DIPLOMA THESIS

Synthesis of Novel Carboline-Based Annulated Heterocyclic Systems for Organic Electronics

conducted at the
Institute of Applied Synthetic Chemistry
at the **TU Wien**

under the supervision of
Univ.Prof. Dipl.-Ing. Dr.techn. Johannes **Fröhlich**

advised by
Univ.Ass. Dipl.-Ing. Paul **Kautny**
and
Senior Lecturer Dipl.-Ing. Dr.techn. Ernst **Horkel**

by
Thomas **Kader**, BSc.

Matr.Nr.: 0928853
Felbigergasse 16/1/5, 1140 Wien

Vienna, March 6, 2016

Danksagung

Zuallererst möchte ich mich bei Univ.Prof. Dr. Johannes Fröhlich für die Möglichkeit bedanken, die hier dargelegte Diplomarbeit in seiner Forschungsgruppe durchzuführen, sowie für den Freiraum den er mir dabei gewährt hat.

Univ.Ass. Dipl.-Ing. Paul Kautny danke ich für die hervorragende fachliche Betreuung und die vielen wertvollen Ratschläge während dieser Arbeit.

Bei Senior Lecturer Dr. Ernst Horkel möchte ich mich für die Unterstützung bei diversen synthetischen Fragestellungen, als auch administrativen Belangen bedanken, sowie für die Durchführung der quantenmechanischen Berechnungen.

Meinen Laborkollegen Dr. Brigitte Holzer und Univ.Ass. Dipl.-Ing. Florian Glöcklhofer, sowie allen anderen Mitgliedern der Forschungsgruppe danke ich für das ausgezeichnete Arbeitsklima und die allgemein große Hilfsbereitschaft.

Bei Paul Getreuer, Helene Kriegner, Martina Rüscher und Eva Schönegger möchte ich mich für ihr Mitwirken an dieser Arbeit im Rahmen von Wahlpraktika bedanken.

Univ.Ass. Dr. Berthold Stöger danke ich für die Durchführung von Kristallstrukturanalysen, sowie für die Bereitstellung eines Teflon-Autoklaven und für die Unterstützung bei der Durchführung von Reaktionen mit ebendiesem.

Besonders möchte ich mich bei meinen Eltern dafür bedanken mir dieses Studium ermöglicht zu haben und für ihre liebevolle Unterstützung in den letzten beinahe 25 Jahren.

Abstract

In recent years organic electronics, based on π-conjugated organic semiconductors, received great attention by both academia and industry, owing to many advantages compared to their inorganic counterparts. Organic light emitting diodes (OLEDs) represent the most advanced technology within the field of organic electronics. OLEDs are already used in great extent for various display applications, but also have potential as future lighting technology.

Phosphorescent OLEDs (PhOLEDs), containing heavy metal complex emitters, are in position to utilize excited singlet and triplet states, resulting in theoretically 100% internal quantum efficiency. In order to avoid quenching effects due to high concentration of excited triplet states, these phosphorescent emitters have to be dispersed in an organic host material.

Recently our research group investigated planarized arylamines as electron donating moieties in oxadiazole based bipolar host materials for PhOLEDs. These studies unveiled, that fully planarized indolo[3,2,1-*jk*]carbazole (ICz) possesses weak acceptor character.

The goal of this thesis was the incorporation of pyridine into the ICz scaffold in order to further increase the acceptor strength of this particular moiety.

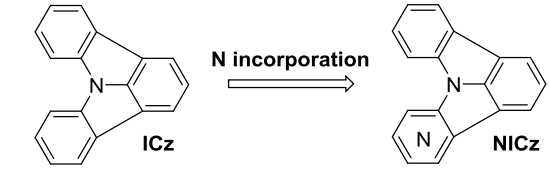

Concept of nitrogen incorporation into the ICz scaffold.

A reliable synthetic approach towards various NICz isomers was established applying traditional methods like nucleophilic substitution and condensation reactions as well as modern transition metal catalyzed methods. The influence of parameters like catalyst, base and solvent on the intramolecular arylation by Pd catalyzed C-H activation as key step in the formation of the ICz derivatives was investigated in detail.

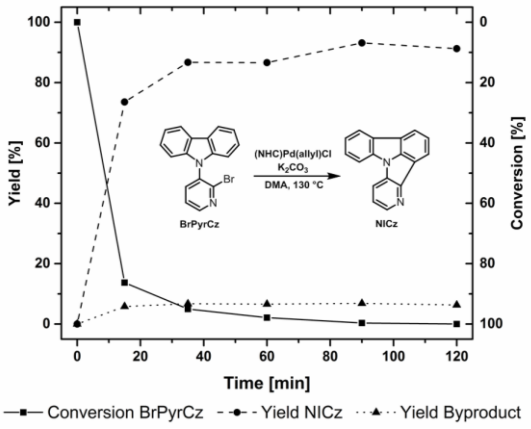

Ring closure towards NICz applying C-H activation.

Furthermore, first investigations towards the incorporation of two pyridine units into the ICz scaffold and on the functionalization of NICz have been conducted.

Kurzfassung

In den letzten Jahren gewann das Gebiet der organischen Elektronik, welches auf π-konjugierten organischen Halbleitern basiert, aufgrund von zahlreichen Vorteilen gegenüber herkömmlichen Technologien zunehmend an Bedeutung. Organische Leuchtdioden (engl. *organic light emitting diodes*, OLEDs) sind die am weitesten fortgeschrittene Technologie im Bereich der organischen Elektronik. OLEDs werden bereits in großem Ausmaß in diversen Bildschirmen genutzt, haben jedoch auch Potential als zukünftige Beleuchtungstechnologie.

Phosphoreszente OLEDs (PhOLEDs) enthalten Metallkomplexe als Emitter und sind in der Lage angeregte Singulett- und Triplettzustände zu verwerten, wodurch eine theoretische interne Quanteneffizienz von 100% erreichbar ist. Um Quenchingeffekte aufgrund hoher Konzentration angeregter Triplettzustände zu vermeiden, müssen diese phosphoreszenten Emitter jedoch in einem organischen Host Material verteilt werden. Vor kurzem untersuchte unsere Forschungsgruppe planarisierte Arylamine als Elektonendonoren in Oxadiazol basierenden bipolaren Host Materialien für PhOLEDs. Die Untersuchungen zeigten, dass vollständig planarisiertes Indolo[3,2,1-*jk*]carbazol (ICz) auch schwachen Akzeptorcharakter aufweist. Das Ziel dieser Arbeit war der Einbau von Pyridin in die ICz Struktur, um die Akzeptorstärke dieses molekularen Bausteins zu erhöhen.

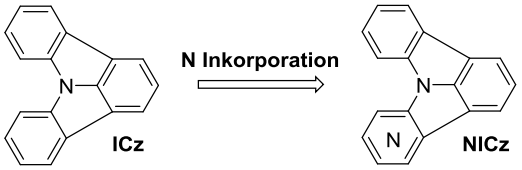

Konzept des Einbaus von Stickstoff in die ICz Struktur.

Ein zuverlässiger synthetischer Zugang zu unterschiedlichen NICz Isomeren wurde unter der Verwendung von klassischen Methoden wie nukleophiler Substitutionen und Kondensationsreaktionen, als auch moderner übergangsmetallkatalysierter Methoden erarbeitet. Die Auswirkungen von Parametern wie Katalysator, Base und Lösungsmittel auf die intramolekulare Arylierung mittels Pd-katalysierter C-H Aktivierung als Schlüsselschritt in der Synthese von NICz wurde detailliert untersucht.

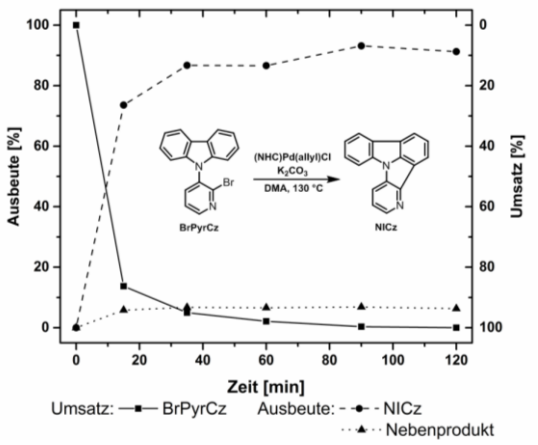

Ringschluss zu NICz mittels C-H Aktivierung.

Weiters wurden erste Untersuchungen zum Einbau von zwei Pyridin Einheiten in die ICz Struktur, sowie zur Funktionalisierung von NICz durchgeführt.

Abbreviations

Besides common abbreviations in the English language and chemical element symbols the below listed short forms are used.

ACN	acetonitrile
aq.	aqueous
CHA	C-H activation
Cz	carbazole
DACH	(±)-*trans*-1,2-diaminocyclohexane
dba	dibenzylideneacetone
DCM	dichloromethane
DMA	dimethylacetamide
DMF	dimethylformamide
DMSO	dimethylsulfoxide
DMT	2,5-dimethoxytetrahydrofuran
dppf	1,1'-bis(diphenylphosphino)-ferrocene
EA	ethyl acetate
E_T	triplet energy
eq.	equivalents
FID	flame ionization detector
GC	gas chromatography
HOMO	highest occupied molecular orbital
ICz	indolo[3,2,1-*j,k*]carbazole
LUMO	lowest unoccupied molecular orbital
MS	mass spectrometry
NBS	*N*-bromosuccinimide
n-BuLi	*n*-butyllithium
NHC	N-heterocyclic carbene
NICz	nitrogen containing ICz
NMR	nuclear magnetic resonance
MW	microwave
OLED	organic light emitting diode
PE	light petrol
PivOH	pivalic acid
PhOLED	phosphorescent OLED
Phen	phenanthroline
r.t.	room temperature
SG	silica gel
THF	tetrahydrofuran
TLC	thin layer chromatography
UV	ultraviolet

General Remarks

Labeling of substances

Identification of substances is achieved by strict sequential numbering. Structurally similar substances receive same numbers combined with additional small Latin letters for further differentiation. Substances previously reported in literature receive Arabic numerals, whereas substances unknown to literature are labeled in Roman numerals.

References to literature citations

References to literature are given within the text by superscript Arabic numbers in square brackets.

Nomenclature

The nomenclature of chemical compounds not described in literature is based on the rules of Chemical Abstracts. Other compounds, reagents and solvents may be described by simplified terms, trivial or trade names.

Table of Contents

A Formular Scheme

A.1 Synthesis of carbolines

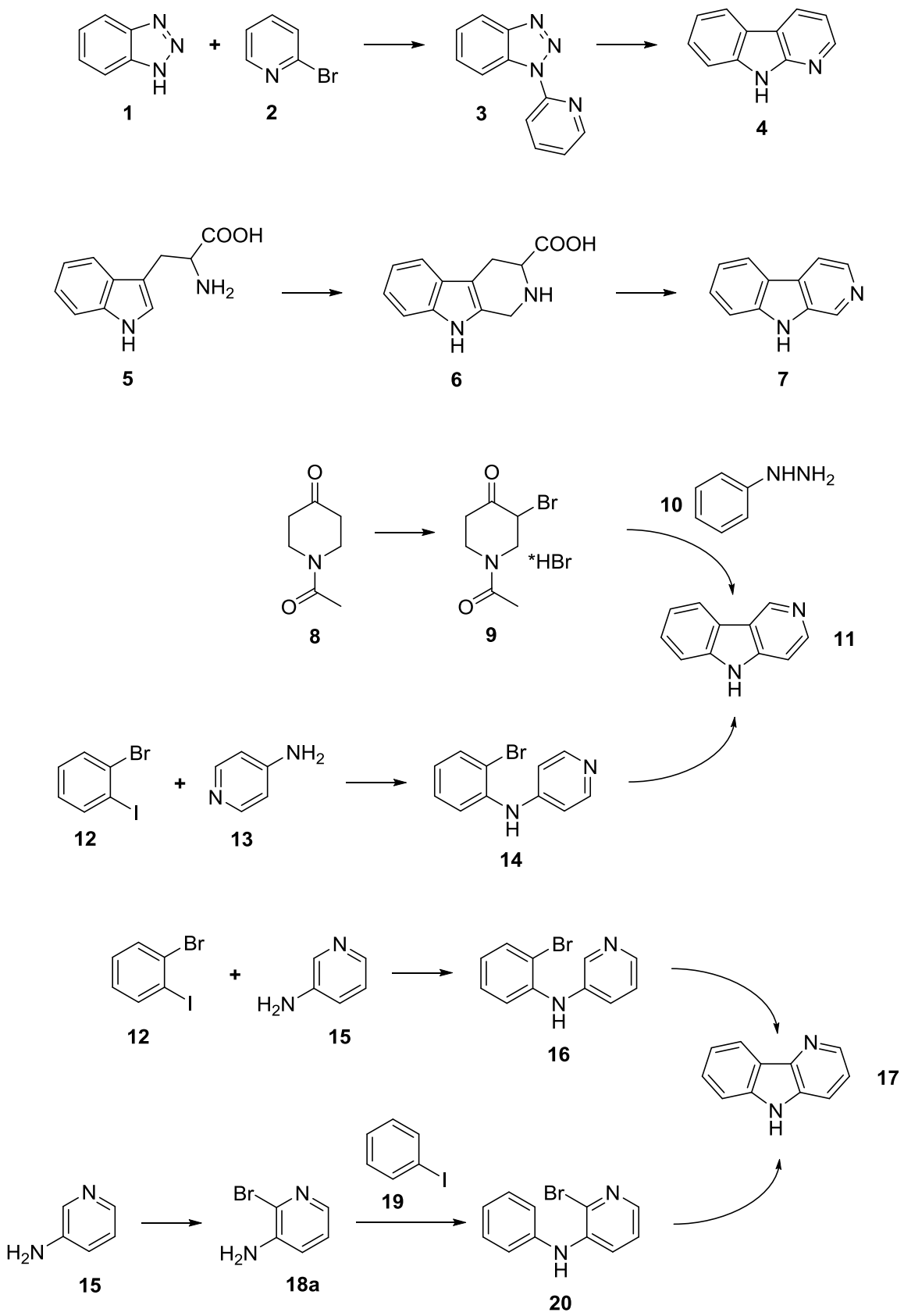

A.2 Carboline strategy

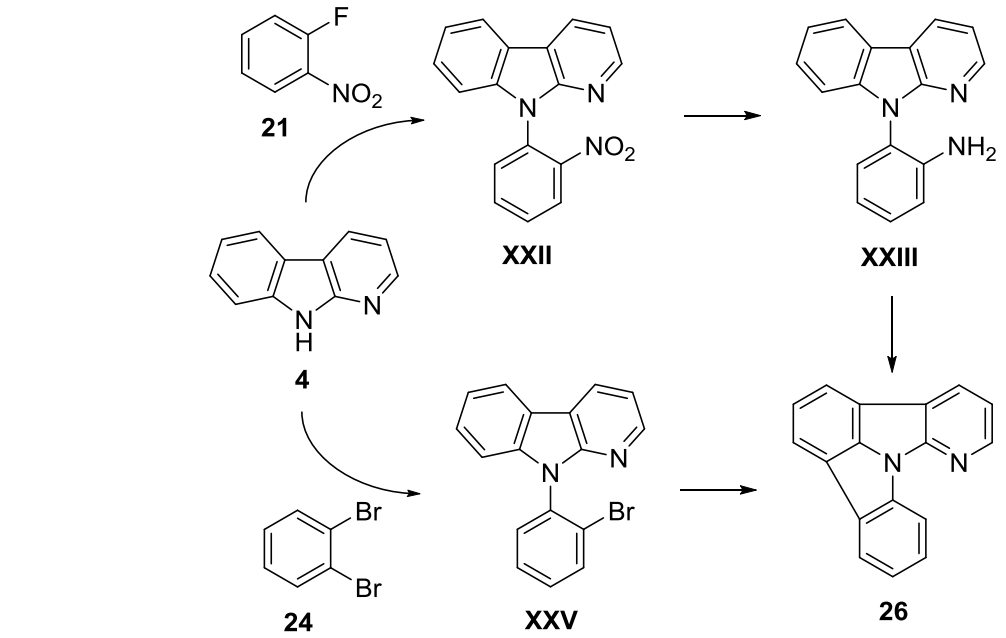

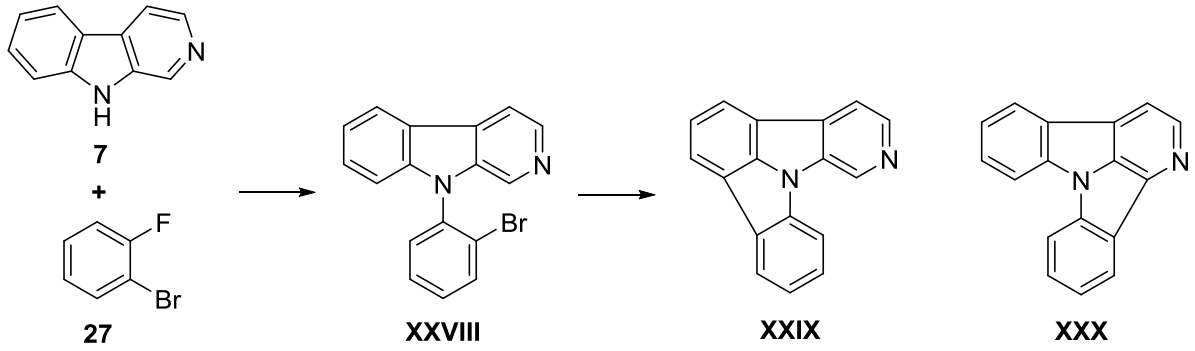

A.3 Carbazole strategy

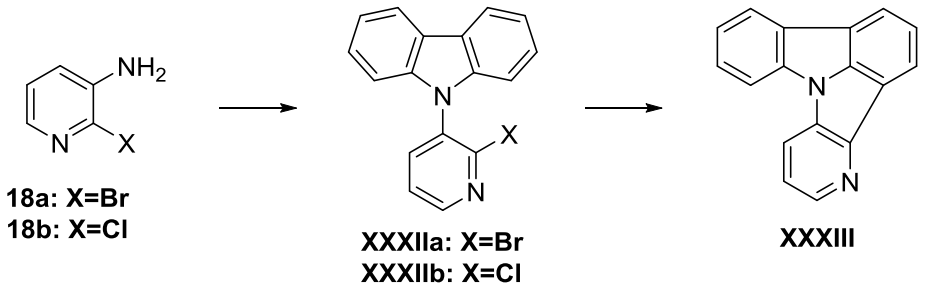

18a: X=Br
18b: X=Cl

XXXIIa: X=Br
XXXIIb: X=Cl

XXXIII

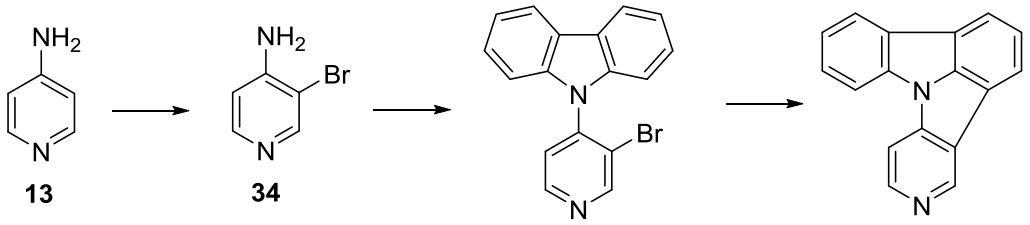

13

34

XXXV

36

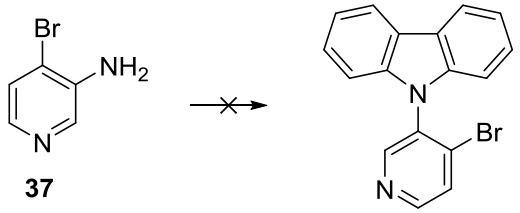

37

XXXVIII

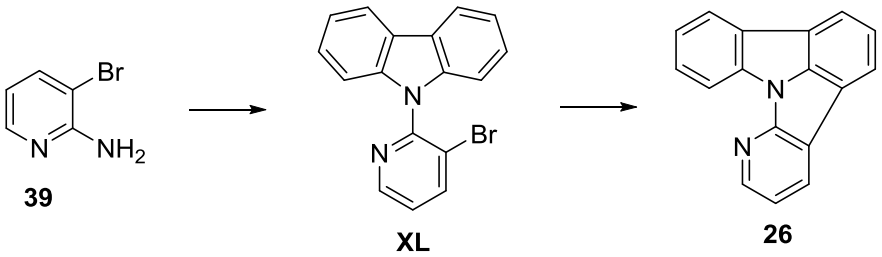

39

XL

26

A.4 Synthesis of Pd-NHC catalyst

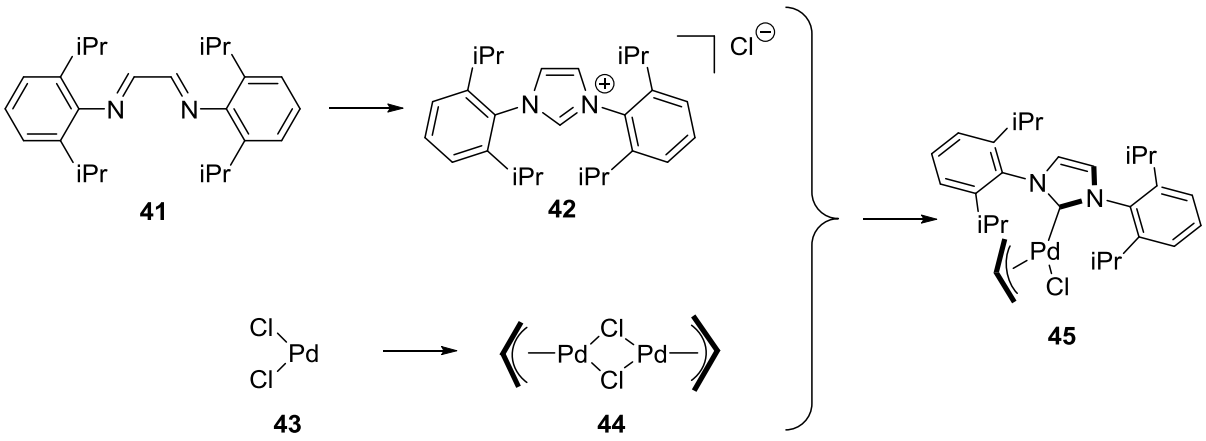

A.5 Synthesis of calibration reference

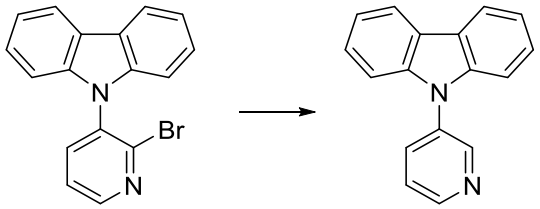

A.6 Syntheses towards substrates for double sided CHA

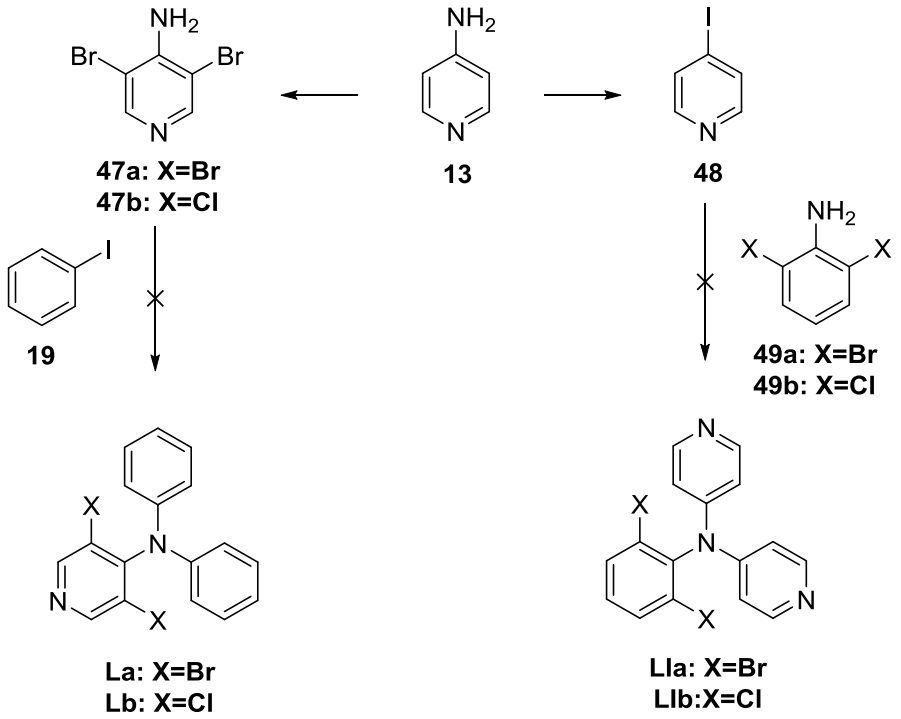

A.7 Functionalization of NICz

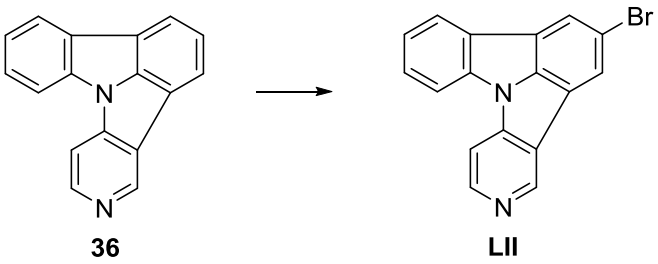

B General Part

B.1 Organic electronics

The emerging field of organic electronics, which deals with electronic devices utilizing carbon-based semiconductors, has recently gained a lot of research interest. Beside Organic Field Effect Transistors (OFETs) and Organic Photovoltaics (OPVs), Organic Light Emitting Diodes (OLEDs) represent the most advanced technology in the field of organic electronics. Typical advantages of organic electronics compared to their inorganic counterparts are low cost processability and the opportunity of light weight or even flexible devices.[1]

B.2 Organic Light Emitting Diodes

Since the first observation of electroluminescence in organic crystals by Pope et al.[2] as well as Helfrich and Schneider[3] in the early 1960s it took almost 20 years until the first vacuum deposited thin film electroluminescent device was reported in 1982 by Vincett et al.[4] A few years later first efficient OLED devices based on small molecules[5] and polymers[6] were developed. Since then a lot of research effort to further increase device performance was made, resulting in the introduction of commercially available products in 1997.[7],[8]

OLEDs are nowadays already used in great extent, particularly in applications for display technology. Whereas in the past only small devices like smartphones employed OLEDs, today also large area OLED TV screens are commercially available.[8] Beside display applications the use of OLEDs for lighting becomes increasingly more appealing. Since nearly 20% of electricity consumption is caused by lighting,[9] the development of energy efficient lighting techniques displays a central role in reducing energy consumption. While incandescent lamps exhibit low efficacy (table B.01), as most energy is wasted on heat formation, more efficient fluorescent lamps contain toxic mercury and high density discharge lamps are only suitable for niche applications. In contrast solid state lighting (inorganic and organic LEDs) shows high efficacy with broad applicability and lack of environmental concerns.[10]–[12]

Table B.01: Energy efficacy of common lighting technologies in Lumen per Watt.[10]

Lighting type	***Energy efficacy [lm/W]***
Incandescent lighting (“light bulb”)	10-17
Compact fluorescence lamp	33-70
High-intensity discharge lamp	25-140
(O)LED	27-94

Although their efficiency is slightly lower compared to inorganic LEDs, OLEDs have the advantage that they can be used as large-area light sources. In contrast LEDs are concentrated point light sources. Hence OLEDs may represent an important future lighting technology. However, one of the major challenges for OLEDs nowadays is to further increase device lifetime, which is particular an issue for blue devices.[13]

B.2.1 Working principle

As already mentioned the working principle of OLEDs is based on electroluminescence. An organic semiconductor is placed between two electrodes and voltage is applied. At the anode holes are injected into the HOMO (highest occupied molecular orbital) of the organic semiconductor, whereas electrons are injected into the LUMO (lowest unoccupied molecular orbital) at the cathode (figure B.01). Driven by the electric field the charges are transported until they recombine and form a formally uncharged excited electron-hole pair, a so called exciton. These excited states can relax by the emission of light or unwanted generation of heat.[14]

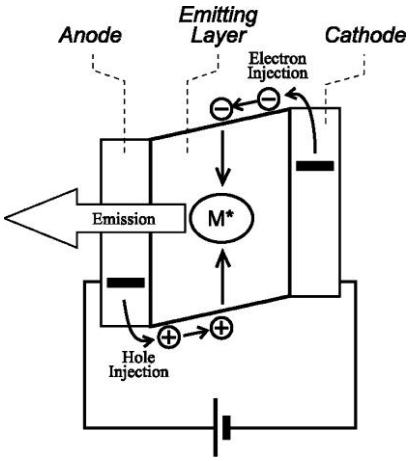

Figure B.01: Working principle of OLEDs.[14]

In the most simple case OLEDs consist of only one layer (emitting layer) between the electrodes (figure B.01). More sophisticated devices use a multi-layer structure with one or more hole- and/or electron-transporting layers between the electrodes and the emitting layer (figure B.02), allowing a more balanced charge carrier transport as the energy barrier for charge injection to adjacent layers is decreased by adjustment of the energy levels of the transporting layers.[15]

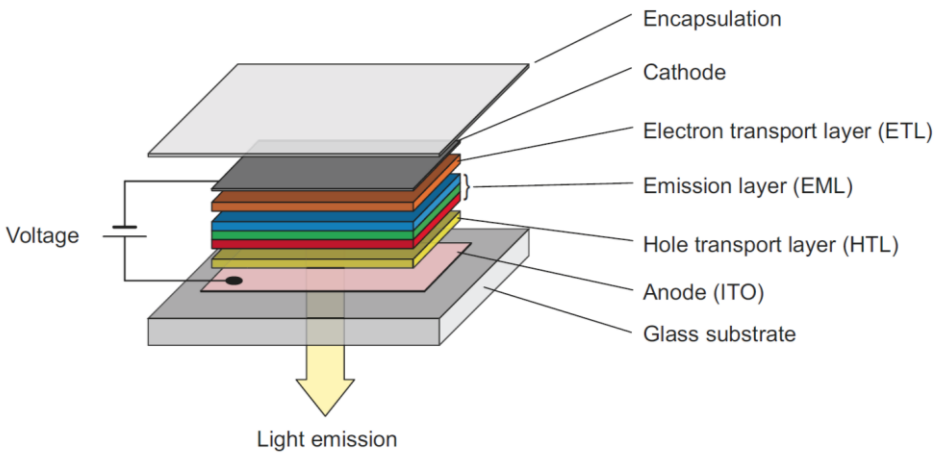

Figure B.02: Multilayer device structure.[16]

B.2.2 Phosphorescent OLEDs

Initially fluorescence based materials, which are capable of using solely singlet excitons, were used in OLEDs. Since the ratio of singlet and triplet excitons in electroluminescent devices is 1:3,[17] such devices are limited to 25% internal quantum efficiency. However, phosphorescent emitters can utilize both singlet and triplet states. Therefore, Phosphorescent OLEDs (PhOLEDs), which were introduced by Forrest et al. in 1998,[18] can theoretically reach 100% internal quantum efficiency. PhOLEDs contain transition metal complexes. Especially Ir complexes are employed as phosphorescent emitters due to their short excited state lifetimes (scheme B.01).[19] The wavelength of the emitted light is determined by the phosphorescent emitter and can be modified by variation of the ligands. White light, as required for lighting applications, can be achieved by the combination of blue, green and red emitters.[20]

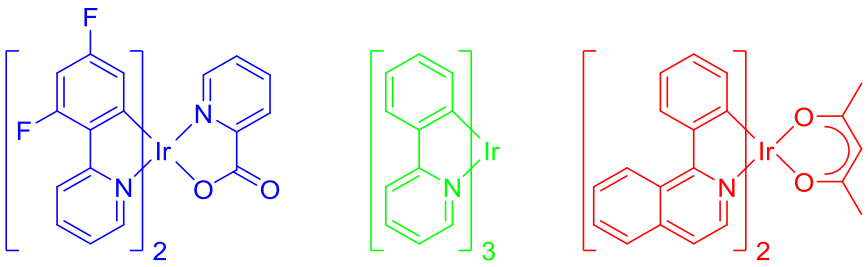

Scheme B.01: Molecular structure of commonly used phosphorescent emitters.[15]

B.2.2.1 Host materials

To prevent undesired competitive effects as concentration dependent quenching of triplet excitons, the phosphorescent emitters (dopants) have to be dispersed in an organic matrix, a so called host material.[20],[21] There are several requirements host materials have to fulfill to achieve efficient devices: a) the triplet energy (E_T) of the host should be higher than the E_T of the dopant, to avoid reverse energy transfer from the emitter to the host; b) energy levels of HOMO and LUMO of the host material should match those of the adjacent layers to decrease the hole and electron injection barrier; c) host materials should have balanced charge carrier transport properties, which is realized by bipolar host materials containing both donor and acceptor subunits within one molecule; d) thermal stability of the host also plays an important role for device performance and lifetime.[15],[22]

B.2.2.2 Arylamine based host materials

Arylamines like carbazole or triphenylamine are commonly used as donor subunits in bipolar host materials.[15] Recently our research group introduced novel bipolar host materials based on oxadiazoles as acceptors and various triarylamines as donors (scheme B.02, right).[23] The increasing degree of planarization, starting from triphenylamine (TPA), phenylcarbazole (PCz) to indolo[3,2,1-*jk*]carbazole (ICz), was utilized to modulate the donor strength of the triarylamine moiety (scheme B.02 left). Increased planarization led to decreased donor strength, as the nitrogen lone pair contributes to the aromaticity of the pyrrole subunits.

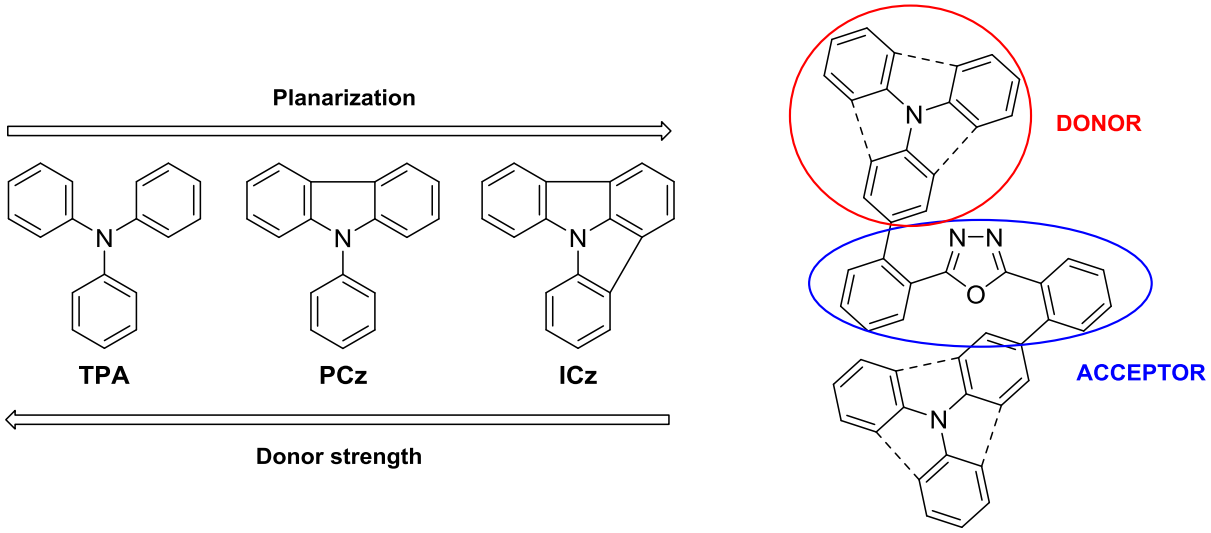

Scheme B.02: Concept of donor strength modulation by planarization (left) and structure of oxadiazole based host materials introduced by Kautny et al.[23]

However, experimental data revealed that the ICz moiety exhibits donor, as well as weak acceptor character. Theoretical calculations further confirmed this observation as they revealed, that for ICz based host material o-ICzPOXD both HOMO and LUMO are located at the opposite ICz moieties (figure B.03), indicating the partial acceptor character of ICz. In contrast the LUMO spreads over the electron withdrawing oxadiazole in TPA and PCz based materials.

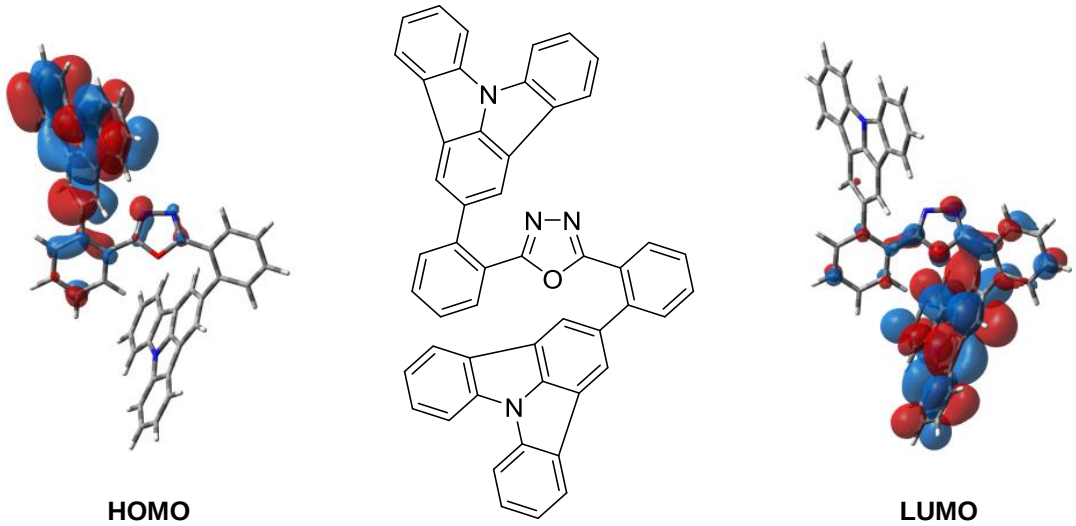

Figure B.03: Spatial distribution of HOMO (left) and LUMO (right) of ICz based host material o-ICzPOXD (middle).[23]

Furthermore, our research group recently developed ICz based **CBP** derivatives, such as **ICzICz** (scheme B.03) exhibiting higher E_T and improved thermal stability compared to widely used host material CBP.[24]

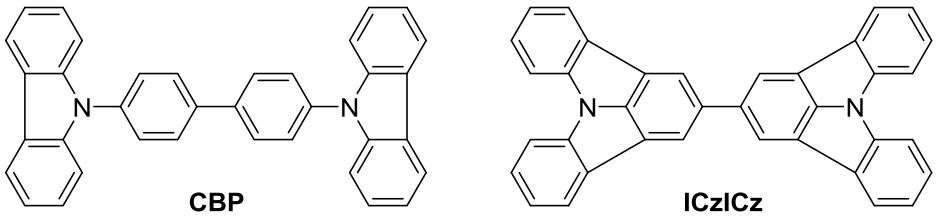

Scheme B.03: Structure of CBP and its derivative ICzICz.

Based on host material **ICzICz** theoretical calculations of HOMO and LUMO levels, as well as E_T of the same scaffold with additionally incorporated nitrogen, as illustrated in scheme B.04, were conducted. Calculations were performed applying density functional theory at B3LYP/6-31G(d) and B3LYP/6-311+G(d) level.

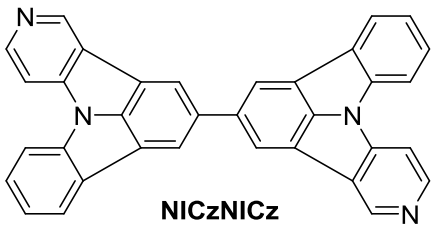

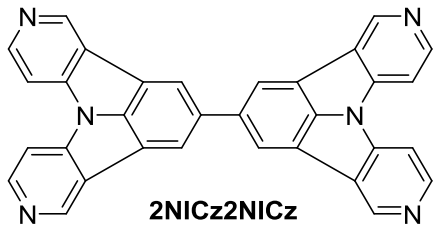

Scheme B.04: Structure of ICzICz derivatives NICzNICz and 2NICz2NICz.

Results of the calculations, which are outlined in table B.02, unveiled that further incorporation of nitrogen into the **ICzICz** scaffold leads to a decrease of both HOMO and LUMO levels, therefore, indicating increased acceptor strength of **NICzNICz** and **2NICz2NICz** compared to **ICzICz**. At the same time E_Ts remain high rendering the application in blue PhOLEDs possible.

Table B.02: HOMO and LUMO levels as well as E_T (all values in eV, energy levels relative to vacuum level) for **ICzICz**, **NICzNICz** and **2NICz2NICz**. Calculated values determined by density functional theory.

	HOMO	***LUMO***	***HOMO***	***LUMO***	***HOMO***	***LUMO***	***E_T***	
	calculated[a]		***calculated[b]***		***experimental[c]***		***calc.[b]***	***exp.[d]***
ICzICz[24]	-5.28	-1.29	-5.62	-1.71	-5.39	-2.18	2.91	2.82
NICzNICz	-5.62	-1.56	-5.92	-1.97	-	-	2.91	-
2NICz2NICz	-5.95	-1.84	-6.29	-2.23	-	-	3.01	-

[a] Calculated applying density functional theory (B3LYP/6-31G(d)). [b] Calculated applying density functional theory (B3LYP/6-311+G(d)). [c] HOMO levels were calculated from the onset of the oxidation peak of cyclic voltammetry measurements. LUMO levels were calculated from HOMO levels and optical bandgap. [d] Estimated from the highest energy vibronic transition in solid solutions of toluene/EtOH (9:1) at 77 K.

The spatial distribution of HOMOs and LUMOs of **NICzNICz** and **2NICz2NICz** are illustrated in figure B.04.

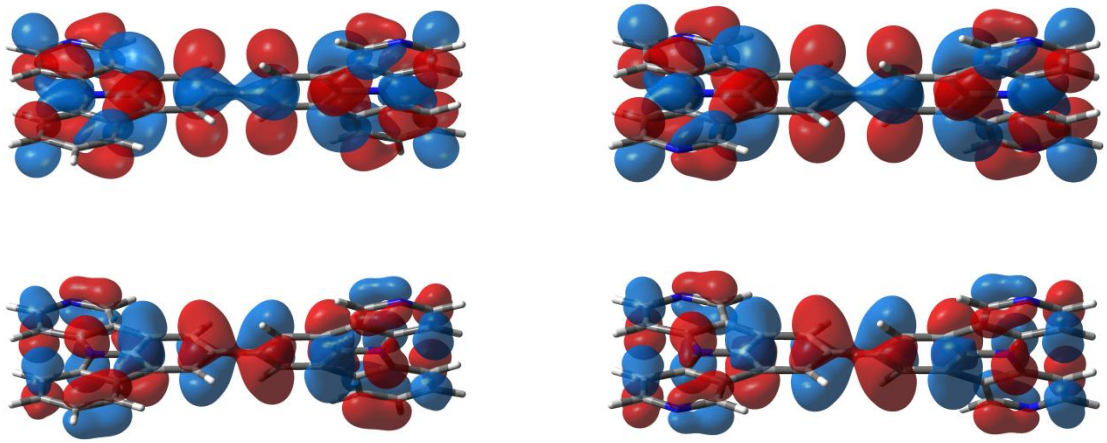

Figure B.04: Spatial distribution of HOMO (bottom) and LUMO (top) of **NICzNICz** (left) and **2NICz2NICz** (right).

B.3 Goal of the thesis

The goal of this work is the introduction of an additional nitrogen atom into one of the benzene rings of ICz (scheme B.05). The incorporation of an electron poor pyridine into ICz should further enhance the acceptor strength of this particular scaffold, as predicted by the theoretical calculations.

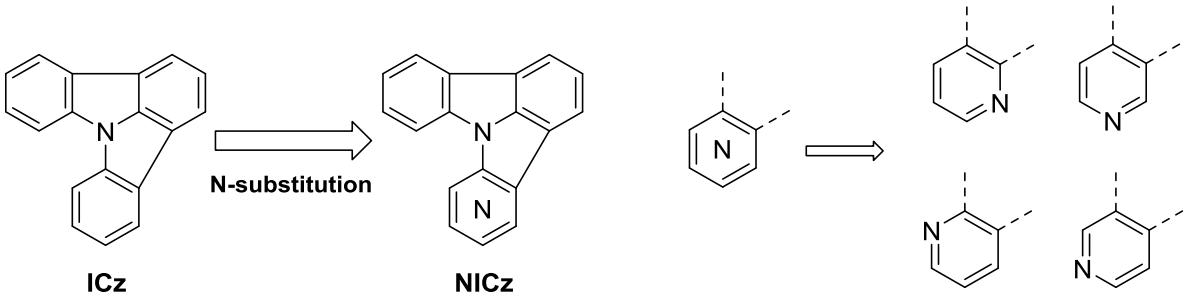

Scheme B.05: Schematic conversion of ICz into nitrogen-containing indolocarbazole (NICz). Possible positions of nitrogen in the pyridine ring result in different NICz isomers (right).

The basic idea behind this approach is illustrated in figure B.05. Gradual modification of donor and acceptor strength of triarylamines is achieved by planarization and control of nitrogen content, which enables specific adjustment of electrochemical properties of the materials. Thus, the development of new building blocks for functional materials with high E_T, good thermal stability and electron transport properties is possible.

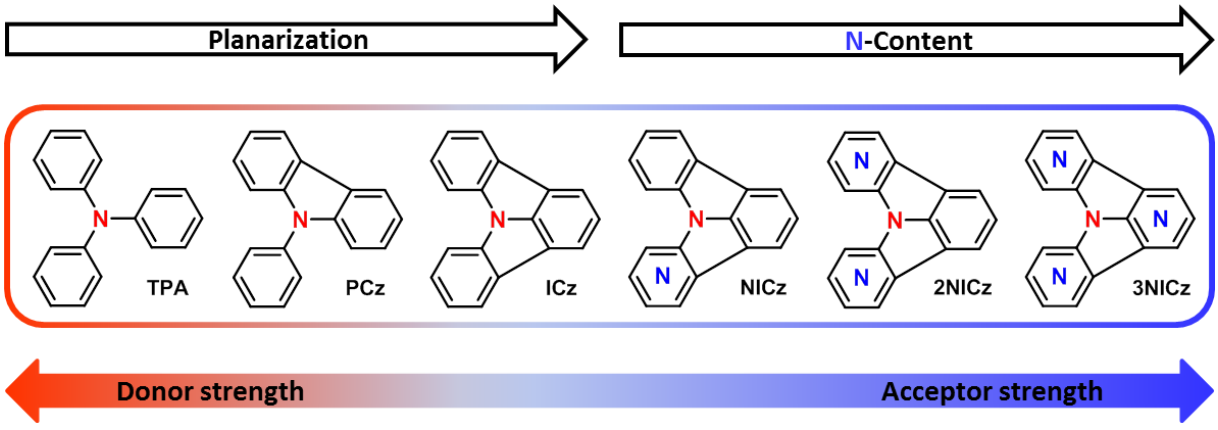

Figure B.05: Concept of modulation of donor and acceptor strength in triarylamines by planarization and N-incorporation.

C Specific Part

C.1 Introduction

The main focus of this thesis is on the development of a reliable and practical synthetic protocol towards the NICz scaffold presented in chapter B.3. Despite for NICz isomers **26** and **36** (scheme C.01), which were synthesized by Wharton et al. *via* flash vacuum pyrolysis,[25],[26] no synthetic protocol towards NICz is described in scientific literature.

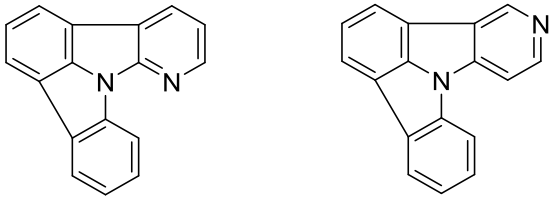

26 **36**

Scheme C.01: NICz isomers **26** and **36**.

Retrosynthetic analysis yields four different ways for the final ring closing reaction towards NICz, which are shown in scheme C.02. These four synthetic paths can be categorized into two approaches, a carboline and a carbazole approach depending on the remaining aromatic tricyclic systems. Each of these two approaches offers two possible substitution patterns, differing in the position that is functionalized for the ring closing reaction.

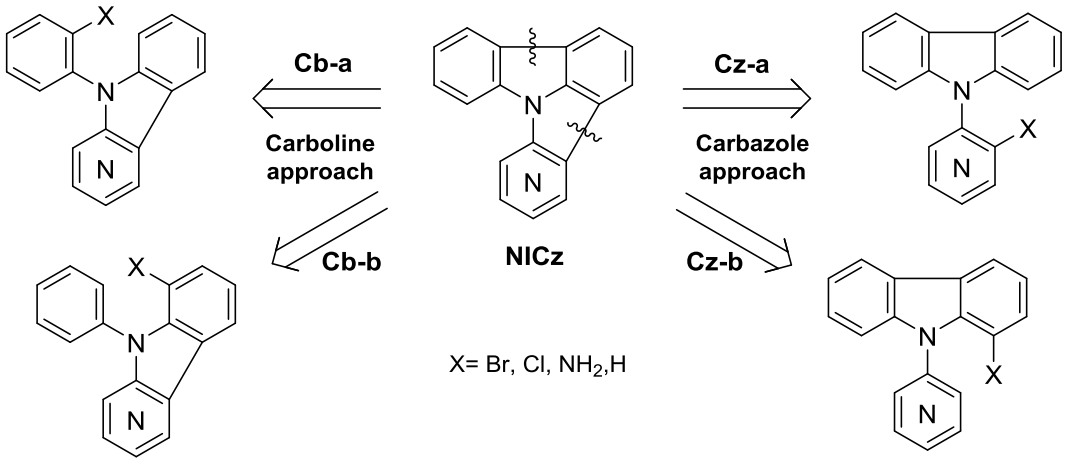

Scheme C.02: Retrosynthetic analysis of NICz scaffold: Substrates for carboline (left) and carbazole (right) approach with different functionalization patterns. Functionalization depending on method chosen for ring closure (X= Br, Cl: CHA, X=NH_2: diazotization, X=H: dehydrogenative ring closure).

Methods for ring closure include Pd catalyzed C-H activation (CHA), diazotization and dehydrogenative ring closure, as these methodologies were all already successfully applied in the synthesis of ICz.[23],[27]–[29] Flash vacuum pyrolysis, which was also employed in the

synthesis of ICz,[30] as well as NICz,[25],[26] was not considered due to the rather impractical reaction conditions of this method, requiring special equipment.

For both approaches only the substitution pattern with functionalization at the isolated ring were investigated, since the appropriate difunctionalized benzene or pyridine substrates are commercially available or easy to synthesize, whereas functionalization of carbolines and carbazoles respectively requires additional synthetic step(s).[31], [32] The two strategies were investigated simultaneously. However, for reasons of better readability the results of the approaches are discussed consecutively in the following chapters. Any overlaps are marked with cross references at the respective places.

C.2 Carboline strategy

Disconnection Cb-a leads to an approach, illustrated in scheme C.03, starting from readily available carbolines and a disubstituted benzene derivative. Disconnecting the pyrrole N of the carbolines and the benzene ring yields the apparent strategy for the synthesis of precursors for ring closure towards NICz by either nucleophilic substitution, Ullmann condensation or Buchwald-Hartwig amination.

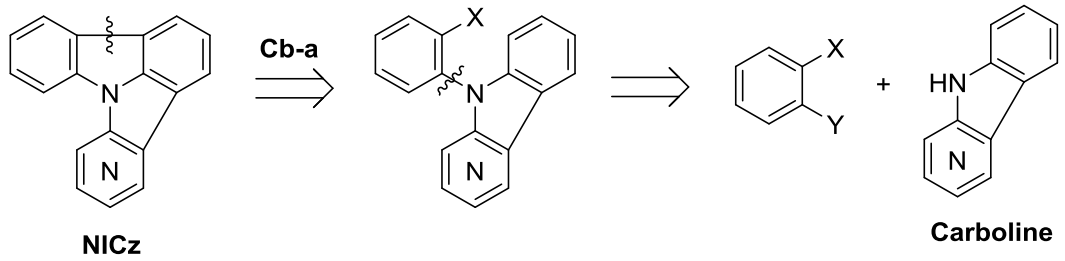

Scheme C.03: Retrosynthetic analysis of the carboline approach: Ring closure (X= Br, Cl: CHA. X= NH_2: diazotization. X= H: dehydrogenative ring closure) and further disconnection step (Y= I, Br: Ullmann, Buchwald-Hartwig. Y= F: nucleophilic substitution) resulting in commercially available disubstituted benzenes and readily accessible carbolines.

However, there is one major drawback of this approach, as there are two possible isomers that can be formed in the ring closing step (scheme C.04) and control of regioselectivity might be difficult despite the different electronic properties of the benzene and pyridine ring.

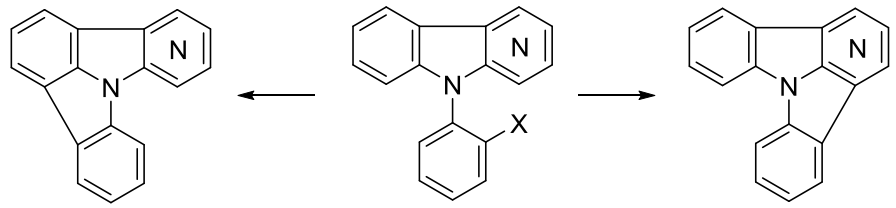

Scheme C.04: Problem of regioselectivity with carboline approach.

C.2.1 Synthesis of carbolines

As all four carbolines (α, β, γ, δ, see scheme C.05) are known to literature, synthesis towards carbolines could be accomplished rather straightforward. The different synthetic approaches used are discussed in the following.

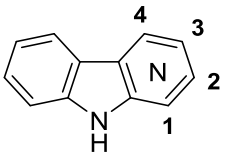

1: α

2: β

3: γ

4: δ

Scheme C.05: Different carbolines with declaration of nitrogen position in the pyridine ring.

C.2.1.1 α-Carboline

Synthesis of α-carboline (**4**) was accomplished by substitution reaction of benzotriazole (**1**) with 2-bromopyridine (**2**), followed by a modified Graebe-Ullmann reaction (scheme C.06).

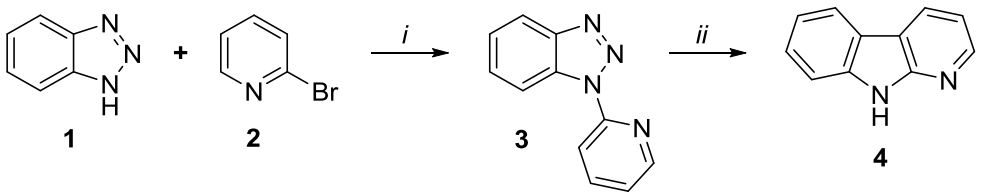

Scheme C.06: Synthesis of α-carboline **4**. *i*: Toluene, reflux. *ii*: Polyphosphoric acid, 130 °C - 140 °C.

Nucleophilic substitution in toluene following the procedure of Katritzky and Wu[33] gave **3** in nearly quantitative yield. The Graebe-Ullmann reaction was done in polyphosphoric acid according to Witkop.[34] However, control of the reaction temperature of the latter was a crucial factor, since this quite exothermic reaction tends to runaway and excessive foaming, when heated too rapidly.

C.2.1.2 β-Carboline

β-Carboline (**7**) was synthesized starting from tryptophane (**5**) (scheme C.07). Pictet-Spengler reaction with formaldehyde in aqueous sodium hydroxide according to Lippke et al.,[35] gave **6** in good yield of nearly 70%. First attempts of decarboxylation and aromatization of **6** using $CuCl_2$ in DMF failed to reproduce the good yields reported in literature[36] giving only 26% of β-carboline (**7**). Therefore, conditions reported from Xin et al.[37] were applied, using selenium dioxide in acetic acid, finally giving **7** with 51% yield.

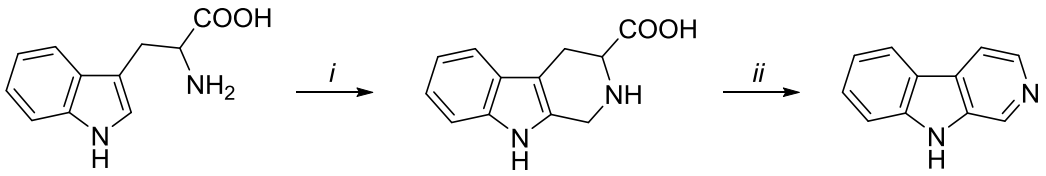

Scheme C.07: Synthetic approach towards β-carboline (**7**). *i*: CH_2O, NaOH, H_2O, r.t. - reflux. *ii:* $CuCl_2$, DMF, 130 °C or SeO_2, AcOH, reflux.

C.2.1.3 γ-Carboline

Synthesis of γ-carboline was done by a modified Fischer indole synthesis starting from **9** (scheme C.08) and phenylhydrazine according to the procedure of Chen et al.[38] Therefore, hydrobromide **9** was isolated in excellent yield (88%) after bromination of commercially available *N*-acetyl-4-piperidone (**8**) with Br_2 in $CHCl_3$. Refluxing in acetic acid with phenylhydrazine, hydrochloride for 24 h gave **11** in rather poor yield of 22%. However, yields could be improved to 36% applying the microwave enhanced method also reported by Chen et al.[38]

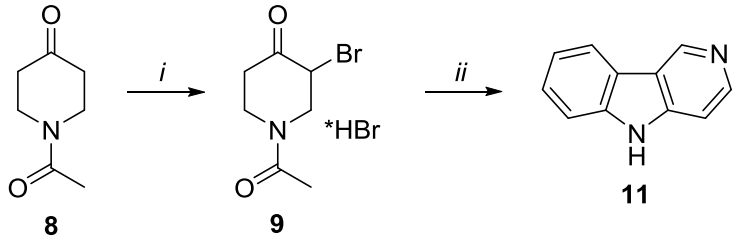

Scheme C.08: Synthesis towards γ-carboline (**11**). *i*: Br_2, $CHCl_3$, 0 °C – r.t.. *ii*: $PhNHNH_2$*HCl, AcOH, reflux or 200 °C (MW).

Nevertheless, also a different approach using a transition metal catalyzed two-step synthesis developed by Iwaki et al.[39] was applied, as illustrated in scheme C.09. Buchwald-Hartwig amination using $Pd_2(dba)_3$ / dppf as catalyst system gave amine **14** in nearly quantitative yield of 99%. Ring closure of **14** by CHA using $Pd(OAc)_2$ yielded carboline **11** (43%).

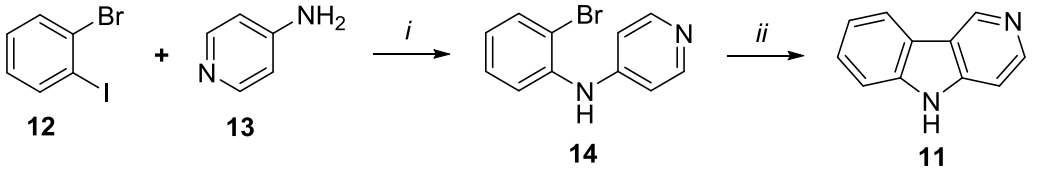

Scheme C.09: Alternative route towards **11** using Buchwald-Hartwig amination followed by CHA. *i:* $Pd_2(dba)_3$, dppf, NaO^tBu, toluene, reflux. *ii*: $Pd(OAc)_2$, Na_2CO_3, DMF, reflux.

C.2.1.4 δ-Carboline

The synthesis of δ-carboline (**17**) was done applying the same strategy as for γ-carboline, using Buchwald-Hartwig amination followed by CHA (scheme C.10). A first approach utilized amine **16**, which was synthesized from 3-aminopyridine (**15**) and 2-bromoiodobenzene (**12**) in excellent yield (90%). However, no selectivity was observed during ring closure and CHA of **16** gave only a mixture of the desired product **17** (7%) and side product **7** (8%). Furthermore, the dehalogenated byproduct **BP1** was formed in about the same amount as both carbolines combined (according to GC-MS).

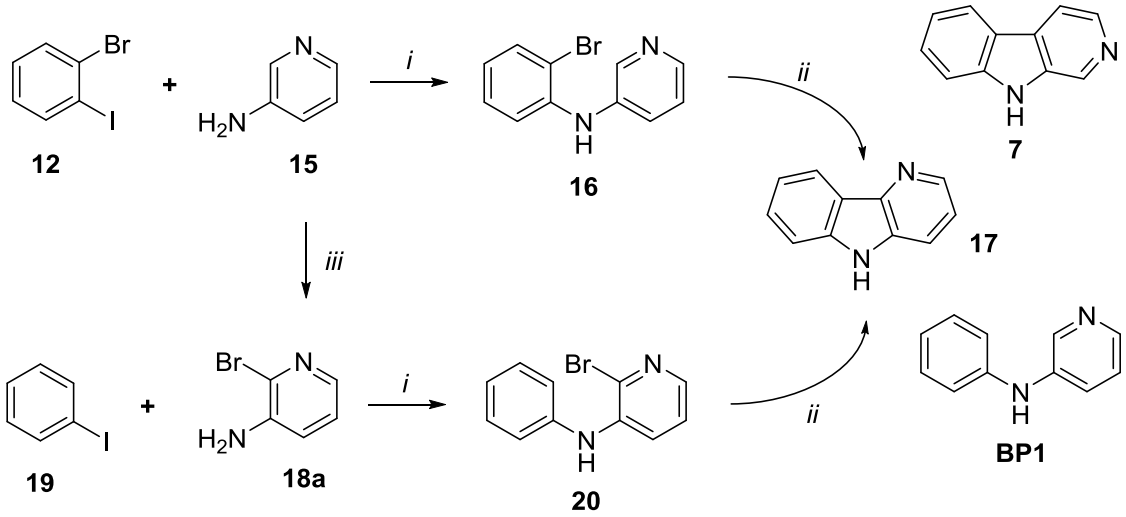

Scheme C.10.: Synthetic approach towards δ-carboline (**11**) using Buchwald-Hartwig amination and CHA, including alternative route by bromination of 3-aminopyridine (**15**) to overcome selectivity problems. *i*: $Pd_2(dba)_3$, dppf, NaO^tBu, toluene, reflux. *ii*: $Pd(OAc)_2$, Na_2CO_3, DMF, reflux. *iii*: NBS, MeOH, r.t., UV-light protection.

In order to overcome the problems with regioselectivity the amine precursor was functionalized at the pyridine ring, since intramolecular CHA at the benzene ring can only form one product. Therefore, **15** was brominated in position 2 with NBS in methanol, according to Cañibano et al.[40] Buchwald-Hartwig amination of **19** with **18a** yielded amine **20** (46%). δ-Carboline (**17**) was isolated after CHA and recrystallization in 39% yield. In contrast to the conversion of **16** side product **BP1** occurred only in minor amounts according to GC-MS.

C.2.2 Ring closure towards NICz

For first experiments towards NICz α-carboline was chosen as starting material, since, as a consequence of the position of the nitrogen in the pyridine ring, the formation of only one NICz isomer is possible in the ring closing reaction, which eliminates any problems with regioselectivity as mentioned before.

C.2.2.1 Diazotization

Synthesis of the amine precursor **XXIII** was accomplished by a $S_{N,Ar}$ reaction of **4** with 2-fluoronitrobenzene (**21**), followed by reduction of the nitro group (scheme C.11.). First experiments towards **XXII** were done applying Cs_2CO_3 as base in DMSO at 130 °C according to a modified procedure by Wharton et al.[30] However, further attempts unveiled that also the weaker base K_2CO_3 could be applied, due to the activation of **21** towards nucleophilic substitution caused by the electron withdrawing nitro group, and **XXII** was isolated in 80% yield. Subsequent reduction was realized applying $SnCl_2*2H_2O$ in ethanol according to Dunlop and Tucker,[28] which gave **XXIII** in excellent yield of 94%.

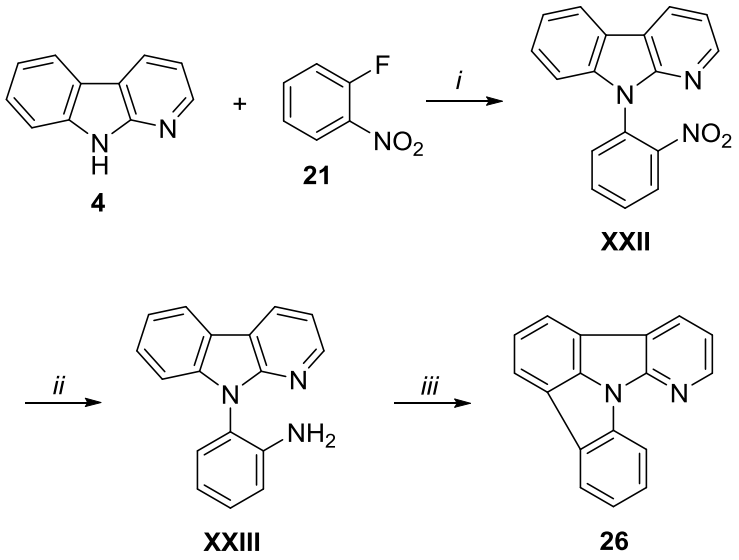

Scheme C.11: Synthesis of **26** by nucleophilic substitution followed by reduction of the nitro group and diazotization. *i*: K_2CO_3, DMSO, 130 °C. *ii*: $SnCl_2*2H_2O$, EtOH, reflux. *iii*: $NaNO_2$, $AcOH/H_2SO_4$, 0 °C – reflux.

Diazotization was accomplished using a procedure from Dunlop and Tucker.[28] However, addition of sodium nitrate in water to **XXIII** dissolved in $AcOH/H_2SO_4$ at 0 °C for *in situ* preparation of the diazonium compound and subsequent heating for decomposition of the diazonium salt under ring closure gave **26** in only 4% yield.

C.2.2.2 C-H Activation

For the synthesis towards the halogenated precursor (scheme C.12) various reaction conditions for Ullmann condensation (Y= I, Br), Buchwald-Hartwig amination (Y= I, Br) and nucleophilic substitution (Y= F), have been tested. The results of this screening are outlined in table C.01.

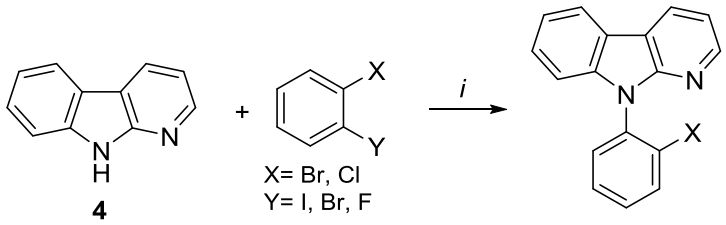

Scheme C.12: Reactions towards CHA precursor.

Ligand accelerated Ullmann condensation applying CuI and *trans*-1,2-diaminocyclohexane (DACH) as catalytic system had been already used in literature for reactions of α-carboline with *para*- and *meta*- substituted dihalogenides.[39],[40] Nevertheless, using this system for *ortho*- substituted dihalogen species, no product formation was observable (according to GC-MS). Further attempts using CuCl and phenanthroline according to Goodbrand and Hu[43] also did not lead to product formation. After all a solvent free Ullmann protocol by Xu et al.[44] using $CuSO_4$*$5H_2O$ and K_2CO_3 at high temperature (230 °C) yielded **XXV** (41%). However, probably caused by the harsh reaction conditions also significant amounts of dehalogenated side product **BP2**, as well as twofold substituted side product **BP3** were formed (scheme C.13).

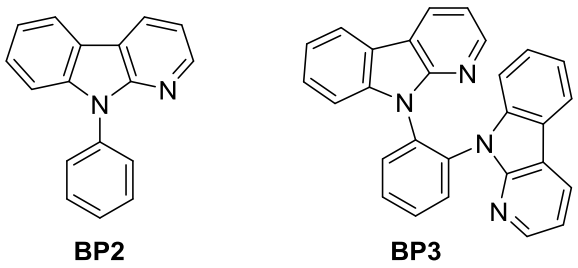

Scheme C.13: Side products of solvent free Ullmann condensation.

Attempts towards Buchwald-Hartwig amination applying Pd-catalyst **45** resulted in no product formation, while nucleophilic substitution in DMSO with Cs_2CO_3 gave only traces of product.

Table C.01: Screening of various reaction conditions for Ullmann condensation, Buchwald-Hartwig amination or nucleophilic substitution towards α-carboline based precursors for CHA, as illustrated in scheme C.12. All reactions were conducted in reaction vials (except for G) using 1 eq. of **4** and 1.1 eq. of dihalogenated substrate. For reaction G a flask with Dean-Stark trap was used.

	Substrate		***Catalyst***	***Ligand***	***Base***	***Solvent***	***T [°C]***	***Time [h]***	***Yield [%]***
	X	***Y***							
A	Cl	Br	CuI	trans-1,2-DACH	K_3PO_4	toluene	110	48	-
B	Br	Br	CuI	trans-1,2-DACH	K_3PO_4	toluene	110	48	-
C	Br	I	CuI	trans-1,2-DACH	K_3PO_4	toluene	110	48	-
D	Cl	Br	CuI	trans-1,2-DACH	K_3PO_4	dioxane	100	48	-
E	Br	Br	CuI	trans-1,2-DACH	K_3PO_4	dioxane	100	48	-
F	Br	I	CuI	trans-1,2-DACH	K_3PO_4	dioxane	100	48	-
G	Br	I	CuCl	phenanthroline	KOH	toluene	110	90	-
H	Br	Br	$CuSO_4{}^*5H_2O$	-	K_2CO_3	-	230	72	41
I	Br	I	Pd-NHC (44)	-	NaO^tBu	toluene	110	24	-
J	Cl	F	-	-	C_2CO_3	DMSO	130	20	traces
K	Br	F	-	-	C_2CO_3	DMSO	130	20	traces

Scale-up of solvent free Ullmann condensation towards **XXV** was done using a Teflon®-autoclave enclosed by a lockable steel jacket, as illustrated in figure C.01. The reaction was performed in a programmable oven. Using this adapted procedure **XXV** was obtained with 14% yield after repeated recrystallization with ethanol. In addition also 12% of **BP2** were isolated. One of the major problems of the scale up was the inaccuracy of the heating program as the oven temperature reached over 260 °C at the end of the first heating cycle. After the reaction a shiny, black graphite-like mixture was obtained, indicating partial thermal decomposition. The molecular structure of **XXV**, seen in figure C.02,

Figure C.01: Teflon®-autoclave (left) with lockable steel jacket (right)

was determined by single crystal diffraction[1] (single crystals obtained after recrystallization with ethanol).

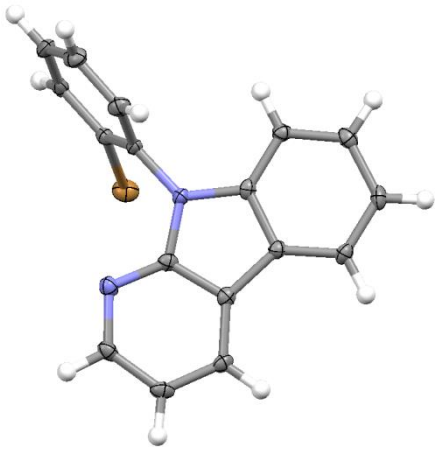

Figure C.02: Molecular structure of **XXV**. Br, C and N atoms are represented by orange, grey and blue ellipsoids drawn at 50% probability levels. Hydrogen atoms (white) are depicted as fixed sizes spheres (radius 0.2 Å).

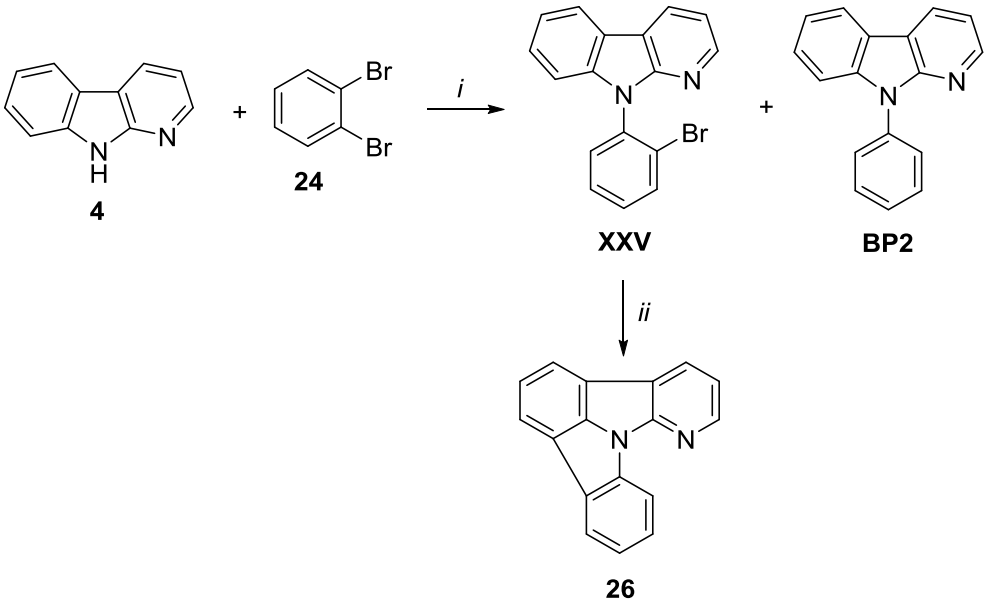

Scheme C.14: Synthetic approach towards **26** using Ullmann condensation and CHA. *i*: $CuSO_4$*$5H_2O$, K_2CO_3, 230 °C. *ii*: Pd-NHC (**45**), K_2CO_3, DMA, 130 °C.

[1] Single crystal structure was determined in collaboration with Dr. Berthold Stöger and the Institute of Chemical Technologies and Analytics, Division of Structural Chemistry. All data were collected on an *APEX II* diffractometer with κ geometry, equipped with a CCD detector using Mo *Kα* irridation at 100 K in a dry stream of nitrogen.

For ring closing reaction of **XXV** towards **26** by CHA the Pd-NHC catalyst **45** (scheme C.15; for synthesis see C.6) was used. However, full conversion took 72 h and gave only a mixture of **26** and **BP2**, at a ratio of roughly 1.3:1 according to GC-MS. This result may be influenced by the position of the nitrogen in the pyridine ring that might cause competitive interactions with the catalyst.

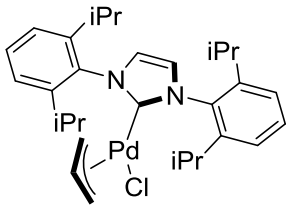

45

Scheme C.15: Catalyst (NHC)Pd(allyl)Cl (**45**).

Therefore, also the halogenated β-carboline derivative was synthesized. In contrast to **XXV**, **XXVIII** can be synthesized by nucleophilic substitution of **27** with β-carboline (**7**) in presence of stoichiometric amounts of Cs_2CO_3 in DMSO (scheme C.16). These findings can be explained by better stabilization of the pyrrole lone pair in **4** compared to **7** due to the position of nitrogen.

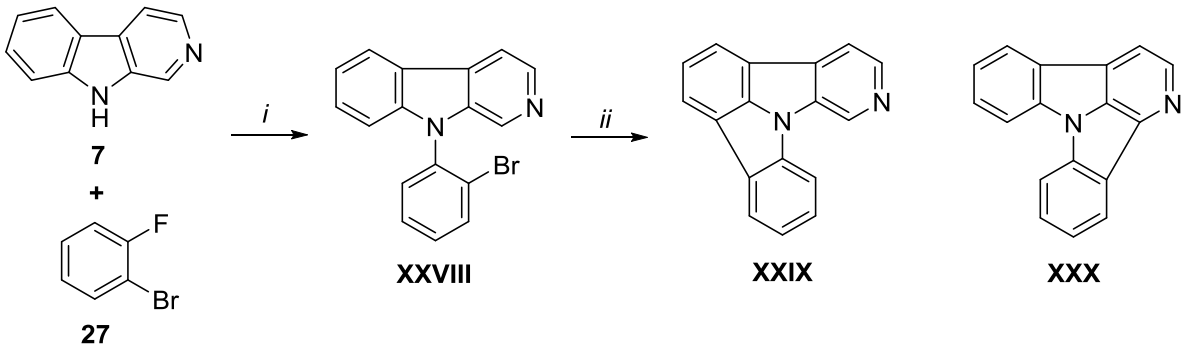

Scheme C.16: Synthesis of β-carboline based NICz by nucleophilic substitution followed by CHA. *i*: Cs_2CO_3, DMSO, 130 °C. *ii*: Pd-NHC (**45**), K_2CO_3, DMA, 130 °C.

Ring closure by CHA of **XXVIII** with catalyst **45** (optimized reaction conditions from C.3.3) gave a mixture of **XXIX** and **XXX** in a ratio of 4:1 with 77% overall yield[2] after stirring at 130 °C over night. The significantly higher yield in the reaction of **XXVIII** confirms the assumption that the reason for the poor results of CHA of **XXV** is the position of the nitrogen within the pyridine ring.

[2] 46% **XXIX** and 8% **XXX** could be isolated after purification with column chromatography. Ratio of remaining mixture (23%) was determined by ^{1}H NMR.

C.2.2.3 Oxidative ring closure

Recently Jones et al.[29] presented a novel route towards ICz using Pd catalyzed dehydrogenative cyclization under oxidative conditions. The applicability of this method for the synthesis of **26** was investigated using the side product of the Ullmann condensation **BP2** (C2.2.2). The use of $Pd(OAc)_2$ as catalyst, the oxidants Ag_2O and CuO and pivalic acid as solvent gave only minor product formation (<5%). Therefore, this approach was no longer pursued.

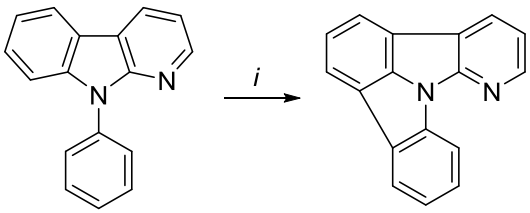

BP2 **26**

Scheme C.17: Synthesis of **26** by dehydrogenative cyclization. *i*: Ag_2O, CuO, $Pd(OAc)_2$, PivOH, 130 °C.

C.3 Carbazole strategy towards NICz

The second approach beside the carboline based synthesis discussed above was the carbazole strategy (Cz-a) as illustrated in scheme C.18. The benefit of this strategy is the exclusion of any problems with regioselectivity, as there is only one isomer that can be formed due to the symmetry of the carbazole moiety. The carbazole derivatives for ring closure towards NICz can be synthesized starting from the corresponding halogenated aminopyridines.

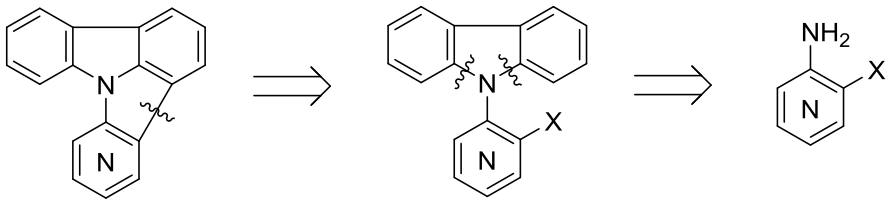

NICz

Scheme C.18: Retrosynthetic approach towards NICz applying the carbazole strategy.

Since investigations on diazotization (C.2.2.1) and oxidative ring closure (C.2.2.3) yielded no convenient results the focus of the carbazole strategy relied on CHA.

C.3.1 Synthesis of the CHA precursor

Although Pd catalyzed N arylation is a common method for the synthesis of carbazoles starting from amines,[45]–[49] a different strategy was chosen, since selectivity problems due to the halogen substituent (X) of the pyridine might occur. A condensation reaction of the amine with 2,5-dimethoxytetrahydrofuran (DMT) **31** can be employed to synthesize carbazole derivatives, as illustrated in scheme C.19.

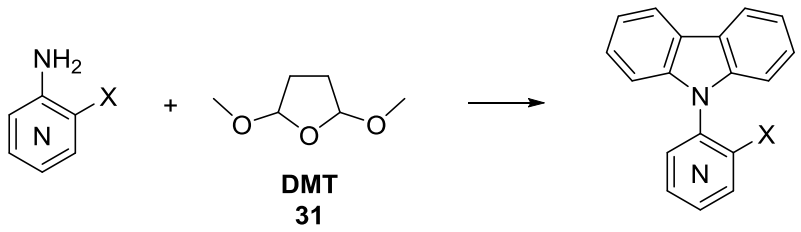

Scheme C.19: Synthesis of carbazoles by condensation reaction of primary amines with 2,5-dimethoxytetrahydrofuran (DMT).

This modified Clauson-Kaas reaction,[50] which is usually applied for the synthesis of pyrroles,[49],[50] can also provide carbazoles.[27],[51]–[55] DMT can hydrolyze under acidic conditions or heat to the 1,4-dialdehyde **A**, which exists under aqueous conditions as 2,5-dihydroxytetrahydrofurane **B.**[52] Both **A** and **B**, as well as DMT itself and further hemiacetal intermediates can act as active species in the reaction. The mechanism of this reaction, which is illustrated in scheme C.20 considering the example of dialdehyde **A**, includes three steps. In a first step dialdehyde **A** reacts with the primary amine to the pyrrole, analogous to a Paal-Knorr pyrrole formation.[58] This pyrrole can react with a further molecule of **A** to give indole, which subsequently can form carbazole with a third equivalent of **A.**[54] This stepwise formation of product was observable by reaction control with GC-MS.

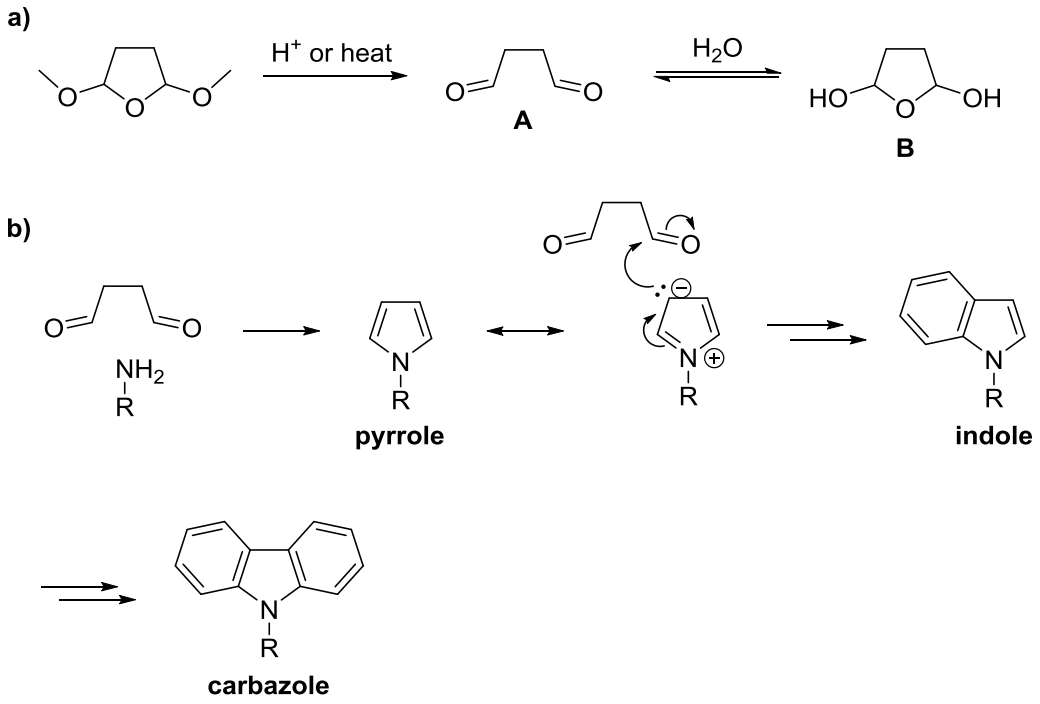

Scheme C.20: Formation of dialdehyde **A** under acidic conditions or heat (a) and stepwise condensation reaction towards carbazole (b).

The condensation reactions were performed using a modified protocol from Lv et al.[27] The corresponding amine was refluxed in AcOH under argon atmosphere with 4 eq. of DMT. If the reactions took longer than 18 h fresh DMT was added (see experimental part for details). Table C.02 gives an overview of reaction times and yields. Whereas all reactions gave rather similar yields of 30% - 50%, there were significant differences in reaction time. The reactions towards **XXXIIa** and **XXXIIb** were completed after 18 h and 34 h. In contrast reactions towards **XXXV** and **XL** were aborted after 120 h and 68 h respectively, although there were still minor amounts of the indole intermediate detectable (GC-MS), as the formation of additional condensation product benzocarbazole was observable. While byproducts from **XXXV** could be removed by column chromatography and subsequent recrystallization, precursor **XL** could not be isolated as entirely pure product, due to the fact that recrystallization was not feasible for **XL** and minor impurities remained after repeated column chromatography. However, condensation was not applicable for amine **37** yielding only traces of **XXXVIII**, which is probably caused by the instability of amine **37**.

Table C.02: Synthesis of carbazole derivatives by modified Clauson-Kaas reaction.

Entry	*Amine*	*Product*	*Time [h]*	*Isolated yield [%]*
1	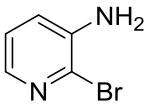 **18a**	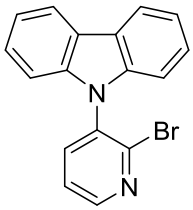 **XXXIIa**	18	52
2	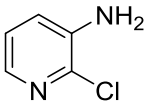 **18b**	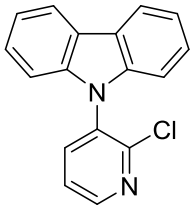 **XXXIIb**	34	41
3	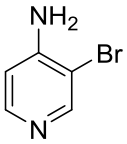 **34**	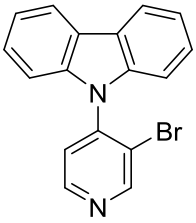 **XXXV**	120	32
4	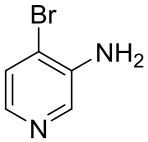 **37**	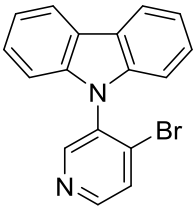 **XXXVIII**	60	traces[a]
5	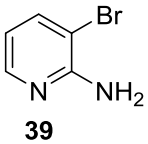 **39**	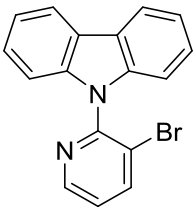 **XL**	68	39[b]

[a] According to GC-MS. [b] Including minor impurities.

C.3.2 CHA-Screening

Since ring closing reaction of precursor **XXV** yielded only poor results (C.2.2.2) a screening was performed for detailed investigations on the influence of different parameters of reaction conditions on the CHA towards NICz. The CHA towards **XXXIII** was selected as model reaction (scheme C.21).

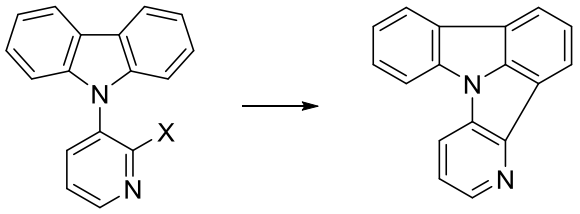

XXXIIa: X=Br
XXXIIb: X=Cl

XXXIII

Scheme C.21: Reaction for the CHA screening.

Within the scope of this screening different catalysts, bases and solvents, as well as the influence of water content and protective atmosphere were investigated. Unless otherwise stated reactions were performed under argon atmosphere in reaction vials using a magnetic stirrer equipped with a metal thermoblock for heating. The vials were sealed using a cap with septum. The reactions were performed using 0.025 mmol of substrate **XXXIIa/b**, 2 eq. base, 10 mol% catalyst and 2 ml solvent at 130 °C.[3] Prior work in our group indicated that the CHA towards ICz requires a certain water content to proceed smoothly. Thus, screening reactions towards NICz with DMA were performed using DMA with a water content of 3000 ppm.

Whereas the base was weighed directly in the vials, starting materials **XXXIIa** or **XXXIIb** and catalyst were added as solutions in the corresponding solvent to ensure accuracy of the used amounts. Furthermore, 1-methylnaphthalene was added to the substrate solution as internal standard for quantification with GC. Solutions were prepared using micropipettes (adjustable piston-driven air displacement pipettes) for addition of specific volumes.[4] The substrate solution and the remaining solvent were added to the base in the reaction vial, using micropipettes and subsequently degassed with argon. The degassed catalyst solution was added *via* syringe through the septum to the reaction mixture. Afterwards the vials were flushed with argon for another two minutes before the reactions were started in a preheated thermoblock. To ensure argon atmosphere during the reaction as well as to enable sampling during the reactions the vials were equipped with argon balloons.

[3] Setting of the thermoblock.
[4] Solutions were freshly prepared for each series. For experiments applying the same conditions different solutions were used to identify systematic errors caused by the preparation of the solutions.

Each reaction was performed three times in three independent experiments in order to prove the reproducibility of the results.[5] Samples were taken after 15 min, 35 min, 60 min and 120 min.[6] Quantification was done using GC with a FID. Therefore, multi-point calibrations for the starting materials **XXXIIa** and **XXXIIb**, product **XXXIII**, dehalogenated side product **46**[7] and internal standard 1-methylnaphthalene were done (see appendix F.1). Each GC sample was measured 3 times. Results of the different experiments are discussed in the following.

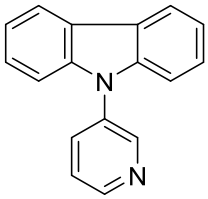

46

Scheme C.22: Dehalogenated byproduct **46**.

[5] Experiments using Pd-NHC (**45**) / K_2CO_3 / DMA were done six times since they were performed during the catalyst and the base screenings.
[6] If required, due to longer reaction times, in some cases further samples were taken.
[7] **46** was prepared by lithiation of **XXXIIa** with *n*-BuLi at -78 °C and subsequent quench with aq. 1N HCl after 1 h reaction time.

C.3.2.1 Catalysts

In the first part of the screening the application of different catalysts was investigated. Beside precatalysts **45** and $PdCl_2(PPh_3)_2$, $Pd(OAc)_2$ in combination with various phosphine ligands was used. The results are outlined in figure C.03 and table C.03.

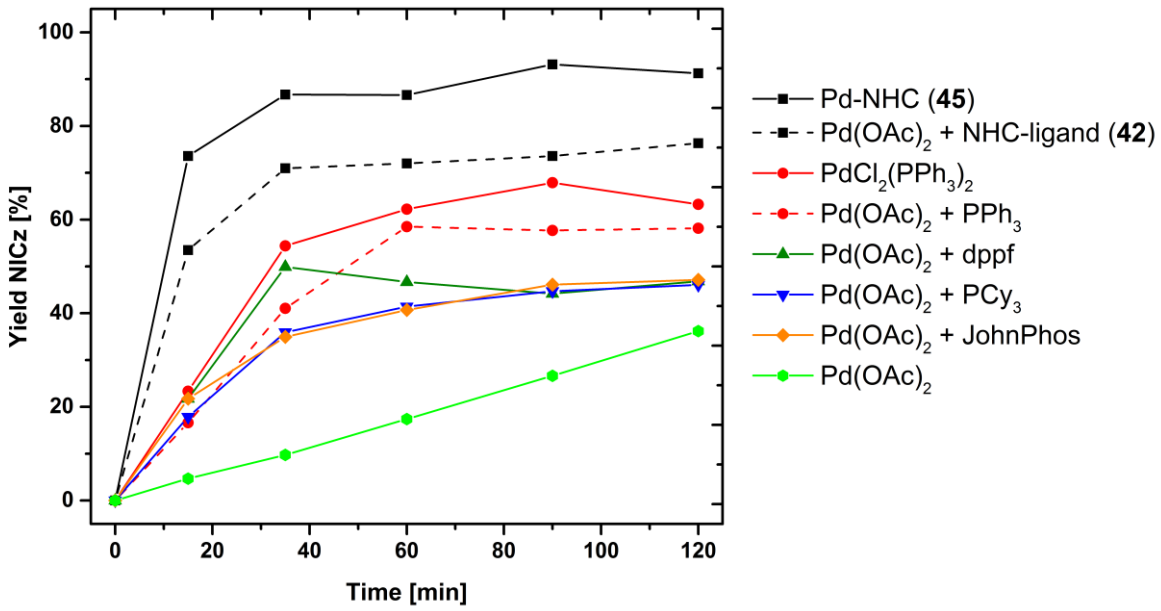

Figure C.03: Results of the screening showing yields of NICz (**XXXIII**) for different catalysts and ligands. Reaction conditions: 10% catalyst and 12% (NHC, dppf) respectively 22% (PPh_3, PCy_3*BF_4, JohnPhos) ligand, 2 eq. K_2CO_3 in DMA (3000 ppm H_2O) at 130 °C.

Table C.03: Results of the screening of different catalyst systems for CHA towards **XXXIII**.

Catalyst[a]	*Ligand*	*Time [min]*[d]	*NICz [%]*	*PyrCz [%]*
(NHC)Pd(allyl)Cl (**45**)	-	60	**93**	7
$Pd(OAc)_2$	NHC (**42**)[b]	120 (91%)	**76**	8
$PdCl2(PPh_3)_2$	-	60	**68**	23
$Pd(OAc)_2$	PPh_3[c]	60	**58**	20
$Pd(OAc)_2$	dppf[b]	35	**50**	25
$Pd(OAc)_2$	PCy_3*BF_4[c]	120 (65%)	**47**	36
$Pd(OAc)_2$	JohnPhos[c]	120 (97%)	**47**	30
$Pd(OAc)_2$	-	120 (71%)	**36**	7

[a] 10%. [b] 12%. [c] 22%. [d] Reaction time until conversion >97% or conversion after 120 min in brackets.

The use of NHC based catalyst **45** gave product yields over 90%, however applying NHC-ligand **42** in combination with $Pd(OAc)_2$ resulted in both lower product yield and increased reaction times. Lower yields were observed for $PdCl_2(PPh_3)_2$ as well as $Pd(OAc)_2$ in combination with PPh_3, at similar conversion rate. Generally the use of phosphine based catalysts resulted in lower product yields due to increased side reaction towards dehalogenated byproduct **46** (figure C.04). Especially application of ligands JohnPhos (structure see scheme C.23) and PCy_3 resulted in significantly increased reaction times and more than 30% of byproduct.

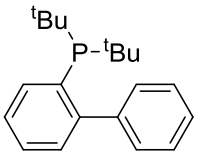

Scheme C.23: Chemical structure of phosphine ligand JohnPhos.

Applying $Pd(OAc)_2$ without any ligand still resulted in slow product formation. In contrast to the other catalytic systems product formation with $Pd(OAc)_2$ as a function of the time exhibits a linear dependence.

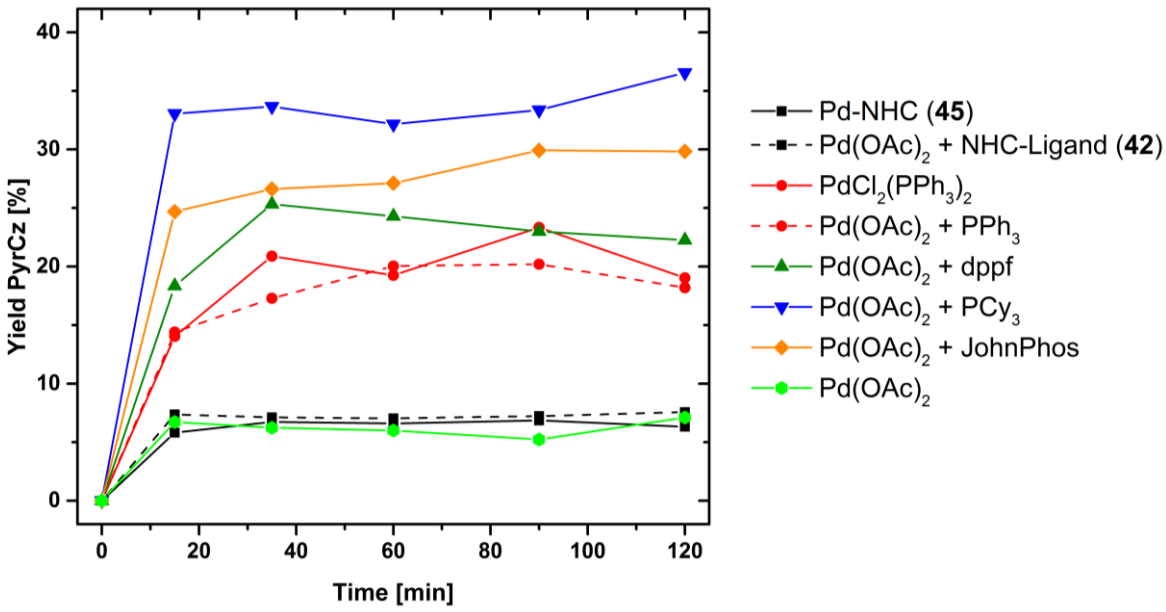

Figure C.04: Formation of side product PyrCz (**46**) for different catalysts. Reaction conditions: 10% catalyst and 12% (NHC, dppf) respectively 22% (PPh_3, PCy_3*BF_4, JohnPhos), 2 eq. K_2CO_3 in DMA (3000 ppm H_2O) at 130 °C.

C.3.2.2 Additives

$BnEt_3NCl$ has been applied as additive for the synthesis of ICz by Lv et al.[27] and pivalic acid (PivOH) is reported in literature to enhance proton transfer and therefore supports cleavage of the C-H bonds in CHA reactions.[59] Thus, the influence of these two additives on the reaction towards NICz was examined using $Pd(OAc)_2$ and PPh_3. Although the reaction applying PivOH as additive started slightly slower, there was no significant influence of the investigated additives on the results of the reactions (see figure C.05).

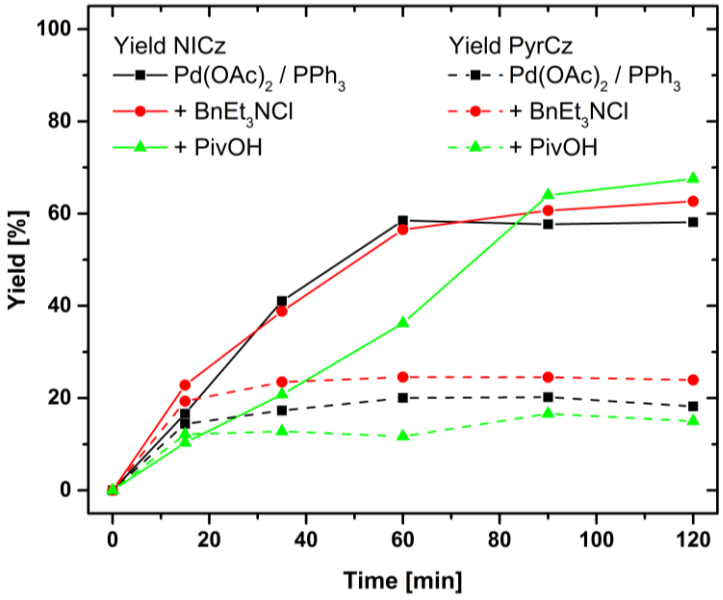

Figure C.05: Influence of different additives on product (NICz) and byproduct (PyrCz) formation using 10% $Pd(OAc)_2$ with 22% PPh_3, 1 eq. $BnEt_3NCl$ or 30% PivOH, 2 eq. K_2CO_3 in DMA at 130 °C.

C.3.2.3 Bases and solvents

Based on the prior results different bases were tested using Pd-NHC (10mol%) as catalyst. As the reaction performed quite well using K_2CO_3, its analog Na_2CO_3 was used to investigate in which extent the use of weaker base influences the outcome. Furthermore, K_3PO_4 was investigated as non-carbonate base and Et_3N to secure a homogenous reaction. The results of these experiments are outlined in figure C.06 and table C.04. As it was expected the use of Na_2CO_3 increased the reaction time. While it had no influence on the yield, the reaction time was tripled (180 min). In contrast reactions applying K_3PO_4 proceeded as quickly as those using K_2CO_3 (>97% conversion after 60 min), yet the product yield was slightly reduced. Reactions with Et_3N led only to minor product formation.

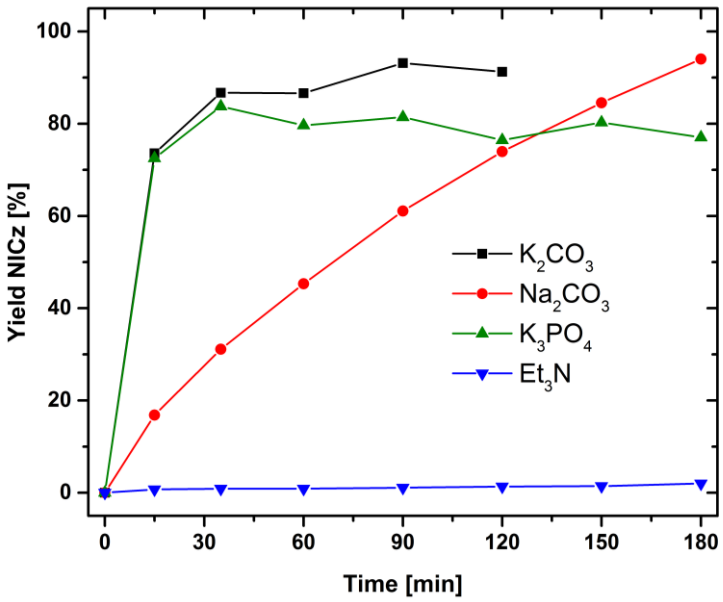

Figure C.06: Product formation using different bases. Reaction conditions: 10% Pd-NHC, 2 eq. base, DMA (3000 ppm H_2O), 130 °C.

Table C.04: Results for experiments applying different bases and solvents with 10% Pd-NHC as catalyst.

Base (2 eq.)	***Solvent***	***Time***	***NICz [%]***	***PyrCz [%]***
K_2CO_3	DMA[a]	60 min[c]	93	7
Na_2CO_3	DMA[a]	180 min[c]	94	2
K_3PO_4	DMA[a]	60 min[c]	84	6
Et_3N	DMA[a]	20 h[d]	10	6
K_2CO_3	toluene[b]	24 h[d]	17	1
K_2CO_3	dioxane[b]	24 h[d]	21	2

[a] 130 °C. [b] 110 °C. [c] Conversion >97%. [d] Reaction aborted.

Furthermore, different solvents were investigated. However, both toluene and dioxane gave only minor product yields (see table C.04). These investigations clearly revealed that the use of Pd-NHC (**45**), K_2CO_3 in DMA (3000 ppm H_2O) is best. Therefore, the next experiments investigated parameters applying these reaction conditions.

C.3.2.4 Pd-NHC amount

Figure C.07 illustrates a comparison of substrate conversion and product formation for different catalyst loadings of Pd-NHC (**45**). While the reaction is basically finished after 1 h with 10mol% of **45**, the use of only 5mol% increased the reaction time to 6 h, lowering the yield of NICz (**XXXIII**) to 73%. Further reduction of the catalyst amount to 2mol% resulted in a significantly longer reaction time of 20 h to achieve full conversion (93%), giving NICz with 52% yield.

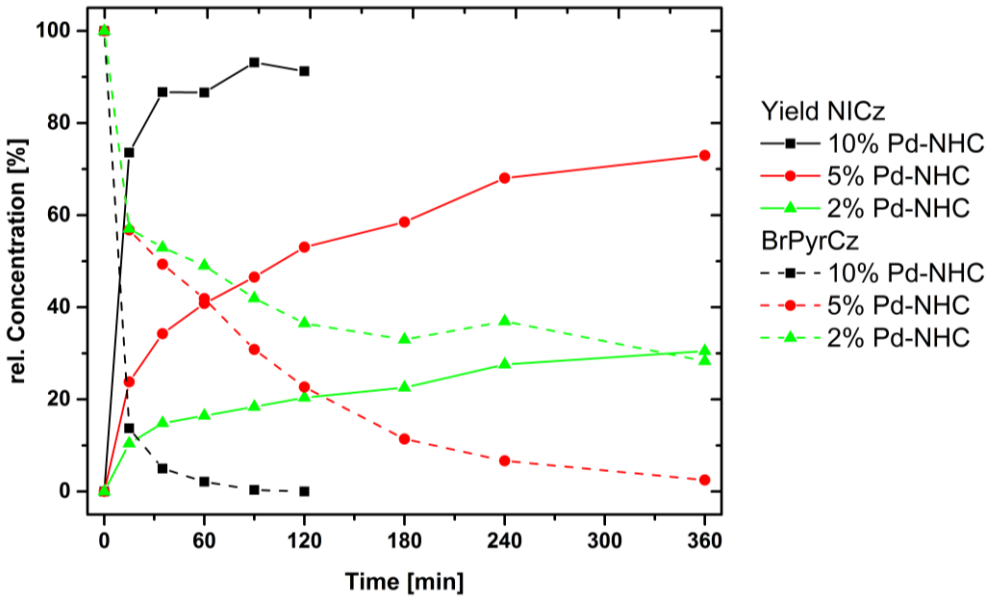

Figure C.07: Substrate concentration (dashed lines) and product yields (full lines) for different amounts of catalyst. Reaction conditions: Pd-NHC, 2 eq. K_2CO_3, DMA, 130 °C.

C.3.2.5 Chlorine substrates

The reactivity towards the chlorine precursor **XXXIIb** (ClPyrCz) was investigated applying Pd-NHC, as well as $PdCl_2(PPh_3)_2$ the most reactive phosphine catalyst in the conversion of **XXXIIa**. The results are illustrated in figure C.08.

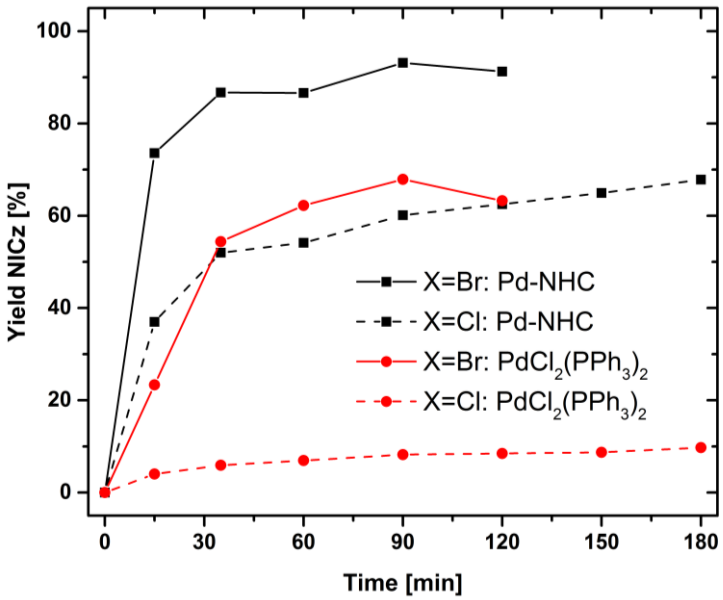

Figure C.08: Product yields for reactions of substrates **XXXIIa** (X=Br) and **XXXIIb** (X=Cl) with Pd-NHC and $PdCl_2(PPh_3)_2$. Reactions performed using 10% catalyst, 2 eq. K_2CO_3, DMA at 130 °C.

While Pd-NHC exhibited approximately the same reactivity towards the chlorine precursor as $PdCl_2(PPh_3)_2$ towards the bromine precursor, the latter gave nearly no product formation with the chlorine substrate. These results further demonstrate the advantages of Pd-NHC, not only as far as yields are concerned, but also for substrate scope of the CHA reaction.

C.3.2.6 Influence of water content and air

As mentioned above a well-defined water content of 3000 ppm was used for the reactions with DMA. To unveil a possible impact of the water amount, reactions using DMA with very low water content (37 ppm and 56 ppm) were investigated. As illustrated in figure C.09 the reactions performed still quite well at these low water concentrations, giving product yields slightly below those of reactions with 3000 ppm water content, but still within the deviations of these experiments. However, it has to be considered that the hygroscopic base K_2CO_3 was not dried prior to the experiments.

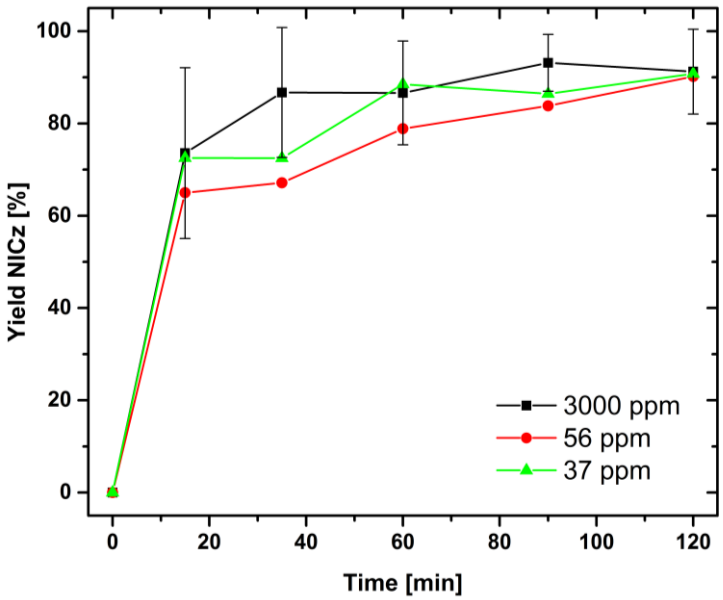

Figure C.09: Yields of NICz for different water contents. Reaction conditions: 10% Pd-NHC, 2 eq. K_2CO_3, DMA at 130 °C.

Furthermore, the influence of oxygen, as well as possible air input during sampling was investigated. For the latter of the experiments each time a sample was taken 1 ml of air was bubbled through the reaction mixture with a syringe. This caused the reaction to slow down and resulted in lower yields as seen in figure C.10. A second experiment was performed without protective atmosphere. The reaction still works under ambient conditions, but with increased reaction times and lower product yields. These findings suggest that the catalytic active species gets partly decomposed in presence of oxygen. The outcome of the experiments illustrates that although protective atmosphere is not strictly necessary for the CHA reaction towards NICz it is still a crucial factor to obtain high yields.

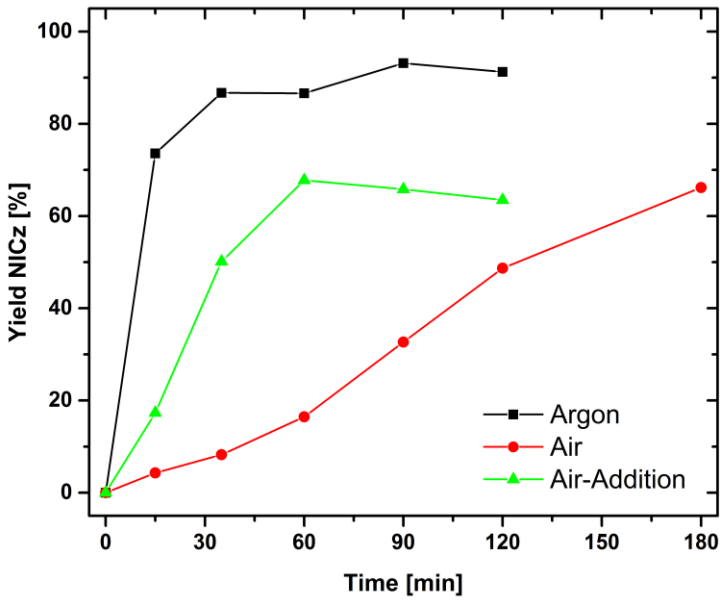

Figure C.10: Yields for **XXXIII** applying 10% Pd-NHC, 2 eq. K_2CO_3 in DMA at 130 °C. Reactions carried out under argon atmosphere (black line), air atmosphere (red line) or argon atmosphere with addition of air during sampling (green line).

C.3.2.7 Conclusion of the screening

The screening clearly showed that the use of Pd-NHC (**45**) with K_2CO_3 in DMA gives by far the best outcome of the reaction owing to a combination of short reaction times, high product yields and only minor side reactions. In contrast the use of phosphine based catalysts occurred to be unfavorable due to increased formation of the side product **46**. Interestingly in all reactions the formation of **46** occurred only at the beginning, suggesting that the side reaction might be involved in the process of catalyst activation.

While the use of solvents different than DMA turned out to be not applicable, different bases, except of Et_3N, showed only minor influence on product formation.

The prior observation during reactions towards ICz, regarding the necessity of a certain water content for the reaction to work smoothly could not be confirmed. Nevertheless the requirement of a certain water content cannot be excluded as the water content of K_2CO_3 was not considered in the reactions. The use of protective atmosphere is an important factor for the reaction, although the reaction also works under ambient atmosphere resulting in lower reactivity and yields.

While the use Na_2CO_3 instead of K_2CO_3 might be an option, as the reaction time is increased in an acceptable extent, the use of lower catalyst amount seemed reasonable, as the catalyst has to be synthesized in a multi-step sequence (see C.6).

C.3.3 Synthesis of NICz

Applying the optimized conditions, ring closure of the carbazole based precursor by CHA was conducted using 5mol% catalyst **45**, 2 eq. K_2CO_3 and DMA (0.01 M) with a water content of 3000 ppm at 130 °C. First reactions were performed in a three necked flask equipped with a condenser. However, these reactions appeared to proceed significantly slower than expected displaying only low conversion after several hours. Though, the reaction could be accelerated when observable condensate in the condenser was flushed into the reaction mixture with additional DMA. A possible explanation for slow conversion was selective removal of water from the reaction mixture due to distillation as result of the significantly lower boiling point of water compared to DMA. Thus, reactions were performed using vials that were sealed with a septum to avoid potential removal of water from the reaction mixture. Applying this setup ring closure of the precursors **XXXIIa**, **XXXIIb** and **XXXV** gave the corresponding NICz isomers in good yields between 70% - 88%. Only the yield of **26** was slightly lower (59%), which is caused by the presence of minor impurities in precursor **XL** (see C.3.1).

Table C.05: Ring closure of carbazole derivatives by CHA towards NICz. Reaction conditions: 5mol% Pd-NHC (**45**), 2 eq. K_2CO_3, DMA (3000 ppm H_2O), 130 °C.

Entry	*Precursor*	*NICz*	*Time [h]*	*Yield [%]*
1	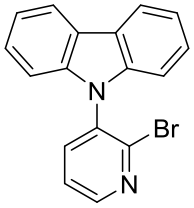 **XXXIIa**	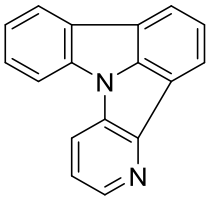 **XXXIII**	8	71
2[a]	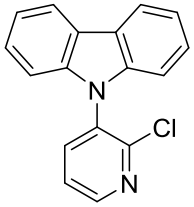 **XXXIIb**	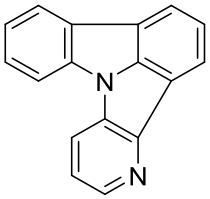 **XXXIII**	2	78
3	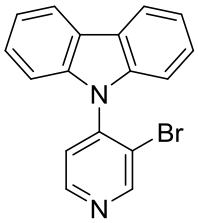 **XXXV**	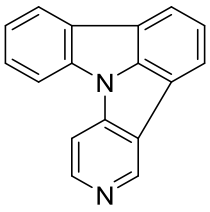 **36**	18	88
4	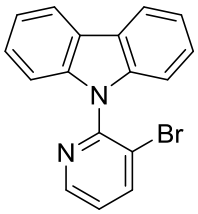 **XL**	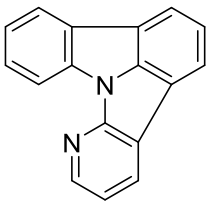 **26**	22	59

[a] Reaction performed in a three necked flask.

C.4 Double sided CHA

Application of the carbazole strategy exclusively allows for the incorporation of the pyridine moiety as a lateral ring (scheme C.24 left). Also the CHA with carboline based precursors gives predominantly these particular isomers (see chapter C.2.2.2). Thus, a different strategy is needed to obtain NICz isomers with the pyridine moiety in the middle ring (scheme C.24 right).

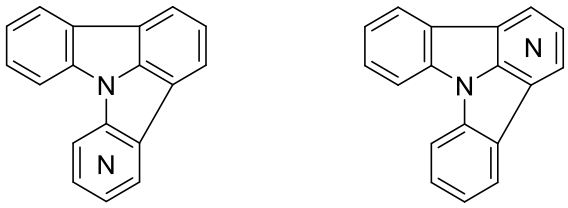

Scheme C.24: Different positions of the pyridine moiety in NICz.

These isomers can be obtained by application of a double sided CHA, as illustrated in scheme C.25. Furthermore, this strategy can be used to synthesize 2NICz derivatives containing two pyridine moieties (TM2 in scheme C.25).

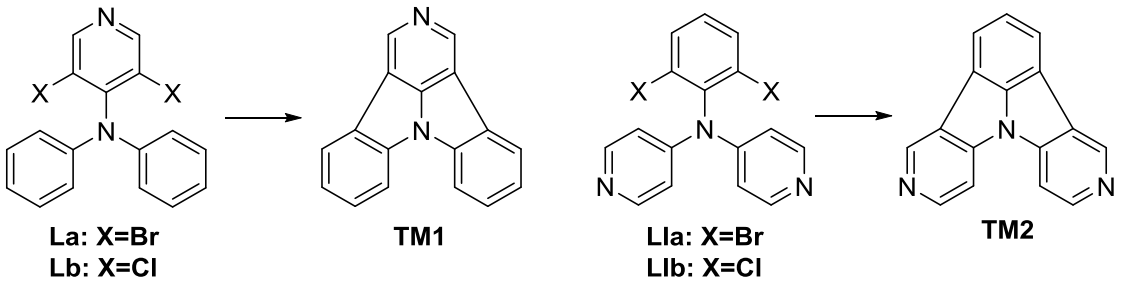

Scheme C.25: Double sided CHA towards **TM1** and **TM2**.

Synthesis of the CHA precursors **L** and **LI** was attempted using the corresponding dihalogenated amines **47** and **49**, as well as iodobenzene (**19**) and 4-iodopyridine (**48**). Amine **47a** was synthesized by twofold bromination of **13** with 2 eq. NBS according to Cañibano[40] with 53% yield. 4-Iodopyridine (**48**) was synthesized by diazotization of amine **13**, followed by reaction with potassium iodide. Caused by the instability of the *in situ* prepared diazonium compound[60] (observable foaming during diazotization), as well as partly decomposition during workup, **48** was isolated in rather poor yields (14%).

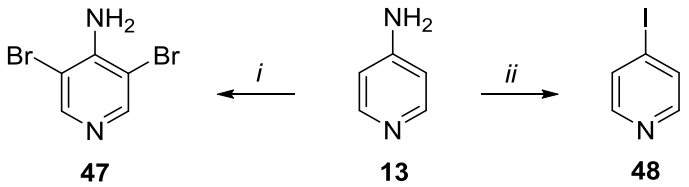

Scheme C.26: Synthesis of compounds **47a** and **48**. *i*: NBS, ACN, r.t., UV-light protection. *ii*: 1. $NaNO_2$, HCl, H_2O, -10 °C; 2. KI, -10 °C – r.t..

For the synthesis towards the dihalogenated precursors **L** and **LI** (scheme C.27) various conditions for Ullmann condensation and Buchwald-Hartwig amination were investigated. Different reaction conditions tested, as well as the results of this screening are outlined in table C.06.

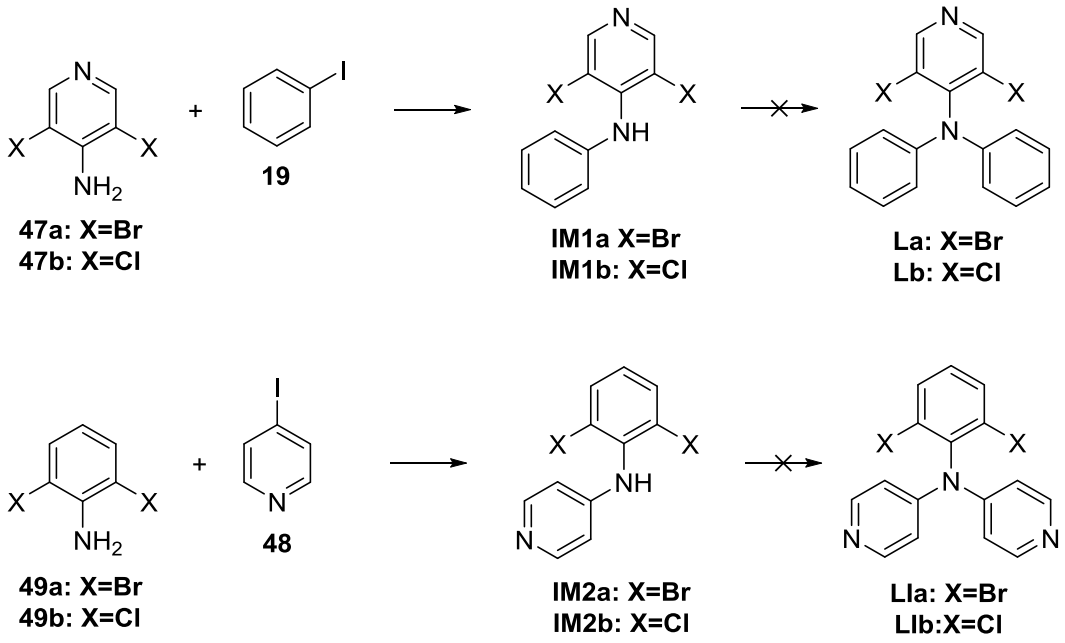

Scheme C.27: Synthesis towards precursors for double sided CHA.

Table C.06: Screening towards precursors for double sided CHA. All reactions were performed in reaction vials stirred in a heating block at 110 °C using 2 ml solvent. Reactions were conducted with 0.05 mmol amine (**47** or **49**), 2.2 eq. of halogen **19**/**48**, 4 eq. base and 10% catalyst.

	substrates	*catalyst*	*base*	*solvent*	*time [h]*	*result* [e]
A	***49a + 48***	Pd-NHC (**45**)	NaO^tBu	toluene	24	-
B	***49a + 48***	$Pd(OAc)_2/PPh_3$	NaO^tBu	toluene	24	-
C	***49a + 48***	$Pd(OAc)_2$/JohnPhos	NaO^tBu	toluene	24	-
D	***49a + 48***	Pd-NHC (**45**)	K_2CO_3	DMA[a]	24	-
E	***47a + 19***	Pd-NHC (**45**)	NaO^tBu	toluene	24	-
F	***49a + 48***	$Pd(OAc)_2$/dppf	NaO^tBu	toluene[b]	48	***IM2a***
G	***49a + 48***	$Pd_2(dba)_3$/dppf	NaO^tBu	toluene	18	***IM2a + LIa (traces)***
H	***49a + 48***	$Pd_2(dba)_3$/dppf	NaO^tBu	dioxane	18	***IM2a***
I	***49b + 48***	$Pd_2(dba)_3$/dppf	NaO^tBu	toluene[b]	48	***IM2b + LIb (traces)***
J	***47b + 19***	$Pd_2(dba)_3$/dppf	NaO^tBu	toluene[b]	48	***IM1b (traces)***
K	***49a + 48***	CuI/DACH	K_3PO_4	toluene	18	***IM2a (traces)***
L	***49a + 48***	CuI/DACH	K_3PO_4	dioxane	18	***IM2a (traces)***
M	***49a + 48***	CuCl/Phen	KOH[c]	toluene	18	-
N	***49b + 48***	CuCl/Phen	KOH[c]	toluene[b]	48	-
O[d]	***47a + 19***	CuCl/Phen	KOH[c]	toluene	188	-
P	***47b + 19***	CuCl/Phen	KOH[c]	toluene[b]	48	-

[a] 130 °C. [b] 3 ml solvent. [c] 8 eq. base. [d] Reaction performed in a three neck flask equipped with a Dean-Stark trap using 1 mmol **47a** and 50 ml toluene. [e] According to GC-MS.

In Buchwald-Hartwig amination reactions starting material was only converted if dppf was applied as ligand. Though, reaction towards **LIa** and **LIb** stopped at the intermediates **IM2a** and **IM2b** respectively and only traces of product formation could be observed,[8] which is probably caused by the steric hindrance of the two halogen substituents on the amine. However, applying the same conditions for the synthesis towards **Lb** only traces of **IM1b** were observed, whereas no product formation was detectable. The use of CuI and 1,2-diaminocyclohexane (DACH) yielded only traces of the intermediates in Ullmann condensations, while no conversion was observed applying CuCl with phenanthroline (Phen).

[8] Reactions were aborted after GC-MS showed no further conversion.

C.5 Functionalization of NICz

For the utilization of NICz in organic electronic applications functionalization of the molecules is a key step in order to incorporate the NICz scaffold into functional organic molecules. First experiments towards bromination of NICz **36** were done applying the same procedure as described for the bromination of ICz[23] using NBS in AcOH/$CHCl_3$ (1:1). The desired product **LII** was obtained with acceptable regioselectivity and 41% yield (crude with approximate 20% impurities according to ^{1}H-NMR).

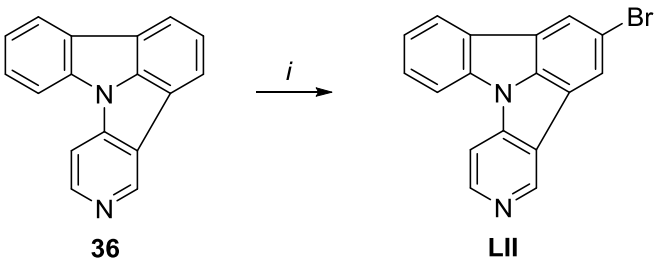

Scheme C.28: Bromination of **36** with NBS. *i*: NBS, AcOH/$CHCl_3$ (1:1), 55 °C.

C.6 Catalyst synthesis

The catalyst (NHC)Pd(allyl)Cl **45** used for CHA reactions was synthesized as depicted in scheme C.29.

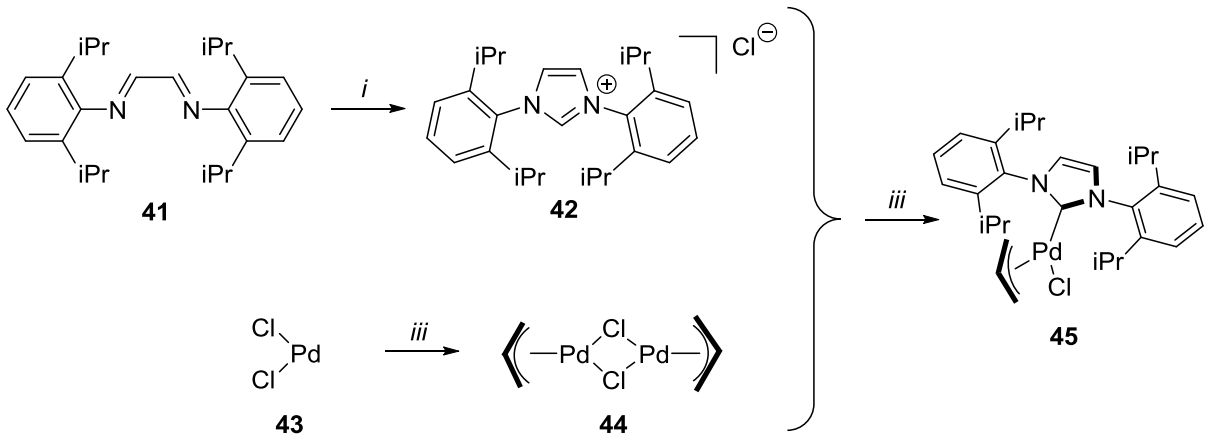

Scheme C.29: Synthesis of catalyst **45**. *i*: 1. paraformaldehyde, toluene, 100 °C; 2. HCl in dioxane, r.t.. *ii*: KCl, H_2O, allyl chloride, r.t.. *iii*: *n*-BuLi, THF, r.t..

According to the procedure by Huang and Nolan[61] imidazolium chloride **42** was isolated in moderate yield (28%) after reaction of diimine **41** with paraformaldehyde in toluene and subsequent acidification with HCl in dioxane. Palladium dimer **44** was prepared according to

the procedure of Marion et al.[62] using $PdCl_2$, KCl and allyl chloride to give **44** as yellow solid with 95% yield. The bench stable Pd-NHC precatalyst **45** was synthesized using a modified protocol from Navarro and Nolan.[63] Addition of **44** to a solution of **42** and *n*-BuLi in THF yielded **45** as slightly yellow solid (77%).

C.7 Summary and outlook

Two different approaches, a carboline and a carbazole strategy, were investigated regarding their applicability in the synthesis of NICz derivatives. In course of these investigations ring closure by diazotization and dehydrogenative ring closing reaction turned out to be not applicable. However, intramolecular arylation by Pd catalyzed CHA became the method of choice. While the corresponding carboline precursors **XXV** and **XXVIII** were obtained in rather low yields, a convenient synthesis towards the carbazole derivatives was developed using a modified Clauson-Kaas reaction.

Detailed investigations on the ring closure by CHA revealed significant impact of the catalytic system on the reaction, especially on byproduct formation. Results from the screening were employed in the synthesis of NICz isomers **26**, **XXXIII** and **36,** which were obtained in good yields from the corresponding carbazole precursors. While CHA could not be applied for α-carboline derivative **XXV**, the conversion of β-carboline derivative **XXVIII** gave a mixture of NICz isomers **XXIX** and **XXX** with limited regioselectivity towards the former isomer (4:1).

A further approach utilizing a double sided CHA could not be realized yet as Ullmann condensation and Buchwald-Hartwig amination towards the corresponding precursors proved to be unsuccessful.

In the future further approaches towards precursors for double sided C-H activation for the remaining NICz isomers as well as additional pyridine incorporation will be investigated. One possible approach are nucleophilic substitution reactions employing arylamines and nitroaryls and subsequent removal of the nitro group by reduction and diazotization (scheme C.30).

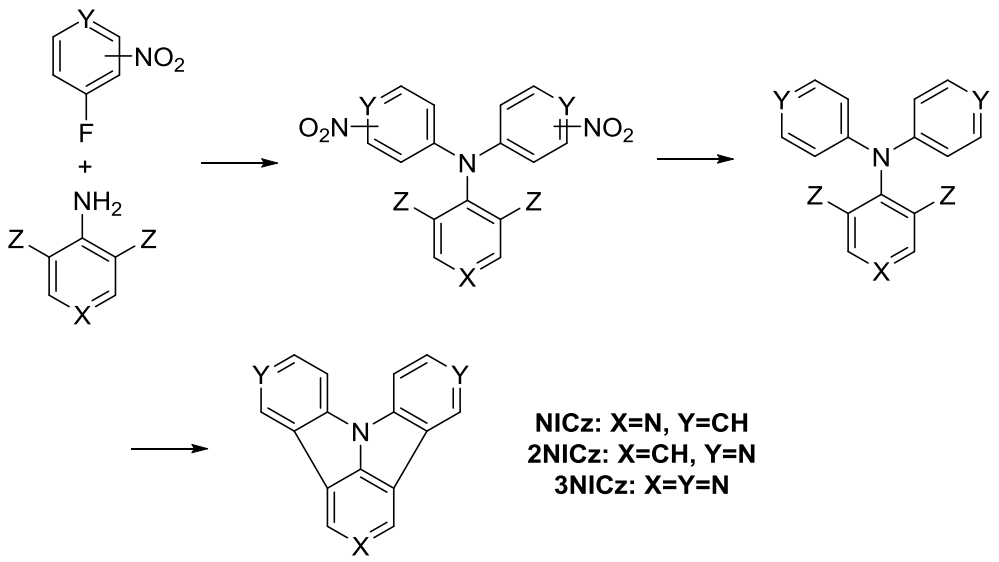

Scheme C.30: Possible synthetic approach towards remaining **NICz** as well as **2NICz** and **3NICz** derivatives.

Furthermore, investigations on the functionalization of NICz will be carried out. Especially adjustment of the reaction conditions to further enhance regioselectivity of the bromination and methods for purification of the obtained compounds will be part of the research. Finally NICz will be incorporated into functional materials like bipolar host materials or electron transporting materials in order to investigate the applicability of NICz in optoelectronic devices (scheme C.31).

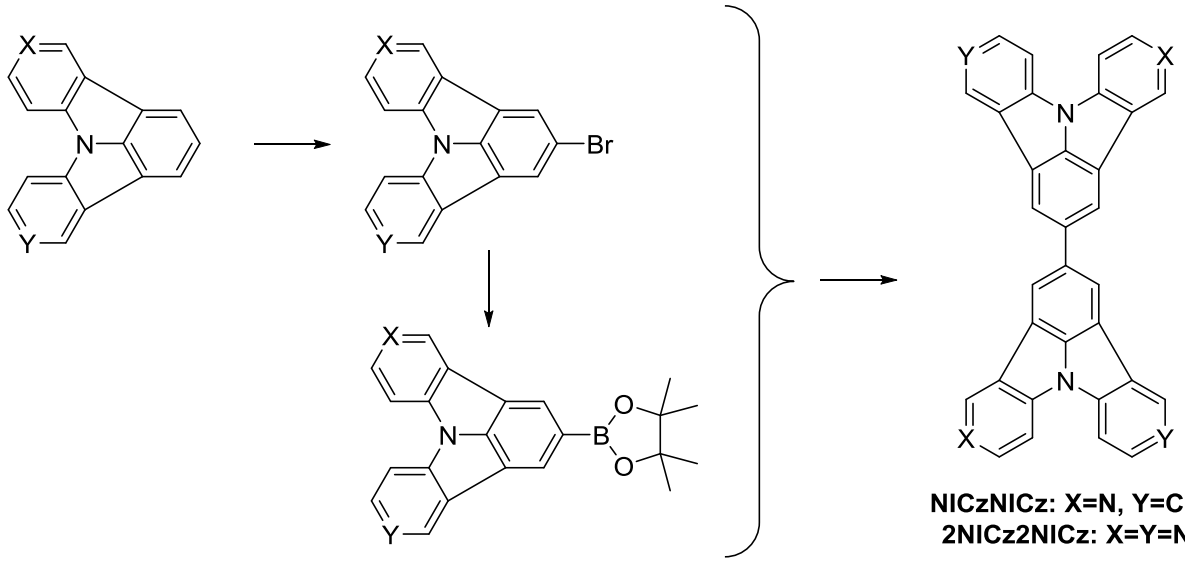

Scheme C.31: Synthetic approach towards **NICzNICz** and **2NICz2NICz** by bromination, followed by lithiation, subsequent quench with boric ester and Suzuki coupling.

D Experimental Part

D.1 General remarks

Unless explicitly mentioned otherwise, all reagents from commercial suppliers were used without further purification. Anhydrous toluene, methanol and THF were absolutized by the *PURESOLV*-system from it-innovative technology inc. Other anhydrous solvents were purchased from commercial suppliers. The commercially available lithiation reagent *n*-BuLi was used without additional quantitative analyses, using the declared value.

Water content of DMA (Sigma Aldrich, puriss. p.a., ≥ 99.5%, stored over molecular sieve) for CHA reactions was adjusted by addition of precise water amounts (gravimetric) to DMA with known water content (determined by Karl Fischer titration prior to use).

D.2 Chromatographic methods

D.2.1 Thin layer chromatography

Thin layer chromatography (TLC) was performed using TLC-aluminum foil (Merck, silica gel 60 F_{254}).

D.2.2 Column chromatography

Preparative column chromatography was performed using a *Büchi Sepacore™ Flash system* which was equipped with the following components:

- Pump-system: 2 *Büchi* pump modules C-605
  Büchi pump manager C-615
- Detector: *Büchi* UV photometer C-635
- Fraction collector: *Büchi* fraction collector C-660

The appropriate PP-cartridges were packed with silica gel (Merck, 40-63 µm).

D.3 Analytical methods

D.3.1 GC-MS measurements

GC-MS measurements were conducted *via* a GC-MS interface from Thermo Scientific™:

- TRACE™ 1300 Gas Chromatograph with a Restek® Rxi®-5Sil MS column (l= 30 m, ID= 0.25 mm, 0.25 µm film, achiral).
- ISQ™ LT Single Quadrupole Mass Spectrometer (electron ionization EI).

D.3.2 GC measurements

GC measurements were accomplished using a TRACE™ 1310 Gas Chromatograph from *Thermo Scientific™* with dual configuration consisting of two AS 1310 autosamplers, *Thermo Scientific™* TR-5MS columns (l= 15 m, ID= 0.25 mm, 1.0 µm film, achiral) and FID detectors (distinguished as front and back FID).

D.3.3 NMR spectroscopy

NMR spectra were recorded using a *Bruker DPX-200* (200 MHz for ^{1}H) or an *Avance DRX-400* (400 MHz for ^{1}H; 100 MHz for ^{13}C) Fourier transform spectrometer. ^{1}H- and ^{13}C-spectra are given as stated: chemical shift in parts per million (ppm) referenced to the according solvent (^{1}H: $CDCl_3$ δ = 7.26 ppm, CD_2Cl_2 δ= 5.32, DMSO-d_6 δ= 2.50 ppm; ^{13}C: $CDCl_3$ δ= 77.0 ppm, CD_2Cl_2 δ= 54.0, DMSO-d_6 δ= 39.5) with tetramethylsilane (TMS) at δ= 0 ppm. Multiplicities of the signals are given as: ^{1}H: s = singlet, d = doublet, t = triplet and m = multiplet.

D.3.4 Karl Fischer titration

Water content of DMA was determined by Karl-Fischer titration using a *Mitsubishi CA-21 Moisture Meter.*

D.4 Microwave assisted reactions

Reactions under microwave irradiation were performed using a *BIOTAGE Initiator EXP EU 355301.*

D.5 Synthesis and characterization of the compounds

Detailed experimental procedures for the synthesis of each compound as well as their characterization are presented in the following chapter.

D.5.1 Synthesis of carbolines

1-(Pyridin-2-yl)-1*H*-benzo[d][1,2,3]triazole (3)

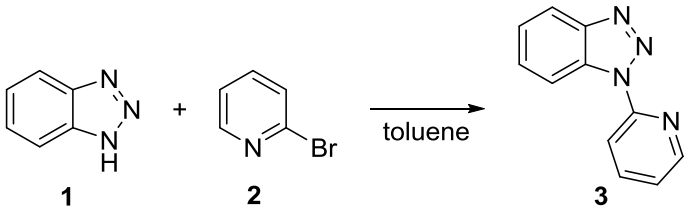

1	**2**	**3**
$C_6H_5N_3$	C_5H_4BrN	$C_{11}H_8N_4$
119,13	158,00	196,21

The synthesis of **3** was done according to Katritzky and Wu.[33]

To a solution of benzotriazole (**1**) (35.74 g, 300 mmol, 2 eq.) in 150 ml anhydrous toluene 2-bromopyridine (**2**) (23.70 g, 150 mmol, 1 eq.) was added. The reaction mixture was heated to reflux for 22 h until full conversion (according to TLC). The reaction mixture was cooled and dissolved in EA and 2 N NaOH. After separation of the phases the organic layer was washed with 2 N NaOH and the aqueous phase was extracted with EA three times. The combined organic layers were washed with sat. aq. NaCl, dried over Na_2SO_4 and concentrated under reduced pressure yielding **3** (28.24 g, 144 mmol, 96%) as white solid.

^{1}H NMR (400 MHz, $CDCl_3$, FID THK118/20): δ= 8.65 (ddd, J= 8.6 Hz, 1.0 Hz, 1.0 Hz, 1H), 8.60 (ddd, J= 5.1 Hz, 2.0 Hz, 0.8 Hz, 1H), 8.30 (ddd, J= 8.2 Hz, 1.0 Hz, 1.0 Hz, 1H), 8.12 (ddd, J= 8.2 Hz, 1.0 Hz, 1.0 Hz, 1H), 7.92 (ddd, J= 8.2 Hz, 7.4 Hz, 2.0 Hz, 1H), 7.60 (ddd, J= 8.6 Hz, 7.0 Hz, 1.2 Hz, 1H), 7.45 (ddd, J= 8.2 Hz, 7.0 Hz, 1.2 Hz, 1H), 7.31 (ddd, J= 7.4 Hz, 5.1 Hz, 1.0 Hz, 1H) ppm.

^{13}C NMR (100 MHz, $CDCl_3$, FID THK118/21): δ= 151.7, 148.3, 146.7, 138.8, 131.5, 128.7, 124.9, 122.2, 119.7, 114.8, 114.4 ppm.

9*H*-Pyrido[2,3-*b*]indole / α-carboline (4)

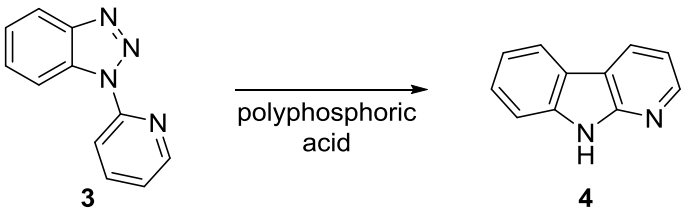

3
$C_{11}H_8N_4$
196,21

4
$C_{11}H_8N_2$
168,20

Synthesis of **4** followed the procedure described by Witkop.[34]

3 (28.25 g, 144 mmol, 1 eq.) was mixed with polyphosphoric acid (226 g, 2304 mmol, 16 eq.) in a three necked flask. The reaction mixture was heated slowly to 120 °C oil bath temperature. After 15 min the viscosity of the mixture was lowered allowing for magnetic stirring. Subsequently, the oil bath temperature was raised to 130 °C – 140 °C. As soon as foam formation could be observed the flask was removed from the oil bath to avoid a runaway reaction. Once no further foam formation was visible the reaction mixture was heated 3 hours at 130 °C – 140 °C oil bath temperature. The cooled reaction mixture was diluted with water and filtrated. 4 N NaOH was added to the filtrate to give basic pH. The resulting white precipitate was filtered and dried *in vacuo*. Crystallization from toluene yielded **4** (7.34 g, 44 mmol, 30%) as beige crystals.

^{1}H NMR (400 MHz, DMSO-d_6, FID THK119/60): δ= 11.79 (bs, 1H), 8.49 (dd, J= 7.8 Hz, 1.6 Hz, 1H), 8.41 (dd, J= 4.7 Hz, 1.6 Hz, 1H), 8.15 (d, J= 7.8 Hz, 1H), 7.51 (d, J= 8.2 Hz, 1H), 7.45 (ddd, J= 8.2 Hz, 6.9 Hz, 1.2 Hz, 1H), 7.24-7.18 (m, 2H) ppm.

^{13}C NMR (100 MHz, DMSO-d_6, FID THK119/61): δ= 151.9, 146.0, 138.8, 128.3, 126.5, 121.1, 120.3, 119.3, 115.1, 114.9, 111.2 ppm.

2,3,4,9-Tetrahydro-1*H*-pyrido[3,4-*b*]indole-3-carboxylic acid (6)

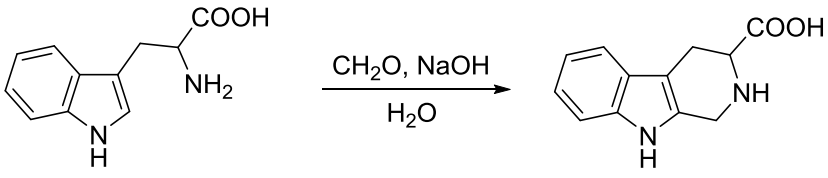

5
$C_{11}H_{12}N_2O_2$
204,23

6
$C_{12}H_{12}N_2O_2$
216,24

Compound **6** was synthesized according to Lippke et al.[35]

To *DL*-tryptophane (**5**) (6.13 g, 30 mmol, 1 eq.) aq. sodium hydroxide solution (1.20 g NaOH, 30 mmol, 1 eq., in 20 ml H_2O) was added and the reaction mixture was stirred until the solid was completely dissolved. After addition of formaldehyde (2.44 g formalin (37wt% formaldehyde in H_2O), 30 mmol, 1 eq.) the reaction was stirred 1 h at r.t. and subsequently heated to reflux for 2 h. To the cooled reaction mixture 6 N HCl was added to give pH ~6. The resulting solid was filtered, washed with H_2O, MeOH, DCM and dried *in vacuo* yielding **6** (4.49 g, 21 mmol, 69%) as light yellow solid.

^{1}H NMR (400 MHz, DMSO-d_6, FID THK084/80): δ= 11.18 (s, 1H), 7.41 (d, J= 7.8 Hz, 1H), 7.33 (d, J= 7.8 Hz, 1H), 7.06 (ddd, J= 8.1 Hz, 7.2 Hz, 1.1 Hz, 1H), 6.98 (m, 1H), 4.32-4.24 (m, 2H), 3.68 (dd, J= 10.4 Hz, 4.9 Hz, 1H), 3.15 (dd, J= 16.2 Hz, 4.9 Hz, 1H), 2.85 (dd, J= 16.0 Hz, 10.5 Hz, 1H) ppm.[9]

^{13}C NMR (100 MHz, DMSO-d_6, FID THK084/81): δ= 170.2, 136.3, 127.8, 126.2, 121.2, 118.6, 117.7, 111.2, 106.5, 56.5, 40.4, 22.9 ppm.

9*H*-Pyrido[3,4-*b*]indole / β-carboline (7)

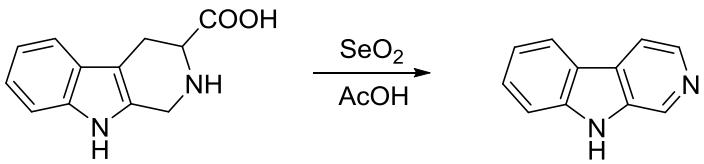

6
$C_{12}H_{12}N_2O_2$
216,24

7
$C_{11}H_8N_2$
168,20

The synthesis of **7** was done according to Xin et al.[37]

To a mixture of **6** (649 mg, 3 mmol, 1 eq.) and SeO_2 (666 mg, 6 mmol, 2 eq.) 15 ml acetic acid was added and the reaction mixture was heated to reflux for 24 h. The reaction mixture was poured into 100 ml ice/water. Afterwards 2 N NaOH was added to give alkaline pH and the mixture was extracted with EA (4x 50 ml). The combined organic layers were washed with sat. aq. NaCl, dried over Na_2SO_4 and the solvent was removed under reduced pressure. **7** was isolated as orange solid (256 mg, 1.52 mmol, 51%).

^{1}H NMR (400 MHz, DMSO-d_6, FID THK113/50): δ= 11.62 (bs, 1H), 8.92 (s, 1H), 8.34 (d, J= 5.5 Hz, 1H), 8.23 (d, J= 8.2 Hz, 1H), 8.09 (dd, J= 5.1 Hz, 1.1 Hz, 1H), 7.60 (d, J= 8.2 Hz, 1H), 7.54 (ddd, J= 8.2 Hz, 7.0 Hz, 1.2 Hz, 1H), 7.24 (ddd, J= 7.8 Hz, 7.0 Hz, 1.2 Hz, 1H) ppm.

^{13}C NMR (100 MHz, DMSO-d_6, FID THK113/51): δ= 140.5, 138.1, 136.0, 134.0, 128.1, 127.4, 121.7, 120.6, 119.2, 114.6, 111.9 ppm.

[9] Two protons were not detected.

N-Acetyl-3-bromo-4-piperidone, hydrobromide (9)

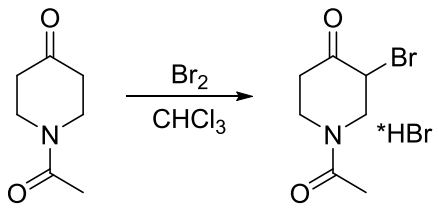

8
$C_7H_{11}NO_2$
141,17

9
$C_7H_{11}Br_2NO_2$
300,98

Compound **9** was prepared according to Denonne et al.[64]

To a solution of 1-acetyl-4-piperidone **8** (4.24 g, 30 mmol, 1 eq.) in 80 ml $CHCl_3$, bromine (5.27 g, 33 mmol, 1.1 eq.) in 5 ml $CHCl_3$ was added slowly at 0 °C. The reaction mixture was stirred for 5 min at 0 °C. Subsequently, the ice/water bath was removed and the reaction was allowed to warm slowly and was further stirred at r.t. for 2 h. The precipitated white solid was filtered, washed with $CHCl_3$ and dried *in vacuo* yielding hydrobromide **9** (7.92 g, 26 mmol, 88%) as white solid.

5*H*-Pyrido[4,3-*b*]indole / γ-carboline (11)

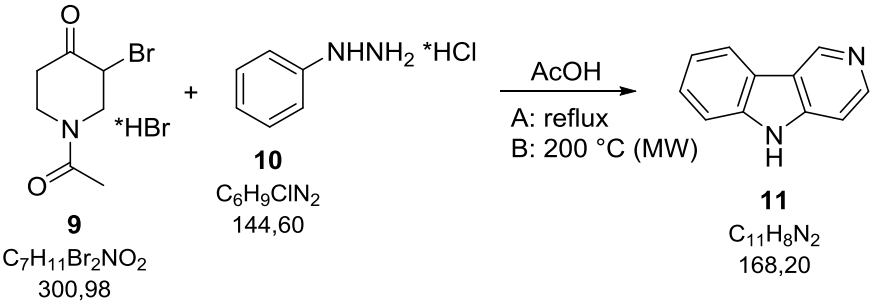

9
$C_7H_{11}Br_2NO_2$
300,98

10
$C_6H_9ClN_2$
144,60

11
$C_{11}H_8N_2$
168,20

Synthesis of **11** followed the procedure described by Chen et al.[38]

Conventional method A:

To hydrobromide **9** (5.21 g, 17.30 mmol, 1 eq.) and phenylhydrazine hydrochloride **10** (3.76 g, 26.00 mmol, 1.5 eq.) in a three necked flask equipped with a condenser and a drying tube filled with $CaCl_2$, 100 ml AcOH were added. The reaction mixture was heated to reflux for 24 h. After cooling the reaction mixture was poured into water and 4 N NaOH was added to give basic pH. The mixture was extracted with EA, the organic layers were dried over Na_2SO_4 and concentrated *in vacuo*. The crude product was purified by column

chromatography (120 g SG, DCM:MeOH 1% → 5%) yielding **11** (0.65 g, 3.86 mmol, 22%) as light brown solid.

Microwave enhanced method B

A microwave reactor vial was charged with hydrobromide **9** (1.20 g, 4 mmol, 1 eq.), hydrochloride **10** (868 mg, 6 mmol, 1.5 eq.) and 20 ml AcOH. The vial was capped with a septum and irradiated for 10 min at 200 °C. The reaction mixture was dissolved in 1 N HCl and repeatedly extracted with EA. 2 N NaOH was added to the aqueous phase to give basic pH. The resulting precipitate was filtered and dried. The crude product was flashed over silica gel (DCM:MeOH ~6:1) yielding **11** (239 mg, 1.42 mmol, 36%) as light brown solid.

^{1}H NMR (400 MHz, DMSO-d_6, FID THK108/20): δ= 11.73 (bs, 1H), 9.34 (s, 1H), 8.42 (d, J= 5.9 Hz, 1H), 8.22 (ddd, J= 7.8 Hz, 1.2 Hz, 0.8 Hz, 1H), 7.57 (ddd, J= 8.2 Hz, 1.0 Hz, 0.9 Hz, 1H), 7.49-7.45 (m, 2H), 7.26 (ddd, J= 7.8 Hz, 7.0 Hz, 1.2 Hz, 1H) ppm.

^{13}C NMR (100 MHz, DMSO-d_6, FID THK108/21): δ= 144.4, 143.5, 142.7, 139.5, 126.6, 120.7, 120.6, 120.0, 119.4, 111.4, 106.3 ppm.

***N*-(2-Bromophenyl)-4-pyridinamine (14)**

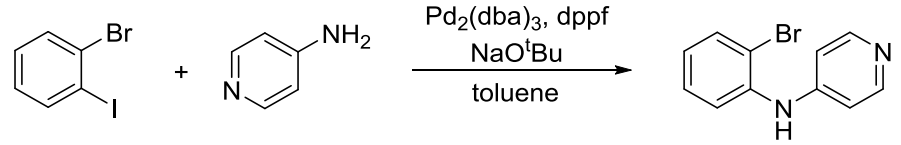

12
C_6H_4BrI
282,91

13
$C_5H_6N_2$
94,12

14
$C_{11}H_9BrN_2$
249,11

Synthesis of **14** was done according to Iwaki et al.[39]

4-Aminopyridine (**13**) (284 mg, 3 mmol, 1 eq.), NaO^{t}Bu (404 mg, 4.2 mmol, 1.40 eq.), $Pd_2(dba)_3$ (28 mg, 0.03 mmol, 1 mol%) and dppf (33 mg, 0.06 mmol, 6 mol%) were suspended in 12 ml anhydrous toluene under argon atmosphere. **12** (1.02 g, 3.60 mmol, 1.20 eq.) was added under argon counterflow. The reaction was heated for 18 h to reflux until full conversion (TLC). The cooled reaction mixture was filtered over celite, washed with Et_2O and concentrated *in vacuo*. Purification *via* column chromatography (40 g SG, DCM:MeOH 1% → 4%) yielded **14** (741 mg, 2.97 mmol, 99%) as grey solid.

^{1}H NMR (400 MHz, $CDCl_3$, FID THK111/30): δ= 8.35 (d, J= 6.2 Hz, 2H), 7.61 (dd, J= 7.8 Hz, 1.6 Hz, 1H), 7.45 (dd, J= 8.2 Hz, 1.6 Hz, 1H), 7.30 (ddd, J= 8.4 Hz, 7.4 Hz, 1.6 Hz, 1H), 6.96 (ddd, J= 8.2 Hz, 7.4 Hz, 1.6 Hz, 1H), 6.88 (dd, J= 5.2 Hz, 1.6 Hz, 2), 6.30 (bs, 1H) ppm.

^{13}C NMR (100 MHz, $CDCl_3$, FID THK111/31): δ= 150.6, 149.4, 137.9, 133.4, 128.2, 124.7, 121.2, 116.2, 110.4 ppm.

5*H*-Pyrido[4,3-*b*]indole / γ-carboline (11)

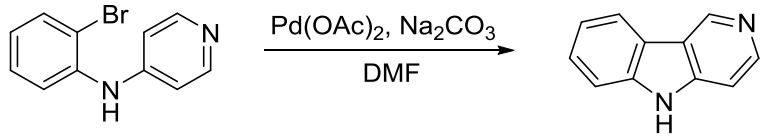

14
$C_{11}H_9BrN_2$
249,11

11
$C_{11}H_8N_2$
168,20

Synthesis of **11** followed the procedure according to Iwaki et al.[39]

A reaction vial was charged with **14** (199 mg, 0.80 mmol, 1 eq.), Na_2CO_3 (119 mg, 1.12 mmol, 1.4 eq.) and $Pd(OAc)_2$ (18 mg, 0.08 mmol, 10 mol%) and flushed with argon. 4 ml degassed DMF were added and the reaction was stirred under argon atmosphere for 24 h at 160 °C until full conversion (TLC). The cooled reaction mixture was diluted with EA, filtered through a celite pad, which was subsequently washed with EA. The filtrate was washed with water and sat. aq. NaCl, dried over Na_2SO_4 and the solvent was evaporated under reduced pressure. Recrystallization from toluene yielded **11** as brown solid (58 mg, 0.34 mmol, 43%).

^{1}H NMR (400 MHz, DMSO-d_6, FID THK108/20): δ= 11.73 (bs, 1H), 9.34 (s, 1H), 8.42 (d, J= 5.9 Hz, 1H), 8.22 (ddd, J= 7.8 Hz, 1.2 Hz, 0.8 Hz, 1H), 7.57 (ddd, J= 7.7 Hz, 1.0 Hz, 0.9 Hz, 1H), 7.49-7.45 (m, 2H), 7.26 (ddd, J= 7.8 Hz, 7.0 Hz, 1.2 Hz, 1H) ppm.

^{13}C NMR (100 MHz, DMSO-d_6, FID THK108/21): δ= 144.4, 143.5, 142.7, 139.5, 126.6, 120.7, 120.6, 120.0, 119.4, 111.4, 106.3 ppm.

N-(2-Bromophenyl)-3-pyridinamine (16)

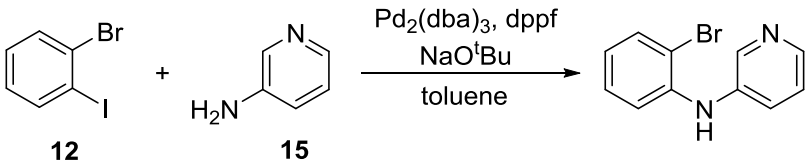

12
C_6H_4BrI
282,91

15
$C_5H_6N_2$
94,12

16
$C_{11}H_9BrN_2$
249,11

Synthesis of **16** was done according to Iwaki et al.[39]

3-Aminopyridine (**15**) (95.8 mg, 1.02 mmol, 1 eq.), **12** (340 mg, 1.20 mmol, 1.2 eq.), NaO^tBu (135 mg, 1.40 mmol, 1.4 eq.), $Pd_2(dba)_3$ (9 mg, 0.01 mmol, 1 mol%) and dppf (11 mg,

0.02 mmol, 2 mol%) were weighed in a glass vial and flushed with argon. 4 ml of degassed anhydrous toluene were added and the reaction was stirred for 21 h until full conversion according to TLC. After cooling to r.t., the reaction mixture was filtered through a celite pad, washed with Et_2O and the solvent was evaporated under reduced pressure. Purification *via* flash chromatography (8 g SG, PE:EA 3:1) gave **16** (229 mg, 0.92 mmol, 90%) as light yellow oil.

^{1}H (400 MHz, CD_2Cl_2, FID THK109/30): δ= 8.45 (d, J= 2.0 Hz, 1H), 8.25 (d, J= 3.9 Hz, 1H), 7.57 (dd, J= 8.6 Hz, 0.8 Hz, 1H), 7.47 (ddd, J= 8.3 Hz, 2.6 Hz, 1.3 Hz, 1H), 7.25-7.19 (m, 3H), 6.86-6.79 (m, 1H), 6.15 (bs, 1H) ppm.

^{13}C (100 MHz, CD_2Cl_2, FID THK109/31): δ= 144.1, 142.7, 141.2, 139.0, 133.7, 128.9, 126.6, 124.3, 122.6, 117.0, 113.5 ppm.

5*H*-Pyrido[3,2-*b*]indole / δ-carboline (17)

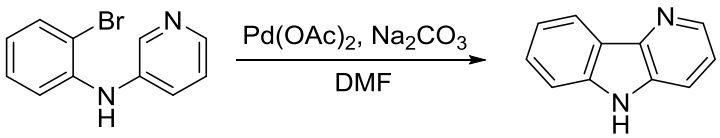

16
$C_{11}H_9BrN_2$
249,11

17
$C_{11}H_8N_2$
168,20

17 was prepared according to Iwaki et al.[39]

16 (250 mg, 1 mmol, 1 eq.), Na_2CO_3 (148 mg, 1.4 mmol, 1.4 eq.) and $Pd(OAc)_2$ (23 mg, 0.1 mmol, 10 mol%) were weighed in a glass vial and flushed with argon. 4 ml degassed DMF was added and the reaction was stirred at 160 °C for 116 h until full conversion (GC-MS). The reaction mixture was cooled to r.t., diluted with EA and filtered over a celite pad. The filtrate was washed with H_2O and sat. aq. NaCl, dried over Na_2SO_4 and concentrated *in vacuo*. The crude product was purified by flash chromatography (16 g SG, PE:EA 50% → 75%) yielding **17** (14 mg, 0.08 mmol, 8%).

^{1}H (400 MHz, DMSO-d_6, FID THK124/30): δ= 11.43 (s, 1H), 8.45 (dd, J= 4.7 Hz, 1.2 Hz, 1H), 8.19 (d, J= 7.8 Hz, 1H), 7.88 (dd, J= 8.2 Hz, 1.6 Hz, 1H), 7.57 (ddd, J= 8.2 Hz, 1.2 Hz, 0.8 Hz, 1H), 7.50 (ddd, J= 8.2 Hz, 7.0 Hz, 1.2 Hz, 1H), 7.38 (dd, J= 8.2 Hz, 4.7 Hz, 1H), 7.24 (ddd, J= 7.6 Hz, 7.3 Hz, 1.1 Hz, 1H) ppm.

^{13}C (100 MHz, DMSO-d_6, FID THK124/31): δ= 141.1, 141.1, 140.4, 132.8, 127.3, 121.5, 120.1, 120.0, 119.3, 117.9, 111.6 ppm.

3-Amino-2-bromopyridine (18a)

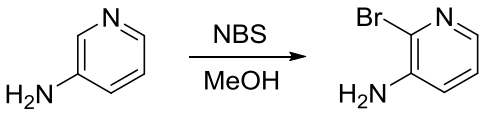

15
$C_5H_6N_2$
94,12

18a
$C_5H_5BrN_2$
173,01

Synthesis of **18a** followed the protocol from Cañibano et al.[40]

3-Aminopyridine (**15**) (4.71 g, 50 mmol, 1eq.) was weighed in a flask and dissolved in 250 ml MeOH. Subsequently, NBS (10.68 g, 60 mmol, 1.2 eq.) was added in small portions and the reaction was stirred for 138 h at r.t. under UV-light protection. The reaction mixture was loaded onto silica gel by evaporation of the solvent under reduced pressure and purified *via* flash chromatography (180 g SG, PE:DCM 55% → 80%) yielding **18a** (3.51 g, 20 mmol, 41%) as red solid.

^{1}H (400 MHz, $CDCl_3$, FID THK116/70): δ= 7.76 (dd, J= 4.3 Hz, 2.0 Hz, 1H), 7.04 (dd, J= 7.8 Hz, 4.3 Hz, 1H), 6.99 (dd, J= 8.0 Hz, 1.8 Hz, 1H), 4.09 (bs, 2H) ppm.

^{13}C (100 MHz, $CDCl_3$, FID THK116/71): δ= 141.4, 139.1, 129.6, 123.6, 121.8 ppm.

2-Bromo-*N*-phenyl-3-pyridinamine (20)

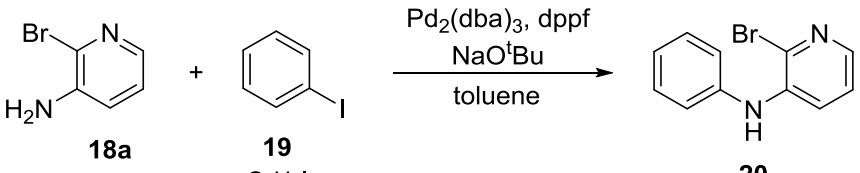

18a
$C_5H_5BrN_2$
173,01

19
C_6H_5I
204,01

20
$C_{11}H_9BrN_2$
249,11

Preparation of **20** followed the procedure from Iwaki et al.[39]

A three necked flask was charged with **18a** (2.77 g, 16 mmol, 1 eq.), NaO^tBu (2.15 g, 22.4 mmol, 1.4 eq.), $Pd_2(dba)_3$ (147 mg, 0.16 mmol, 1 mol%) and dppf (177 mg, 0.32 mmol, 2 mol%) and subsequently flushed with argon. 64 ml degassed anhydrous toluene and iodobenzene (**19**) (3.92 g, 19.2 mmol, 1.2 eq.) were added through a septum and the reaction was refluxed under argon atmosphere for 40 h. The reaction mixture was then cooled to r.t., filtered through a celite pad and washed with Et_2O. After evaporation of the solvent *in vacuo* the crude product was purified *via* flash chromatography (120 g SG, PE:EA 10% → 20%) yielding **20** (1.83 g, 7.3 mmol, 46%) as light brown solid.

^{1}H (400 MHz, $CDCl_3$, FID THK123/20): δ= 7.85 (dd, J= 4.7 Hz, 1.6 Hz, 1H), 7.43 (dd, J= 8.0 Hz, 1.8 Hz, 1H), 7.39-7.34 (m, 2H), 7.18-7.07 (m, 4H), 6.16 (bs, 1H) ppm.

^{13}C (100 MHz, $CDCl_3$, FID THK123/21): δ= 140.0, 139.9, 139.3, 131.8, 129.7, 123.9, 123.3, 121.2, 121.0 ppm.

5*H*-Pyrido[3,2-*b*]indole / δ-carboline (17)

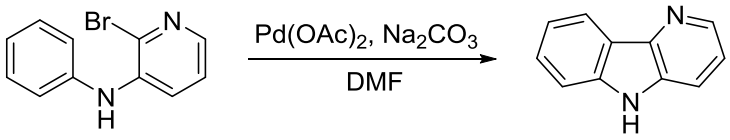

20
$C_{11}H_9BrN_2$
249,11

17
$C_{11}H_8N_2$
168,20

Synthesis of **17** was done according to Iwaki et al.[39]

A glass vial was charged with **20** (249 mg, 1 mmol, 1 eq.), Na_2CO_3 (148 mg, 1.4 mmol, 1.4 eq.) and $Pd(OAc)_2$ (22 mg, 0.1 mmol, 10 mol%) and subsequently flushed with argon. 4 ml degassed DMF was added and the reaction was stirred under argon atmosphere for 24 h at 160 °C until full conversion according to GC-MS. The cooled reaction mixture was diluted with EA and flashed through a celite pad. The filtrate was washed with H_2O and sat. aq. NaCl, dried over Na_2SO_4 and concentrated under reduced pressure. The crude product was purified *via* column chromatography (8 g SG, PE:EA 40% → 70%). **17** (65 mg, 0.39 mmol, 39%) was obtained after crystallization from toluene as green solid.

^{1}H (400 MHz, DMSO-d_6, FID THK124/30): δ= 11.43 (s, 1H), 8.45 (dd, J= 4.7 Hz, 1.2 Hz, 1H), 8.19 (d, J= 7.8 Hz, 1H), 7.88 (dd, J= 8.2 Hz, 1.6 Hz, 1H), 7.57 (ddd, J= 8.2 Hz, 1.2 Hz, 0.8 Hz 1H), 7.50 (ddd, J= 8.2 Hz, 7.0 Hz, 1.2 Hz, 1H), 7.38 (dd, J= 8.2 Hz, 4.7 Hz, 1H), 7.24 (ddd, J= 7.6 Hz, 7.3 Hz, 1.1 Hz, 1H) ppm.

^{13}C (100 MHz, DMSO-d_6, FID THK124/31): δ= 141.1, 141.1, 140.4, 132.8, 127.3, 121.5, 120.1, 120.0, 119.3, 117.9, 111.6 ppm.

D.5.2 Synthesis of carboline derivatives

9-(2-Nitrophenyl)-9*H*-pyrido[2,3-*b*]indole (XXII)

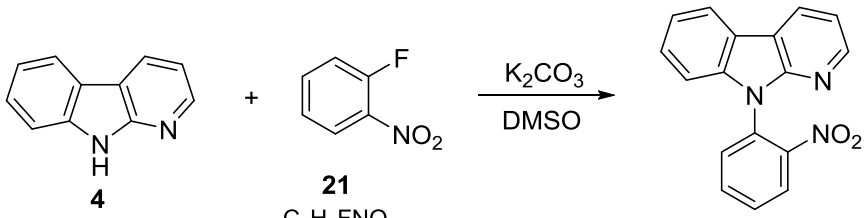

4
$C_{11}H_8N_2$
168,20

21
$C_6H_4FNO_2$
141,10

XXII
$C_{17}H_{11}N_3O_2$
289,29

The synthesis of **XXII** was done according a modified procedure from Wharton et al.[30]

α-Carboline (**4**) (505 mg, 3 mmol, 1 eq.) was dissolved in 8 ml DMSO. **21** (466 mg, 3.3 mmol, 1.1 eq.) and K_2CO_3 (456 mg, 3.3 mmol, 1.1 eq.) were added and the reaction was stirred for 4 h at 120 °C. The cooled reaction mixture was poured into H_2O and extracted repeatedly with DCM. The combined organic layers were dried over Na_2SO_4 and concentrated *in vacuo*. Purification *via* column chromatography (90 SG, PE:DCM 90% → 100%) gave **XXII** (695 mg, 2.40 mmol, 80%) as yellow solid.

^{1}H (400 MHz, CD_2Cl_2, FID THK102/20): δ= 8.42 (dd, J= 7.8 Hz, 1.6 Hz, 1H), 8.36 (dd, 5.1 Hz, 1.6 Hz, 1H), 8.21 (dd, J= 8.2 Hz, 1.6 Hz, 1H), 8.17 (ddd, J= 7.6 Hz, 1.2 Hz, 0.8 Hz, 1H), 7.87 (ddd, J= 8.0 Hz, 7.6 Hz, 1.5 Hz, 1H), 7.77 (dd, J= 8.1 Hz, 1.5 Hz, 1H), 7.69 (ddd, J= 8.2 Hz, 7.4 Hz, 1.6 Hz, 1H), 7.52 (ddd, J= 7.6 Hz, 7.6 Hz, 1.2 Hz, 1H), 7.41-7.37 (m, 2H), 7.27 (dd, J= 7.6 Hz, 4.9 Hz, 1H) ppm.

^{13}C (100 MHz, CD_2Cl_2, FID THK102/21): δ= 152.2, 147.3, 146.9, 139.9, 134.8, 131.2, 130.5, 129.5, 129.1, 127.9, 126.5, 122.0, 122.0, 121.9, 117.4, 117.1, 110.3 ppm.

2-(9*H*-Pyrido[2,3-*b*]indol-9-yl)aniline (XXIII)

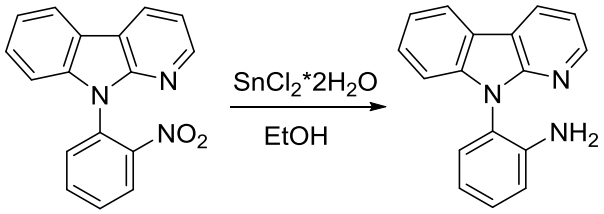

XXII
$C_{17}H_{11}N_3O_2$
289,29

XXIII
$C_{17}H_{13}N_3$
259,31

Preparation of **XXIII** was done according to Dunlop and Tucker.[28]

XXII (1.67 g, 5.8 mmol, 1 eq.) was suspended in 20 ml ethanol. $SnCl_2*2H_2O$ (4.56 g, 20.3 mmol, 3.5 eq.) was added and the mixture was refluxed for 2 h until full conversion (TLC). After the reaction mixture was cooled to r.t. it was poured into H_2O giving a yellow precipitate. 2 N NaOH was added to give basic pH, resulting in a color change to blue. The mixture was extracted three times with DCM. The combined organic layers were washed with H_2O, dried over Na_2SO_4 and concentrated under reduced pressure. After the crude product was flashed over a silica gel pad (DCM:Et_2O 12:1), **XXIII** (1.42 g, 5.48 mmol, 94%) was obtained as brown solid.

^{1}H (400 MHz, CD_2Cl_2, FID THK101/20): δ= 8.46-8.42 (m, 2H), 8.17 (d, J= 7.8 Hz, 1H), 7.48 (ddd, J= 8.2 Hz, 7.4 Hz, 1.2 Hz, 1H), 7.36-7.31 (m, 2H), 7.27-7.22 (m, 3H), 6.98 (dd, J= 8.2 Hz, 1.2 Hz, 1H), 6.92 (ddd, J= 7.8 Hz, 7.4 Hz, 1.2 Hz, 1H), 3.70 (bs, 2H) ppm.

^{13}C (100 MHz, CD_2Cl_2, FID THK101/21): δ= 152.5, 147.1, 145.0, 140.5, 130.2, 130.2, 128.9, 127.5, 122.4, 121.6, 121.5, 121.2, 119.2, 117.5, 116.9, 116.5, 111.2 ppm.

9-(2-Bromophenyl)-9*H*-pyrido[2,3-*b*]indole (XXV)

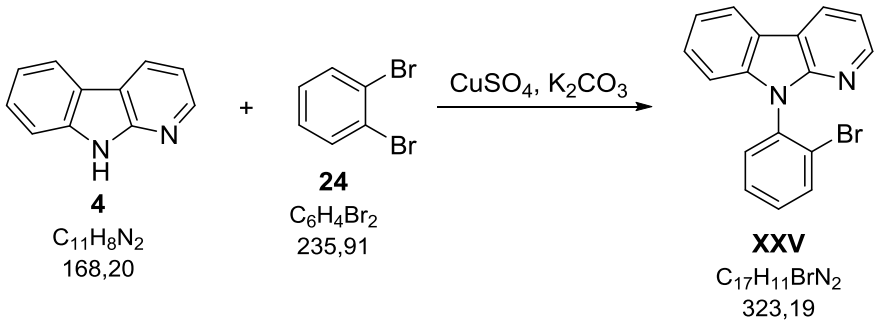

The synthesis of **XXV** followed a modified protocol from Xu et al.[44]

α-Carboline (**4**) (1.68 g, 10 mmol, 1 eq.), K_2CO_3 (1.38 g, 10 mmol, 1 eq.) and $CuSO_4*5H_2O$ (125 mg, 0.5 mmol, 5 mol%) were weighed in a Teflon autoclave and overlaid with **24** (2.83 g, 12 mmol, 1.2 eq.). The autoclave was placed in a steel jacket and heated in an oven for 22 h at 220 °C. After cooling the residue was dissolved in H_2O and DCM. The phases were separated and the aqueous phase was extracted twice with DCM. The combined organic layers were dried over Na_2SO_4 and concentrated *in vacuo*. The crude product was purified by column chromatography (180 g SG, PE:DCM 66% → 75%). Crystallization from ethanol yielded **XXV** (443 mg, 1.37 mmol, 14%) as white crystals.

^{1}H (400 MHz, CD_2Cl_2, FID THK091/120): δ= 8.44-8.42 (m, 2H), 8.17 (d, J= 7.8 Hz, 1H), 7.88 (dd, J= 8.2 Hz, 1.6 Hz, 1H), 7.61-7.53 (m, 2H), 7.50-7.45 (m, 2H), 7.37-7.33 (m, 1H), 7.26 (dd, 7.4 Hz, 5.1 Hz, 1H), 7.11 (ddd, J= 8.2 Hz, 1.2 Hz, 0.8 Hz, 1H) ppm.

^{13}C (100 MHz, CD_2Cl_2, FID THK091/121): δ= 152.7, 147.1, 140.6, 136.3, 134.5, 132.1, 131.0, 129.3, 128.9, 127.5, 124.5, 121.6, 121.4, 121.3, 116.7, 116.7, 110.9 ppm.

9-(2-Bromophenyl)-9*H*-pyrido[3,4-*b*]indole (XXVIII)

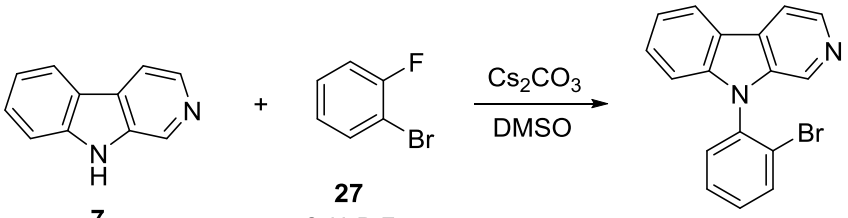

7
$C_{11}H_8N_2$
168,20

27
C_6H_4BrF
175,00

XXVIII
$C_{17}H_{11}BrN_2$
323,19

β-Carboline (**7**) (336 mg, 2 mmol, 1 eq.) and Cs_2CO_3 (717 mg, 2.2 mmol, 1.1 eq.) were weighed in a glass vial. 4 ml DMSO and **27** (350 mg, 2 mmol, 2 eq.) were added and the reaction mixture was stirred for 24 h at 130 °C. After cooling the reaction mixture was poured into H_2O and extracted three times with DCM. The combined organic layers were dried over Na_2SO_4 and concentrated under reduced pressure. After purification *via* flash chromatography (40 g SG, DCM:Et_2O 0% → 5%) **XXVIII** (229 mg, 0.71 mmol, 35%) was obtained as light brown solid.

^{1}H (400 MHz, $CDCl_3$, FID THK191/20): δ= 8.55-8.53 (m, 2H), 8.21 (ddd, J= 7.8 Hz, 1.2 Hz, 0.8 Hz, 1H), 8.03 (dd, J= 5.1 Hz, 1.2 Hz, 1H), 7.89 (dd, J= 7.8 Hz, 1.3 Hz, 1H), 7.59-7.45 (m, 4H), 7.36 (ddd, J= 7.5 Hz, 7.1 Hz, 1.0 Hz, 1H), 7.15 (d, J= 8.6 Hz, 1H) ppm.

^{13}C (100 MHz, $CDCl_3$, FID THK191/21): δ= 141.6, 140.0, 136.8, 135.8, 134.4, 133.3, 130.8, 130.7, 129.0, 128.9, 128.6, 123.4, 121.8, 121.4, 120.7, 114.6, 110.8 ppm.

D.5.3 Synthesis of carbazole derivatives

General procedure 1 (GP1): condensation reaction with 2,5-dimethoxytetrahydrofuran (DMT)

The condensation reactions with **31** were done according to a modified protocol from Lv et al.[27]

To a solution of the corresponding amine in acetic acid (~ 0.07 M) 4 eq. of **31** were added. The reaction was then refluxed under argon atmosphere. Depending on the progress of the reaction (reaction control via GC-MS) fresh DMT (**31**) was added. After full conversion or observation of additional condensation side products the reaction was cooled to r.t., poured into iced 2 N HCl and repeatedly extracted with DCM. The combined organic layers were washed with water and 2 N NaOH, dried over Na_2SO_4 and concentrated *in vacuo*.

9-(2-Bromopyridin-3-yl)-9*H*-carbazole (XXXIIa)

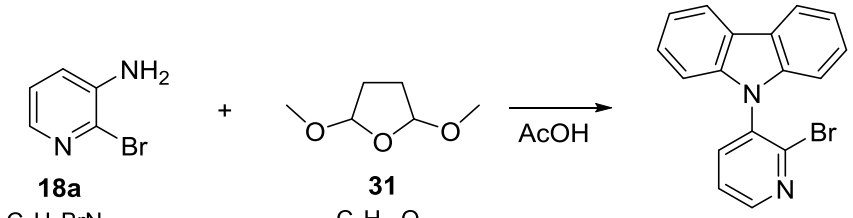

18a
$C_5H_5BrN_2$
173,01

31
$C_6H_{12}O_3$
132,16

XXXIIa
$C_{17}H_{11}BrN_2$
323,19

Synthesis of **XXXIIa** was done according to the general procedure GP1.

18a (1.73 g, 10 mmol, 1 eq.) and **31** (5.29 g, 40 mmol, 4 eq.) were refluxed in 150 ml AcOH for 18 h. After work up the crude product was flashed over a silica gel pad (DCM). Recrystallization from EtOH gave **XXXIIa** (1.69 g, 5.23 mmol, 52%) as orange crystals.

^{1}H (400 MHz, CD_2Cl_2, FID THK136/70): δ= 8.59 (dd, J= 4.7 Hz, 2.0 Hz, 1H), 8.18 (d, J= 7.8 Hz, 2H), 7.86 (dd, J= 7.8 Hz, 2.0 Hz, 1H), 7.56 (dd, J= 7.8 Hz, 4.7 Hz, 1H), 7.44 (ddd, J= 8.1 Hz, 7.4 Hz, 1.3 Hz, 2H), 7.35-7.31 (m, 2H), 7.07 (d, J= 8.2 Hz, 2H) ppm.

^{13}C (100 MHz, CD_2Cl_2, FID THK136/71): δ= 150.7, 144.1, 141.2, 140.1, 134.9, 126.8, 124.6, 124.1, 121.1, 121.0, 110.4 ppm.

9-(2-Chloropyridin-3-yl)-9*H*-carbazole (XXIIb)

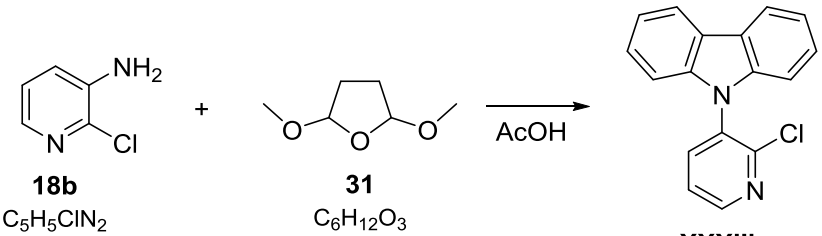

18b
$C_5H_5ClN_2$
128,56

31
$C_6H_{12}O_3$
132,16

XXXIIb
$C_{17}H_{11}ClN_2$
278,74

Synthesis of **XXXIIb** was done according to the general procedure GP1.

18b (1.29 g, 10 mmol, 1 eq.) and **31** (5.28 g, 40 mmol, 4 eq.) were refluxed in 150 ml AcOH for 34 h. After 20 h additional **31** (0.66 g, 5 mmol, 0.5 eq.) was added to the reaction. For purification the crude product was flashed over a silica gel pad (DCM) yielding **XXXIIb** (1.15 g, 4.13 mmol, 41%) as orange solid.

^{1}H (400 MHz, CD_2Cl_2, FID THK128/40): δ= 8.60 (dd, J= 4.7 Hz, 2.0 Hz, 1H), 8.18 (ddd, J= 7.8 Hz, 1.2 Hz, 0.8 Hz, 2H), 7.92 (dd, J= 7.8 Hz, 2.0 Hz, 1H), 7.54 (dd, J= 7.8 Hz, 5.1 Hz, 1H), 7.44 (ddd, J= 8.0 Hz, 7.3 Hz, 1.2 Hz, 2H), 7.34 (ddd, J= 7.6 Hz, 7.4 Hz, 1.0 Hz, 2H), 7.09 (ddd, J= 8.2 Hz, 0.8 Hz, 0.8 Hz, 2H) ppm.

^{13}C (100 MHz, CD_2Cl_2, FID THK128/41): δ= 151.3, 150.2, 141.2, 140.3, 132.6, 126.8, 124.3, 124.1, 121.1, 121.0, 110.3 ppm.

4-Amino-3-bromopyridine (34)

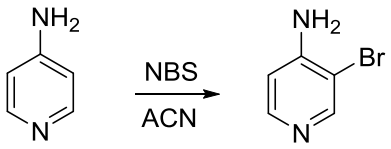

13
$C_5H_6N_2$
94,12

34
$C_5H_5BrN_2$
173,01

Preparation of **34** was done according to Cañibano et al.[40]

13 (4.71 g, 50 mmol, 1 eq.) was dissolved in 250 ml ACN. NBS (10.68 g, 60 mmol, 1.2 eq.) was added and the reaction was stirred at r.t. for 48 h under exclusion of UV light. Afterwards the solvent was removed under reduced pressure. The residue was dissolved in H_2O and EA. The aqueous phase was extracted repeatedly with EA. The combined organic layers were washed twice with H_2O, dried over Na_2SO_4 and concentrated under reduced pressure.

Purification *via* column chromatography (180 g SG, PE:EA 25% → 80%) yielded **34** (2.89 g, 16.7 mmol, 33%) as white solid.

^{1}H (400 MHz, $CDCl_3$, FID THK152/40): δ= 8.39 (s, 1H), 8.10 (d, J= 5.5 Hz, 1H), 6.60 (d, J= 5.5 Hz, 1H), 4.71 (bs, 2H) ppm.

^{13}C (100 MHz, $CDCl_3$, FID THK152/41): δ= 151.4, 150.0, 148.6, 109.8, 106.9 ppm.

9-(3-Bromopyridin-4-yl)-9*H*-carbazole (XXXV)

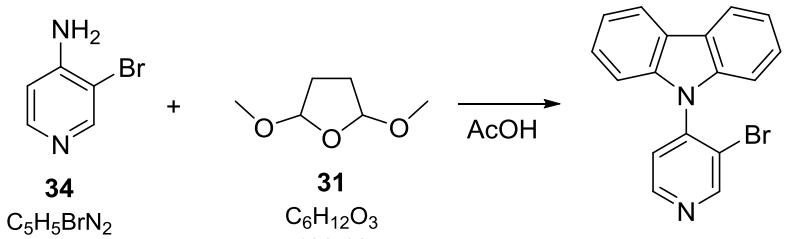

34
$C_5H_5BrN_2$
173,01

31
$C_6H_{12}O_3$
132,16

XXXV
$C_{17}H_{11}BrN_2$
323,19

Synthesis of **XXXV** was done according to the general procedure GP1.

34 (2.60 g, 15 mmol, 1 eq.) and **31** (7.93 g, 60 mmol, 4 eq.) were refluxed in 225 ml AcOH for 120 h. During the reaction further **31** (11.89 g, 90 mmol, 6 eq.) was added. After column chromatography (180 g SG, PE:DCM 40% → 60%) followed by crystallization from EtOH **XXXV** (1.53 g, 4.73 mmol, 32%) was obtained as light yellow solid.

^{1}H (400 MHz, CD_2Cl_2, FID THK168/60): δ= 9.05 (s, 1H), 8.75 (d, J= 5.1 Hz, 1H), 8.17 (d, J= 7.4 Hz, 2H), 7.50 (d, J= 5.1 Hz, 1H), 7.44 (ddd, J= 8.2 Hz, 7.4 Hz, 1.1 Hz, 2H), 7.34 (ddd, J= 7.8 Hz, 7.3 Hz, 1.0 Hz, 2H), 7.14 (d, J= 8.2 Hz, 2H) ppm.

^{13}C (100 MHz, CD_2Cl_2, FID THK168/61): δ= 155.0, 150.7, 145.0, 140.4, 126.8, 125.8, 124.3, 121.4, 121.3, 121.0, 110.7 ppm.

9-(3-Bromopyridin-2-yl)-9*H*-carbazole (XL)

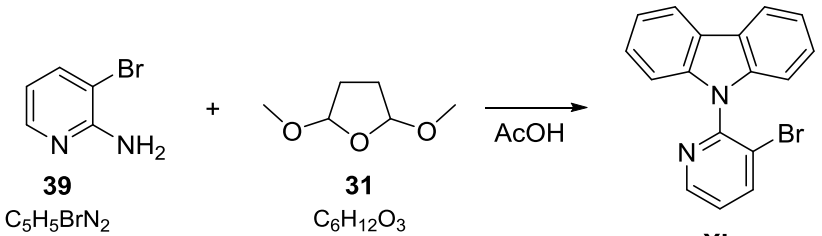

39
$C_5H_5BrN_2$
173,01

31
$C_6H_{12}O_3$
132,16

XL
$C_{17}H_{11}BrN_2$
323,19

Synthesis of **XL** was done according to the general procedure GP1.

39 (1.73 g, 10 mmol, 1 eq.) and **31** (5.29 g, 40 mmol, 4 eq.) were refluxed for 68 h. During the reaction additional **31** (7.93 g, 60 mmol, 6 eq.) was added. Purification *via* repeated column chromatography (120 g, SG, PE:DCM 40% → 60%) yielded **XL** (1.25 g, 3.87 mmol, 39%) as brown oil including minor impurities.

^{1}H (400 MHz, CD_2Cl_2, FID THK178/30): δ= 8.69 (dd, J= 4.7 Hz, 2.0 Hz, 1H), 8.24 (dd, J= 8.2 Hz, 1.6 Hz, 1H), 8.15 (d, J= 7.4 Hz, 2H), 7.44-7.38 (m, 3H), 7.32 (ddd, J= 7.8 Hz, 7.2 Hz, 1.0 Hz, 2H), 7.19-7,17 (m, 2H) ppm.

D.5.4 Ring closure towards NICz

D.5.4.1 Diazotization

Pyrido[3',2':4,5]pyrrolo[3,2,1-*jk*]carbazole (26)

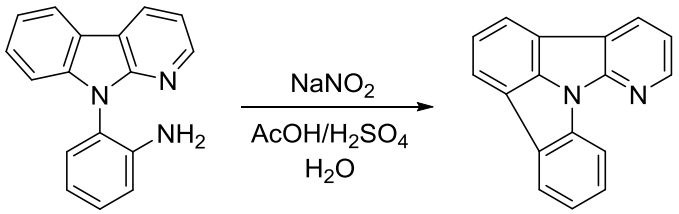

XXIII
$C_{17}H_{13}N_3$
259,31

26
$C_{17}H_{10}N_2$
242,28

Synthesis of **26** was done according to Dunlop and Tucker.[28]

XXIII (468 mg, 1.8 mmol, 1 eq.) was dissolved in 4.6 ml AcOH and 1 ml H_2SO_4 and cooled to 0 °C using an ice/water cooling bath. $NaNO_2$ (137 mg, 1.98 mmol, 1.1 eq.) dissolved in 2.9 ml H_2O was added slowly keeping the temperature below 4 °C. After the addition the reaction mixture was stirred 5 min at 4 °C before it was refluxed for 90 min. The reaction mixture was cooled to r.t. and poured into H_2O. 2 N NaOH was added to give basic pH and the mixture was extracted repeatedly with DCM. The combined organic layers were dried over Na_2SO_4 and concentrated *in vacuo*. Purification *via* column chromatography yielded **26** (17 mg, 0.07 mmol, 4%) as white solid.

^{1}H (400 MHz, $CDCl_3$, FID THK190/10): δ= 8.55 (dd, J= 4.9 Hz, 1.8 Hz, 1H), 8.38 (dd, J= 7.6 Hz, 1.8 Hz, 1H), 8.31 (d, J= 7.8 Hz, 1H), 8.13 (d, J= 7.8 Hz, 1H), 8.08 (d, J= 7.4 Hz, 1H), 8.0 (d, J= 7.4 Hz, 1H), 7.63-7.58 (m, 2H), 7.41 (ddd, J= 7.8 Hz, 7.4 Hz, 0.8 Hz, 1H), 7.29 (dd, J= 7.8 Hz, 5.1 Hz, 1H) ppm.

D.5.4.2 CHA

General procedure 2 (GP2): CHA

A glass vial was charged with the corresponding precursor, K_2CO_3 (2 eq.) and (NHC)Pd(allyl)Cl (**45**) (5 mol%). The vial was closed using a cap with septum and flushed with argon. Degassed DMA (0.1M) with a water content of 3000 ppm was added *via* a syringe. The vial was then placed in a preheated oil bath (130 °C) and the reaction was stirred under argon atmosphere until full conversion. After the reaction was cooled to r.t. the mixture was poured into water and extracted repeatedly with DCM. The combined organic layers were dried over Na_2SO_4 and concentrated under reduced pressure.

Pyrido[2',3':4,5]pyrrolo[3,2,1-*jk*]carbazole (XXXIII)

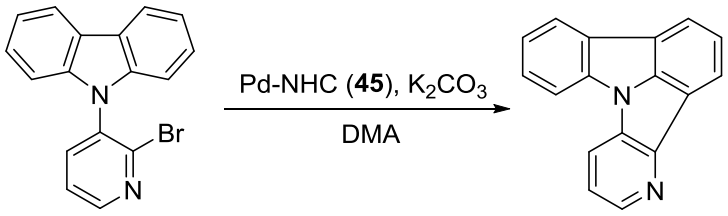

XXXIIa
$C_{17}H_{11}BrN_2$
323,19

XXXIII
$C_{17}H_{10}N_2$
242,28

Synthesis of **XXXIII** was done according to the general procedure GP2.

XXXIIa (485 mg, 1.50 mmol, 1 eq.), K_2CO_3 (414 mg, 3 mmol, 2 eq.) and **45** (44 mg, 0.075 mmol, 5 mol%) in 15 ml DMA were stirred for 8 h at 130 °C. Following work up the crude product was purified *via* column chromatography (PE:DCM 80% → 100%). **XXXIII** (258 mg, 1.06 mmol, 71%) was obtained as light brown solid.

^{1}H (400 MHz, $CDCl_3$, FID THK143/30): δ= 8.57 (d, J= 1.4 Hz, 1H), 8.24 (d, J= 7.4 Hz, 1H), 8.06-8.02 (m, 2H), 7.99 (dd, J= 8.2 Hz, 1.2 Hz, 1H), 7.70 (d, J= 8.2 Hz, 1H), 7.61 (dd, J= 7.4 Hz, 7.4 Hz, 1H), 7.48 (ddd, J= 7.8 Hz, 7.4 Hz, 1.2 Hz, 1H), 7.37-7.30 (m, 2H) ppm.

^{1}3C (100 MHz, $CDCl_3$, FID THK143/31): δ= 148.1, 143.7, 142.9, 138.6, 132.8, 129.4, 126.9, 123.6, 123.1, 122.2, 121.1, 120.2, 120.1, 118.9, 118.4, 117.4, 112.0 ppm.

Pyrido[2',3':4,5]pyrrolo[3,2,1-*jk*]carbazole (XXXIII)

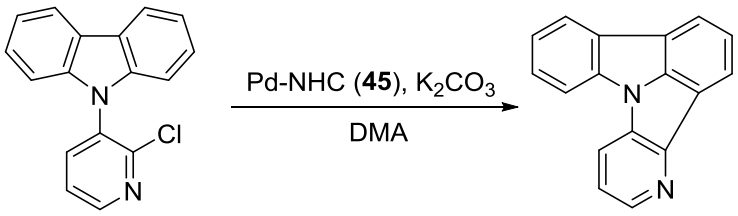

XXXIIb
$C_{17}H_{11}ClN_2$
278,74

XXXIII
$C_{17}H_{10}N_2$
242,28

Synthesis of **XXXIII** was done according to the general procedure GP2. In contrast to the general procedure the reaction was performed in a three necked flask.

XXXIIb (279 mg, 1 mmol, 1 eq.), K_2CO_3 (276 mg, 2 mmol, 2 eq.) and **45** (29 mg, 0.05 mmol, 5 mol%) in 10 ml DMA were stirred for 2 h at 130 °C. Following to work up the crude product was purified *via* column chromatography (16 g, SG, PE:DCM 80% → 100%). **XXXIII** (190 mg, 0.78 mmol, 78%) was obtained as yellow solid.

^{1}H (400 MHz, $CDCl_3$, FID THK143/30): δ= 8.57 (d, J= 1.4 Hz, 1H), 8.24 (d, J= 7.4 Hz, 1H), 8.06-8.02 (m, 2H), 7.99 (dd, J= 8.2 Hz, 1.2 Hz, 1H), 7.70 (d, J= 8.2 Hz, 1H), 7.61 (dd, J= 7.4 Hz, 7.4 Hz, 1H), 7.48 (ddd, J= 7.8 Hz, 7.4 Hz, 1.2 Hz, 1H), 7.37-7.30 (m, 2H) ppm.

^{13}C (100 MHz, $CDCl_3$, FID THK143/31): δ= 148.1, 143.7, 142.9, 138.6, 132.8, 129.4, 126.9, 123.6, 123.1, 122.2, 121.1, 120.2, 120.1, 118.9, 118.4, 117.4, 112.0 ppm.

Pyrido[3',4':4,5]pyrrolo[3,2,1-*jk*]carbazole (36)

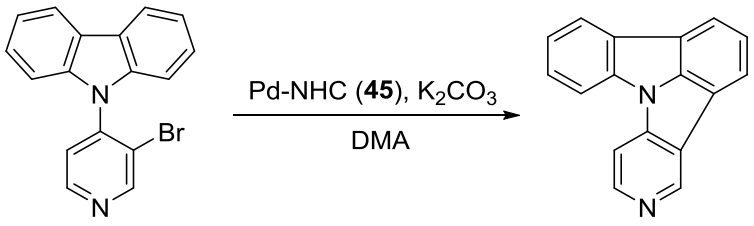

XXXV
$C_{17}H_{11}BrN_2$
323,19

36
$C_{17}H_{10}N_2$
242,28

Synthesis of **36** was done according to the general procedure GP2.

XXXV (323 mg, 1 mmol, 1 eq.), K_2CO_3 (276 mg, 2 mmol, 2 eq.) and **45** (29 mg, 0.05 mmol, 5 mol%) in 10 ml DMA were stirred for 18 h at 130 °C. After workup the crude product was flashed over a silica gel pad (DCM:Et_2O 1:1) yielding **36** (213 mg, 0.88 mmol, 88%) as white solid.

^{1}H (400MHz, CD_2Cl_2, FID THK177/60): δ= 9.29 (s, 1H), 8.66 (d, J= 5.5 Hz, 1H), 8.10 (d, J= 7.8 Hz, 1H), 8.03 (dd, J= 9.8 Hz, 7.4 Hz, 2H), 7.85 (d, J= 8.2 Hz, 1H), 7.73 (dd, J= 5.5 Hz, 1.2 Hz, 1H), 7.62-7.54 (m, 2H), 7.40 (ddd, J= 7.9 Hz, 7.7 Hz, 0.9 Hz, 1H) ppm.

^{13}C (100 MHz, CD_2Cl_2, FID THK177/61): δ= 147.3, 145.2, 144.1, 142.9, 138.8, 131.1, 127.7, 126.5, 124.5, 123.8, 123.5, 120.7, 120.5, 119.3, 116.8, 113.4, 108.0 ppm.

Pyrido[3',2':4,5]pyrrolo[3,2,1-*jk*]carbazole (26)

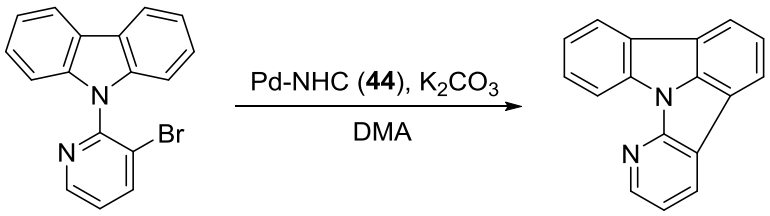

XL
$C_{17}H_{11}BrN_2$
323,19

26
$C_{17}H_{10}N_2$
242,28

Synthesis of **26** was done according to the general procedure GP2.

XL (335 mg, 1.04 mmol, 1 eq.), K_2CO_3 (276 mg, 2 mmol, 2 eq.) and **45** (29 mg, 0.05 mmol, 5 mol%) in 10 ml DMA were stirred for 22 h at 130 °C. After work up the crude product was purified *via* column chromatography (40 g SG, PE:DCM 45% → 60%) yielding **26** (148 mg, 0.61 mmol, 59%) as white solid.

^{1}H (400 MHz, $CDCl_3$, FID THK190/10): δ= 8.55 (dd, J= 4.9 Hz, 1.8 Hz, 1H), 8.38 (dd, J= 7.6 Hz, 1.8 Hz, 1H), 8.31 (d, J= 7.8 Hz, 1H), 8.13 (d, J= 7.8 Hz, 1H), 8.08 (d, J= 7.4 Hz, 1H), 8.0 (d, J= 7.4 Hz, 1H), 7.63-7.58 (m, 2H), 7.41 (ddd, J= 7.8 Hz, 7.4 Hz, 0.8 Hz, 1H), 7.29 (dd, J= 7.8 Hz, 5.1 Hz, 1H) ppm.

Pyrido[4',3':4,5]pyrrolo[3,2,1-jk]carbazole (XXIX)

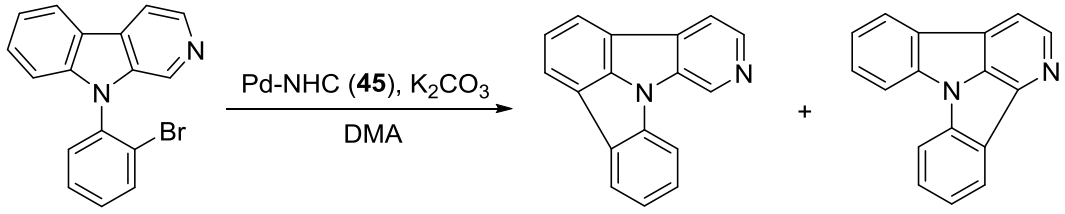

XXVIII
$C_{17}H_{11}BrN_2$
323,19

XXIX
$C_{17}H_{10}N_2$
242,28

XXX
$C_{17}H_{10}N_2$
242,28

Synthesis of **XXIX** was done according to the general procedure GP2.

XXVIII (162 mg, 0.5 mmol, 1 eq.), K_2CO_3 (138 mg, 1 mmol, 2 eq.) and **45** (14 mg, 0.025 mmol, 5 mol%) in 5 ml DMA were stirred for 18 h at 130 °C. After work up the crude product was purified by column chromatography (16 g SG, DCM:Et_2O 2% → 5%) yielding **XXIX** (56 mg, 0.23 mmol, 46%) as yellow solid as well as **XXX** (10 mg, 0.04 mmol, 8%) as green solid.

XXIX: ^{1}H (400 MHz, $CDCl_3$, FID THK194/20): δ= 9.34 (s, 1H), 8.63 (d, J= 8.6 Hz, 1H), 8.19-8.13 (m, 3H), 8.08 (dd, J= 5.4 Hz, 1.1 Hz, 1H), 7.95 (ddd, J= 8.2 Hz, 1.2 Hz, 0.8 Hz, 1H), 7.67 (dd, J= 7.4 Hz, 7.4 Hz, 1H), 7.62 (ddd, J= 8.2 Hz, 7.4 Hz, 1.2 Hz, 1H), 7.43 (ddd, J= 7.6 Hz, 7.4 Hz, 0.8 Hz, 1H) ppm.

XXX: ^{1}H (400 MHz, $CDCl_3$, FID THK194/10): δ= 8.87 (d, J= 5.1 Hz, 1H), 8.39 (d, 7.8 Hz, 1H), 8.16 (ddd, J= 7.8 Hz, 1.2 Hz, 0.8 Hz, 1H), 7.91-7.86 (m, 3H), 7.69-7.61 (m, 2H), 7.45-7.38 (m, 2H) ppm.

D.5.5 Synthesis of the Pd-NHC catalyst

1,3-Bis[2,6-bis(1-methylethyl)phenyl]imidazoliumchlorid (42)

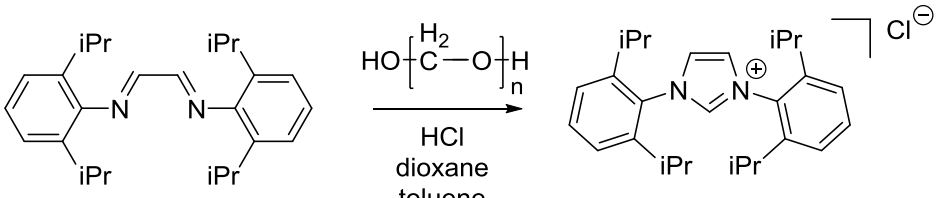

41
$C_{26}H_{36}N_2$
376,59

42
$C_{27}H_{37}ClN_2$
425,05

Synthesis of **42** was done according to Huang and Nolan.[61]

To a mixture of **41** (22.97 g, 61 mmol, 1 eq.) and paraformaldehyde (1.83 g, 61 mmol, 1 eq.) 500 ml toluene were added. The reaction mixture was heated for 1 h to 100 °C. Afterwards the reaction was cooled to 40 °C and HCl in dioxane (22.43 ml, 61 mmol, 1 eq., 2.7 N) was added. Subsequently the reaction mixture was stirred for 3 h at 40 °C and overnight at r.t. before the suspension was filtrated. Recrystallization from $CHCl_3$ yielded **42** (7.37 g, 17.3 mmol, 28%) as pink crystals.

^{1}H (200 MHz, $CDCl_3$, FID PAG003/20): δ= 9.95 (bs, 1H), 8.13 (s, 2H), 7.58 (t, J= 7.6 Hz, 2H), 7.35 (d, J= 7.8 Hz, 4H), 2.45 (quintet, J= 6.9 Hz, 4H), 1.31-1.22 (m, 24H) ppm.

Di-μ-chloro-bis(η^3-2-propenyl)dipalladium (44)

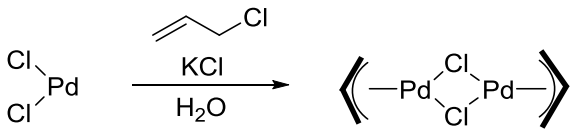

43
Cl_2Pd
177,32

44
$C_6H_{10}Cl_2Pd$
377,86

44 was synthesized according to Marion et al.[62]

43 (2.13 g, 12 mmol, 2 eq.) and KCl (1.70 g, 22.8 mmol, 3.8 eq.) were dissolved in 270 ml degassed H_2O and stirred at r.t. After 30 min allyl chloride (2.79 g, 39 mmol, 6.5 eq.) was added and the reaction mixture was stirred for 17 h at r.t. Subsequently, the reaction mixture was extracted three times with $CHCl_3$. The combined organic layers were dried over Na_2SO_4 and concentrated under reduced pressure yielding **44** (2.15 g, 5.69 mmol, 95%) as yellow solid.

^{1}H (200 MHz, $CDCl_3$, FID PAG001/10): δ= 5.55-5.36 (m, 2H), 4.10 (d, J= 6.6 Hz, 4H), 3.03 (d, J= 12.1 Hz, 4H) ppm.

[1,3-Bis[2,6-bis(1-methylethyl)phenyl]-1,3-dihydro-2*H*-imidazol-2-yliden]chloro(η^3-2-propen-1-yl)palladium (45)

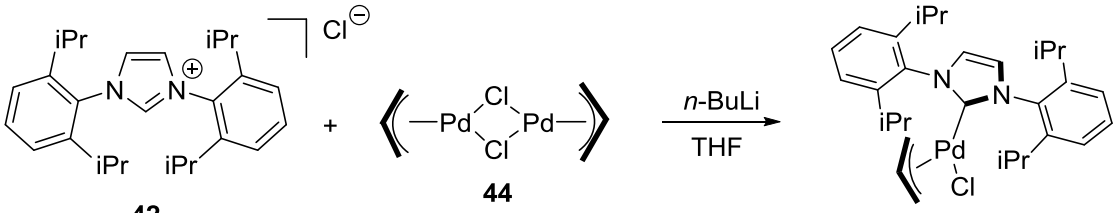

42
$C_{27}H_{37}ClN_2$
425,05

44
$C_6H_{10}Cl_2Pd$
377,86

45
$C_{30}H_{41}N_2ClPd$
571,52

Synthesis of **45** followed the procedure from Navarro and Nolan.[63]

To a solution of **42** (10.75 g, 25.29 mmol, 5 eq.) in 150 ml anhydrous THF was added *n*-BuLi (10.32 ml, 25.80 mmol, 5.1 eq., 2.5 M in hexane) slowly at room temperature. After 30 min **44** (2.15 g, 5.06 mmol, 1 eq.) was added and the reaction mixture was stirred 2 h at room temperature. Subsequently, the reaction mixture was filtered and the filtrate concentrated under reduced pressure. Purification *via* flash column chromatography (180 g SG, DCM:Et_2O 0% → 5%) yielded **45** (2.23 g, 3.90 mmol, 77%) as beige solid.

^{1}H (200 MHz, $CDCl_3$, FID PAG012/40): δ= 7.45 (t, J= 7.7 Hz, 2H), 7.31-7.27 (m, 4H), 7.18 (s, 2H), 4.93-4.73 (m, 1H), 3.92 (dd, J= 7.5 Hz, 1.7 Hz, 1H), 3.21-3.05 (m, 3H), 2.95-2.76 (m, 3H), 1.60 (dd, J= 6.0 Hz, 6.0 Hz 1H), 1.43-1.34 (m, 12H), 1.20 (d, J= 6.8 Hz, 6H), 1.11 (d, J= 6.8 Hz, 6H) ppm.

D.5.6 Synthesis of calibration reference

9-(Pyridin-3-yl)-9*H*-carbazole (46)

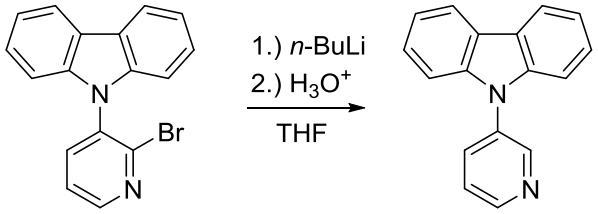

XXXIIa
$C_{17}H_{11}BrN_2$
323,19

46
$C_{17}H_{12}N_2$
244,30

XXXIIa (323 mg, 1 mmol, 1 eq.) was dissolved in 10 ml anhydrous THF and cooled to -80 °C under argon atmosphere with an acetone/$N_{2,fl}$ cooling bath. *n*-BuLi (0.6 ml, 1.4 mmol, 1.4 eq., 2.5 M in hexane) was added slowly keeping the temperature below -70 °C. The reaction mixture was stirred for 1 h at this temperature before 2 ml 1 N HCl was added slowly. The reaction mixture was allowed to warm to r.t. and stirred overnight. 1 N HCl and Et_2O were added to the reaction mixture and the layers were separated. The aqueous layer was repeatedly extracted with Et_2O. The combined organic layers were washed with sat. aq. NaCl, dried over Na_2SO_4 and concentrated *in vacuo*. Column chromatography (16 g SG, DCM) yielded **46** (183 mg, 0.75 mmol, 75%) as yellow solid.

^{1}H (400 MHz, CD_2Cl_2, FID THK142/30): δ= 8.88 (d, J= 2.3 Hz, 1H), 8.72 (dd, J= 4.7 Hz, 1.6 Hz, 1H), 8.17 (ddd, J= 7.8 Hz, 1.2 Hz, 0.8 Hz, 2H), 7.93 (ddd, J= 8.2 Hz, 2.7 Hz, 1.6 Hz, 1H), 7.58 (ddd, J= 8.1 Hz, 4.8 Hz, 0.8 Hz, 1H), 7.47-7.39 (m, 4H), 7.33 (ddd, J= 7.8 Hz, 6.8 Hz, 1.2 Hz, 2H) ppm.

^{13}C (100 MHz, CD_2Cl_2, FID THK142/31): δ= 149.1, 141.3, 135.0, 134.9, 126.8, 125.0, 124.1, 121.0, 120.9, 110.0 ppm.[10]

[10] One carbon not detected.

D.5.7 Further reactions

4-Amino-3,5-dibromopyridine (47)

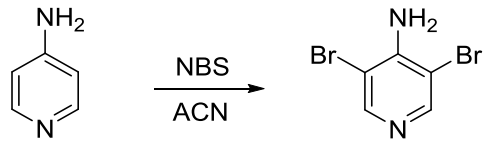

13
$C_5H_6N_2$
94,12

47
$C_5H_4Br_2N_2$
251,91

Synthesis of **47** was done according to Cañibano et al.[40]

4-Aminopyridine (**13**) (2.35 g, 25 mmol, 1 eq.) was dissolved in 125 ml ACN. NBS (8.90 g, 50 mmol, 2 eq.) was added and the reaction was stirred for 48 h under UV-light protection. The formed precipitate was filtrated and washed with ACN and MeOH. The filtrate was evaporated under reduced pressure. Purification *via* flash chromatography (180 g SG, PE:EA 25%) yielded **47** (3.32 g, 13.18 mmol, 53%) as yellow solid.

^{1}H (400 MHz, $CDCl_3$, FID THK154/30): δ= 8.30 (s, 2H), 5.08 (bs, 2H) ppm.

^{13}C (100 MHz, $CDCl_3$, FID THK154/31): δ= 149.9, 147.7, 106.0 ppm.

4-Iodopyridine (48)

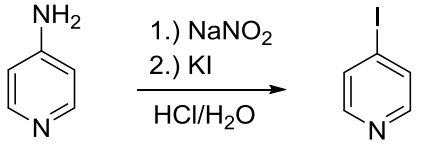

13
$C_5H_6N_2$
94,12

48
C_5H_4IN
205,00

The reaction, workup and purification were done under UV-light protection. 4-Aminopyridine (**13**) (5.65 g, 60 mmol, 1 eq.) was dissolved in 100 ml 3.5 N HCl, stirred mechanically and cooled to -15 °C in an ice/NaCl cooling bath. $NaNO_2$ (4.35 g, 63 mmol, 1.05 eq.) dissolved in 20 ml H_2O was added slowly over a period of 20 min, keeping the temperature below -10 °C. After addition the reaction was stirred for further 20 min at -12 °C. Subsequently, small amounts of urea were added. 5 min later KI (10.96 g, 66 mmol, 1.1 eq.) dissolved in 20 ml H_2O was added dropwise. Then the reaction was stirred 15 min at -10 °C and 1 h at 0 °C. Subsequently, the reaction was allowed to warm to r.t. and 2 N NaOH was added to give basic pH. The mixture was extracted three times with Et_2O. The combined organic layers

were washed with sat. aqueous $Na_2S_2O_5$ solution and H_2O, dried over Na_2SO_4 and concentrated under reduced pressure. Purification *via* column chromatography (12 g KG, DCM:Et_2O 3% → 10%) gave a white solid. Since the solid turned dark after a few hours it was dissolved in DCM, washed with sat. aqueous $Na_2S_2O_5$, dried over Na_2SO_4 and the solvent was evaporated *in vacuo* to give **48** (1.76 g, 8.59 mmol, 14%) as off-white solid.

^{1}H (200 MHz, $CDCl_3$, FID THK170/30): δ= 8.27 (d, J= 5.7 Hz, 2H), 7.68 (d, J= 5.8 Hz, 2H) ppm.

E Bibliography

[1] S. R. Forrest, “The path to ubiquitous and low-cost organic electronic appliances on plastic.,” *Nature*, vol. 428, no. 6986, pp. 911–918, 2004.

[2] M. Pope, H. P. Kallmann, and P. Magnante, “Electroluminescence in Organic Crystals,” *J. Chem. Phys.*, vol. 38, no. 8, p. 2042, 1963.

[3] W. Helfrich and W. G. Schneider, “Recombination Radiation in Anthracene Crystals,” *Phys. Rev. Lett.*, vol. 14, no. 7, pp. 229–231, Feb. 1965.

[4] P. S. Vincett, W. A. Barlow, R. A. Hann, and G. G. Roberts, “Electrical conduction and low voltage blue electroluminescence in vacuum-deposited organic films,” *Thin Solid Films*, vol. 94, no. 2, pp. 171–183, 1982.

[5] C. W. Tang and S. A. Vanslyke, “Organic electroluminescent diodes,” *Appl. Phys. Lett.*, vol. 51, no. 12, pp. 913–915, 1987.

[6] J. H. Burroughes, D. D. C. Bradley, A. R. Brown, R. N. Marks, K. Mackay, R. H. Friend, P. L. Burns, and A. B. Holmes, “Light-emitting diodes based on conjugated polymers,” *Nature*, vol. 347, no. 6293, pp. 539–541, Oct. 1990.

[7] “OLED Community Honors Ted Thoma,” 2011. [Online]. Available: http://www.reuters.com/article/idUS193415+27-Sep-2011+BW20110927. [Accessed: 12-Feb-2016].

[8] J.-H. Jou, S. Kumar, A. Agrawal, T.-H. Lia, and S. Sahooa, “Approaches for fabricating high efficiency organic light emitting diodes,” *J. Mater. Chem. C*, vol. 3, no. 13, pp. 2974–3002, 2015.

[9] International Energy Agency, “Energy Efficiency.” [Online]. Available: http://www.iea.org/topics/energyefficiency/subtopics/lighting/. [Accessed: 13-Feb-2016].

[10] US Department of Energy, “Lighting Basics.” [Online]. Available: http://energy.gov/eere/energybasics/articles/lighting-basics. [Accessed: 06-Feb-2016].

[11] Y. Sun, N. C. Giebink, H. Kanno, B. Ma, M. E. Thompson, and S. R. Forrest, “Management of singlet and triplet excitons for efficient white organic light-emitting devices,” *Nature*, vol. 440, no. 7086, pp. 908–912, 2006.

[12] H. Sasabe and J. Kido, “Development of high performance OLEDs for general lighting,” *J. Mater. Chem. C*, vol. 1, p. 1699, 2013.

[13] S. Scholz, D. Kondakov, B. Lüssem, and K. Leo, “Degradation mechanisms and reactions in organic light-emitting devices,” *Chem. Rev.*, vol. 115, no. 16, pp. 8449–8503, 2015.

[14] Y. Shirota and H. Kageyama, “Charge Carrier Transporting Molecular Materials and Their Applications in Devices,” *Chem. Rev.*, vol. 107, no. 4, pp. 953–1010, 2007.

[15] Y. Tao, C. Yang, and J. Qin, “Organic host materials for phosphorescent organic light-emitting diodes.,” *Chem. Soc. Rev.*, vol. 40, no. 5, pp. 2943–70, 2011.

[16] W. Brütting, J. Frischeisen, T. D. Schmidt, B. J. Scholz, and C. Mayr, “Device efficiency of organic light-emitting diodes: Progress by improved light outcoupling,” *Phys. Status Solidi Appl. Mater. Sci.*, vol. 210, no. 1, pp. 44–65, 2013.

[17] M. A. Baldo, D. F. O’Brien, M. E. Thompson, and S. R. Forrest, “Excitonic singlet-triplet ratio in a semiconducting organic thin film,” *Phys. Rev. B*, vol. 60, no. 20, pp. 14422–14428, Nov. 1999.

[18] M. A. Baldo, D. F. O’Brien, Y. You, A. Shoustikov, S. Sibley, M. E. Thompson, and S. R. Forrest, “Highly efficient phosphorescent emission from organic electroluminescent devices,” *Nature*, vol. 395, no. 6698, pp. 151–154, Sep. 1998.

[19] A. Köhler, J. S. Wilson, and R. H. Friend, “Fluorescence and Phosphorescence in Organic Materials,” *Adv. Mater.*, vol. 14, no. 10, pp. 701–707, 2002.

[20] X. Yang, G. Zhou, and W.-Y. Wong, “Functionalization of phosphorescent emitters and their host materials by main-group elements for phosphorescent organic light-emitting devices,” *Chem. Soc. Rev.*, vol. 44, no. 23, pp. 8484–8575, 2015.

[21] M. H. Tsai, H. W. Lin, H. C. Su, T. H. Ke, C. C. Wu, F. C. Fang, Y. L. Liao, K. T. Wong, and C. I. Wu, “Highly efficient organic blue electrophosphorescent devices based on 3,6-Bis(triphenylsilyl)carbazole as the host material,” *Adv. Mater.*, vol. 18, no. 9, pp. 1216–1220, 2006.

[22] S. J. Yeh, M. F. Wu, C. T. Chen, Y. H. Song, Y. Chi, M. H. Ho, S. F. Hsu, and C. H. Chen, “New dopant and host materials for blue-light-emitting phosphorescent organic electroluminescent devices,” *Adv. Mater.*, vol. 17, no. 3, pp. 285–289, 2005.

[23] P. Kautny, D. Lumpi, Y. Wang, A. Tissot, J. Bintinger, E. Horkel, B. Stöger, C. Hametner, H. Hagemann, D. Ma, and J. Fröhlich, “Oxadiazole based bipolar host materials employing planarized triarylamine donors for RGB PHOLEDs with low

efficiency roll-off," *J. Mater. Chem. C*, vol. 2, no. 11, p. 2069, 2014.

[24] P. Kautny, Z. Wu, J. Eichelter, E. Horkel, B. Stöger, J. Chen, D. Ma, J. Fröhlich, and D. Lumpi, "Indolo[3,2,1-jk]carbazole based planarized CBP derivatives as host materials for PhOLEDs," *submitted*, 2016.

[25] L. A. Crawford, H. McNab, A. R. Mount, J. Verhille, and S. I. Wharton, "Synthesis of azapyrrolo[3,2,1-jk]carbazoles, azaindolo[3,2,1-jk]carbazoles, and carbazole-1-carbonitriles by gas-phase cyclization of aryl radicals," *Synthesis (Stuttg).*, no. 6, pp. 923–928, 2010.

[26] J. B. Henry, S. I. Wharton, E. R. Wood, H. McNab, and A. R. Mount, "Specific indolo[3,2,1-jk]carbazole conducting thin-film materials production by selective substitution," *J. Phys. Chem. A*, vol. 115, no. 21, pp. 5435–5442, 2011.

[27] J. Lv, Q. Liu, J. Tang, F. Perdih, and K. Kranjc, "A facile synthesis of indolo[3,2,1-jk]carbazoles via palladium-catalyzed intramolecular cyclization," *Tetrahedron Lett.*, vol. 53, no. 39, pp. 5248–5252, 2012.

[28] H. G. Dunlop and S. H. Tucker, "Attempts to prepare Optically Active Tervalent Nitrogen Compounds. Part I. Syntheses of 1:9-Phenylenecarbazole and Derivatives," J. Chem. Soc. (resumed), pp. 1945-1956, 1939.

[29] A. W. Jones, M. L. Louillat-Habermeyer, and F. W. Patureau, "Strained dehydrogenative ring closure of phenylcarbazoles," *Adv. Synth. Catal.*, vol. 357, no. 5, pp. 945–949, 2015.

[30] S. I. Wharton, J. B. Henry, H. McNab, and A. R. Mount, "The production and characterisation of novel conducting redox-active oligomeric thin films from electrooxidised indolo[3,2,1-jk]carbazole," *Chem. - A Eur. J.*, vol. 15, no. 22, pp. 5482–5490, 2009.

[31] A. R. Katritzky, G. W. Rewcastle, and L. M. Vazquez de Miguel, "Improved syntheses of substituted carbazoles and benzocarbazoles via lithiation of the (dialkylamino)methyl (aminal) derivatives," *J. Org. Chem.*, vol. 53, no. 4, pp. 794–799, Feb. 1988.

[32] M. A. Ponce and R. Erra-Balsells, "Synthesis and isolation of bromo-β-carbolines obtained by bromination of β-carboline alkaloids.," *J. Heterocycl. Chem.*, vol. 38, no. 5, pp. 1087–1095, 2001.

[33] A. R. Katritzky and J. Wu, “A simple, versatile synthetic route to N-1-aryl-, -heteroaryl-, -acylmethyl-, -carboxymethyl- and -alkyl-benzotriazoles via regiospecific or highly regioselective substitutions of benzotriazole.,” *Synthesis (Stuttg).*, no. 6, pp. 597–600, 1994.

[34] B. Witkop, “Studies on Carboline Anhydronium Bases,” *J. Am. Chem. Soc.*, vol. 75, no. 14, pp. 3361–3370, Jul. 1953.

[35] K. P. Lippke, W. G. Schunack, W. Wenning, and W. E. Müller, “beta-Carbolines as benzodiazepine receptor ligands. 1. Synthesis and benzodiazepine receptor interaction of esters of beta-carboline-3-carboxylic acid.,” *J. Med. Chem.*, vol. 26, no. 4, pp. 499–503, 1983.

[36] R. Meesala, M. N. Mordi, and S. M. Mansor, “Copper-catalyzed protodecarboxylation and aromatization of tetrahydro-??-carboline-3-carboxylic acids,” *Synlett*, vol. 25, no. 1, pp. 120–122, 2014.

[37] B. Xin, W. Tang, Y. Wang, G. Lin, H. Liu, Y. Jiao, Y. Zhu, H. Yuan, Y. Chen, and T. Lu, “Design, synthesis and biological evaluation of β-carboline derivatives as novel inhibitors targeting B-Raf kinase,” *Bioorg. Med. Chem. Lett.*, vol. 22, no. 14, pp. 4783–4786, 2012.

[38] J. Chen, W. Chen, and Y. Hu, “Microwave-enhanced Fischer reaction: An efficient one-pot synthesis of gamma-carbolines,” *Synlett*, no. 1, pp. 0077–0082, 2008.

[39] T. Iwaki, A. Yasuhara, and T. Sakamoto, “Novel synthetic strategy of carbolines via palladium-catalyzed amination and arylation reaction,” *J. Chem. Soc. Perkin Trans. 1*, no. 11, pp. 1505–1510, 1999.

[40] V. Cañibano, J. F. Rodríguez, M. Santos, M. A. Sanz-Tejedor, M. C. Carreño, G. González, and J. L. García-Ruano, “Mild Regioselective Halogenation of Activated Pyridines with N-Bromosuccinimide,” *Synthesis (Stuttg).*, vol. 2001, no. 14, pp. 2175–2179, 2001.

[41] Y. H. Son, Y. J. Kim, M. J. Park, H.-Y. Oh, J. S. Park, J. H. Yang, M. C. Suh, and J. H. Kwon, “Small single–triplet energy gap bipolar host materials for phosphorescent blue and white organic light emitting diodes,” *J. Mater. Chem. C*, vol. 1, no. 33, p. 5008, 2013.

[42] M. J. Cho, S. J. Kim, S. H. Yoon, J. Shin, T. R. Hong, H. J. Kim, Y. H. Son, J. S. Kang, H. A. Um, T. W. Lee, J. Bin, B. S. Lee, J. H. Yang, G. S. Chae, J. H. Kwon, and D. H.

Choi, “New Bipolar Host Materials for Realizing Blue Phosphorescent Organic Light-Emitting Diodes with High Efficiency at 1000 cd/m 2,” *ACS Appl. Mater. Interfaces*, 2014.

[43] H. B. Goodbrand and N. X. Hu, “Ligand-accelerated catalysis of the Ullmann condensation: Application to hole conducting triarylamines,” *J. Org. Chem.*, vol. 64, no. 2, pp. 670–674, 1999.

[44] H. Xu, K. Yin, and W. Huang, “Highly improved electroluminescence from a series of novel Eu111 complexes with functional single-coordinate phosphine oxide ligands: Tuning the intramolecular energy transfer, morphology, and carrier injection ability of the complexes,” *Chem. - A Eur. J.*, vol. 13, no. 36, pp. 10281–10293, 2007.

[45] K. Nozaki, K. Takahashi, K. Nakano, T. Hiyama, H. Z. Tang, M. Fujiki, S. Yamaguchi, and K. Tamao, “The double N-arylation of primary amines: Toward multisubstituted carbazoles with unique optical properties,” *Angew. Chemie - Int. Ed.*, vol. 42, no. 18, pp. 2051–2053, 2003.

[46] A. Kuwahara, K. Nakano, and K. Nozaki, “Double N -Arylation of Primary Amines : Carbazole Synthesis from 2 , 2 ′ -Biphenyldiols,” *J. Org. Chem.*, no. 2, pp. 413–419, 2005.

[47] T. Kitawaki, Y. Hayashi, A. Ueno, and N. Chida, “One-step construction of carbazoles by way of the palladium-catalyzed double N-arylation reaction and its application to the total synthesis of murrastifoline-A,” *Tetrahedron*, vol. 62, no. 29, pp. 6792–6801, 2006.

[48] Y. Zhou and J. G. Verkade, “Highly efficient ligands for the palladium-assisted double N-arylation of primary amines for one-sep construction of carbazoles,” *Adv. Synth. Catal.*, vol. 352, no. 4, pp. 616–620, 2010.

[49] S. H. Kim, M. Kim, J. G. Verkade, and Y. Kim, “A tuned bicyclic proazaphosphatrane for catalytically enhanced n-arylation reactions with aryl chlorides,” *European J. Org. Chem.*, vol. 2015, no. 9, pp. 1954–1960, 2015.

[50] N. Clauson-Kaas, F. Limborg, and J. Fakstorp, “Alkoxylation of simple furans and related reactions.,” *Acta Chem. Scand.*, vol. 2, pp. 109–115, 1948.

[51] T. A. Wynn, “Clauson-Kaas pyrrole synthesis.,” in *Name React. Heterocycl. Chem. II*, John Wiley & Sons, Inc., 2011, pp. 42–52.

[52] B. S. Gourlay, P. P. Molesworth, J. H. Ryan, and J. A. Smith, “A new and high yielding

synthesis of unstable pyrroles via a modified Clauson-Kaas reaction.," *Tetrahedron Lett.*, vol. 47, no. 5, pp. 799–801, 2006.

[53] C. Kashima, S. Hibi, T. Maruyama, and Y. Omote, "The convenient and one-pot synthesis of N-substituted carbazoles," *Tetrahedron Lett.*, vol. 27, no. 19, pp. 2131–2134, 1986.

[54] C. Kashima, S. Hibi, T. Maruyama, K. Harada, and Y. Omote, "A convenient and one-pot synthesis of 9-substituted carbazoles from primary amine hydrochlorides and 2,5-dimethoxytetrahydrofuran," *J. Heterocycl. Chem.*, vol. 24, no. 4, pp. 913–916, 1987.

[55] S. Govindaraji, P. Nakache, V. Marks, Z. Pomerantz, A. Zaban, and J. P. Lellouche, "Novel carboxylated pyrrole- and carbazole-based monomers. Synthesis and electro-oxidation features," *J. Org. Chem.*, vol. 71, no. 24, pp. 9139–9143, 2006.

[56] J. P. Lellouche, Z. Pomerantz, and S. Ghosh, "Towards hybrid carbazole/pyrrole-based carboxylated monomers: Chemical synthesis, characterisation and electro-oxidation properties," *Tetrahedron Lett.*, vol. 52, no. 51, pp. 6903–6907, 2011.

[57] D. H. Lee, S. G. Lee, D. I. Jung, and J. T. Hahn, "Synthesis of heteroaromatic derivatives with nitrogen atoms: tripyrrolyl pyrimidine and tripyrrolyl[1,3,5]triazine.," *Asian J. Chem.*, vol. 25, no. 1, pp. 501–504, 2013.

[58] V. Amarnath, D. C. Anthony, K. Amarnath, W. M. Valentine, L. A. Wetterau, and D. G. Graham, "Intermediates in the Paal-Knorr synthesis of pyrroles," *J. Org. Chem.*, vol. 56, no. 24, pp. 6924–6931, Nov. 1991.

[59] M. Lafrance and K. Fagnou, "Palladium-catalyzed benzene arylation: Incorporation of catalytic pivalic acid as a proton shuttle and a key element in catalyst design," *J. Am. Chem. Soc.*, vol. 128, no. 51, pp. 16496–16497, 2006.

[60] M. A. Bartucci, P. M. Wierzbicki, C. Gwengo, S. Shajan, S. H. Hussain, and J. W. Ciszek, "Synthesis of dihydroindolizines for potential photoinduced work function alteration," *Tetrahedron Lett.*, vol. 51, no. 52, pp. 6839–6842, Dec. 2010.

[61] J. Huang and S. P. Nolan, "Efficient Cross-Coupling of Aryl Chlorides with Aryl Grignard Reagents (Kumada Reaction) Mediated by a Palladium/Imidazolium Chloride System," *J. Am. Chem. Soc.*, vol. 121, no. 42, pp. 9889–9890, Oct. 1999.

[62] N. Marion, O. Navarro, J. Mei, E. D. Stevens, N. M. Scott, and S. P. Nolan, "Modified (NHC)Pd(allyl)Cl (NHC = N-Heterocyclic Carbene) Complexes for Room-Temperature

Suzuki−Miyaura and Buchwald−Hartwig Reactions," *J. Am. Chem. Soc.*, vol. 128, no. 12, pp. 4101–4111, Mar. 2006.

[63] O. Navarro and S. P. Nolan, "Large-scale one-pot synthesis of N-heterocyclic carbene-Pd(allyl)Cl complexes," *Synthesis (Stuttg).*, no. 2, pp. 366–367, 2006.

[64] F. Denonne, S. Celanire, A. Valade, S. Defays, and V. Durieux, "Cyclobutoxy-dihydrothiazolopyridines and related compounds as histamine H3 ligands and their preparation and use in the treatment of diseases.," 30-Jul-2009, WO2009092764A1.

F Appendix

F.1 GC calibration for CHA screening

For quantification of screening results a calibration was done with both brominated and chlorinated starting material **XXXIIa/b**, product **XXXIII**, by product **46** an internal standard 1-methylnaphthalene. The weight of the samples, which were dissolved in 25 ml DCM for stock solutions are listed in table F.01. The dilution series can be seen in table F.02. Each sample was measured three times on both detectors (referred to below as front and back FID). The average peak areas for the different compounds are given in table F.03 (front FID) and table F.04 (back FID). In figure F.01 (front FID) and figure F.02 (back FID) the peak area is plotted against the sample concentration and the linear fitted calibration curves are displayed.

Table F.01: Sample weight for calibration, dissolved in 25 ml DCM for stock solutions.

	sample weight [mg]	***concentration stock solution [mg/ml]***
Standard	23.8	0.952
BrPyrCz (**XXXIIa**)	25.8	1.032
ClPyrCz (**XXXIIb**)	29.3	1.172
NICz (**XXXIII**)	28.7	1.148
PyrCz (**46**)	28.3	1.132

Table F.02: Concentration of the compounds in diluted samples.

Sample	***Dilution***	***Standard [mg/ml]***	***BrPyrCz [mg/ml]***	***ClPyrCz [mg/ml]***	***NICz [mg/ml]***	***PyrCz [mg/ml]***
A	1:10	0.0952	0.1032	0.1172	0.1148	0.1132
B	1:20	0.0476	0.0516	0.0586	0.0574	0.0566
C	1:50	0.01904	0.02064	0.02344	0.02296	0.02264
D	1:100	0.00952	0.01032	0.01172	0.01148	0.01132
E	1:200	0.00476	0.00516	0.00586	0.00574	0.00566
F	1:1000	0.000952	0.001032	0.001172	0.001148	0.001132

Table F.03: Average peak area of three measurements of samples A-F with front FID.

Sample	*Standard [pA*min]*	*BrPyrCz [pA*min]*	*ClPyrCz [pA*min]*	*NICz [pA*min]*	*PyrCz [pA*min]*
A	1.3924	0.6542	0,9807	1.1227	1.1130
B	0.6770	0.3131	0.4751	0.5465	0.5391
C	0.2559	0.1175	0.1850	0.2053	0.1987
D	0.1200	0.0586	0.0932	0.1007	0.0962
E	0.0610	0.0292	0.0451	0.0489	0.0465
F	0.0117	0.0061	0.0082	0.0092	0.0091

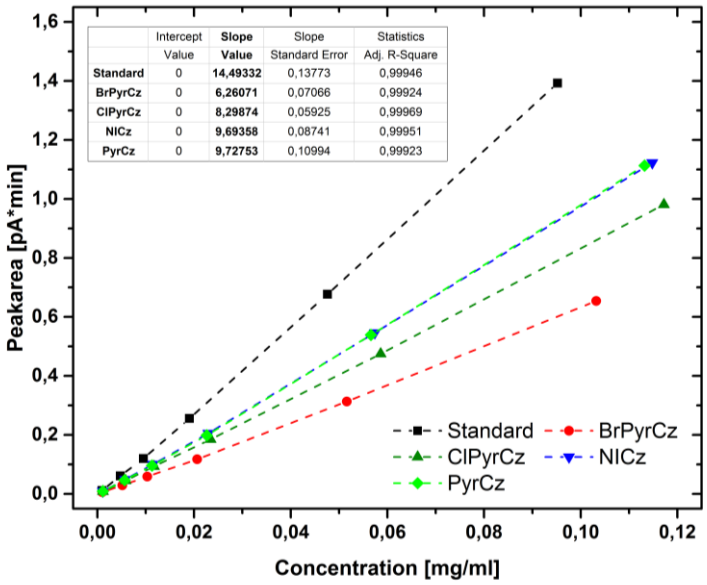

Figure F.01: Calibration curves for front FID.

Table F.04: Average peak area of three measurements of samples A-F with back FID.

Sample	*Standard [pA*min]*	*BrPyrCz [pA*min]*	*ClPyrCz [pA*min]*	*NICz [pA*min]*	*PyrCz [pA*min]*
A	1.6557	0.8916	1.2390	1.4131	1.3827
B	0.8133	0.4334	0.6016	0.6965	0.6809
C	0.3303	0.1706	0.2419	0.2721	0.2627
D	0.1613	0.0846	0.1203	0.1330	0.1274
E	0.0777	0.0414	0.0603	0.0642	0.0634
F	0.0158	0.0078	0.0124	0.0113	0.0117

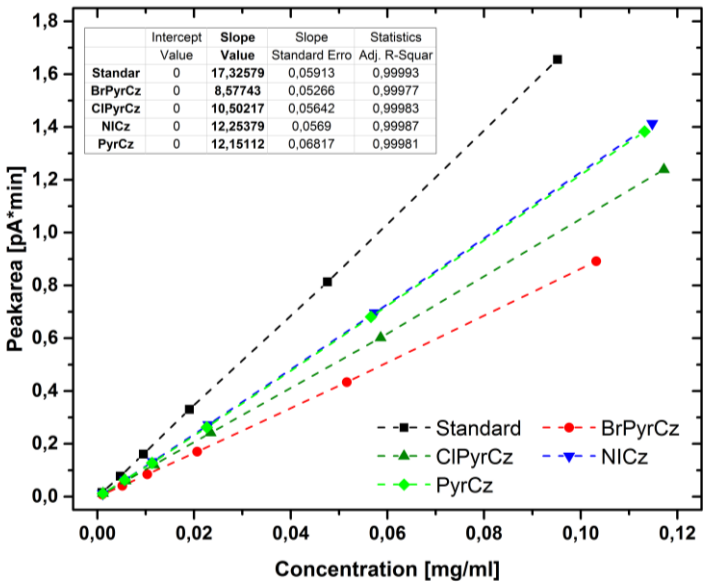

Figure F.02: Calibration for back FID.

Table F.05: Slope of linear regression curves for front and back FID. All curves are set to go through origin (intercept x=0).

	slope	
	front FID	***back FID***
Standard	14.4933	17.3258
BrPyrCz (**XXXIIa**)	6.2607	8.5774
ClPyrCz (**XXXIIb**)	8.2987	10.5022
NICz (**XXXIII**)	9.6936	12.2538
PyrCz (**46**)	9.7275	12.1511

Table F.06: Single point data of calibration samples from front FID.

Sample	*Standard [pA*min]*	*BrPyrCz [pA*min]*	*ClPyrCz [pA*min]*	*NICz [pA*min]*	*PyrCz [pA*min]*
A-1	1.3904	0.6429	1.0041	1.1094	1.0959
A-2	1.3676	0.6425	0.9550	1.1009	1.0916
A-3	1.4193	0.6771	0.9831	1.1577	1.1516
B-1	0.7061	0.3231	0.4880	0.5664	0.5590
B-2	0.6771	0.3094	0.4690	0.5395	0.5331
B-3	0.6478	0.3069	0.4682	0.5335	0.5253
C-1	0.2629	0.1191	0.1871	0.2078	0.2016
C-2	0.2545	0.1142	0.1835	0.1997	0.1933
C-3	0.2503	0.1193	0.1844	0.2084	0.2011
D-1	0.1232	0.0580	0.0939	0.1006	0.0950
D-2	0.1244	0.0583	0.0928	0.0986	0.0954
D-3	0.1124	0.0594	0.0929	0.1028	0.0981
E-1	0.0608	0.0283	0.0450	0.0094	0.0459
E-2	0.0602	0.0291	0.0451	0.0093	0.0457
E-3	0.0620	0.0302	0.0453	0.0088	0.0479
F-1	0.0113	0.0064	0.0074	0.0488	0.0093
F-2	0.0121	0.0060	0.0088	0.0486	0.0091
F-3	0.0118	0.0058	0.0084	0.0493	0.0088

Table F.07: Single point data of calibration samples from back FID.

Sample	*Standard [pA*min]*	*BrPyrCz [pA*min]*	*ClPyrCz [pA*min]*	*NICz [pA*min]*	*PyrCz [pA*min]*
A-1	1.7120	0.9164	1.2414	1.4497	1.4237
A-2	1.6231	0.8703	1.1678	1.3842	1.3509
A-3	1.6319	0.8882	1.3077	1.4055	1.3735
B-1	0.8028	0.4311	0.6118	0.6970	0.6802
B-2	0.8040	0.4309	0.6045	0.6920	0.6799
B-3	0.8330	0.4381	0.5885	0.7004	0.6827
C-1	0.3567	0.1722	0.2442	0.2729	0.2675
C-2	0.3140	0.1692	0.2424	0.2719	0.2590
C-3	0.3201	0.1704	0.2391	0.2715	0.2616
D-1	0.1761	0.0882	0.1184	0.1362	0.1320
D-2	0.1541	0.0837	0.1214	0.1327	0.1261
D-3	0.1537	0.0820	0.1210	0.1302	0.1242
E-1	0.0754	0.0392	0.0619	0.0611	0.0609
E-2	0.0789	0.0434	0.0600	0.0670	0.0655
E-3	0.0789	0.0417	0.0589	0.0645	0.0637
F-1	0.0165	0.0078	-	0.0114	0.0119
F-2	0.0150	0.0079	-	0.0103	0.0114
F-3	0.0158	0.0077	0.0124	0.0121	0.0118

F.2 CHA screening: results

The detailed screening results of each experiment, as well as the average values of experiments applying the same reaction conditions are outlined in table F.08 – F.15. Starting materials **XXXIIa** and **XXXIIb** are referred to below as BrPyrCz and ClPyrCz, product **XXXIII** and dehalogenated byproduct **46** as NICz and PyrCz.

Table F.08: Results for experiments applying different catalysts. Reaction conditions: 10% catalyst (entry), 2 eq. K_2CO_3, DMA (3000 ppm H_2O), 130 °C.

Entry	*Time [min]*	*Experiment 1*			*Experiment 2*			*Experiment 3*			*Conversion BrPyrCz*		*Yield NICz*		*Yield PyrCz*	
		Conversion BrPyrCz [%]	*Yield NICz [%]*	*Yield PyrCz [%]*	*Conversion BrPyrCz [%]*	*Yield NICz [%]*	*Yield PyrCz [%]*	*Conversion BrPyrCz [%]*	*Yield NICz [%]*	*Yield PyrCz [%]*	*Average [%]*	*Standard deviation*	*Average [%]*	*Standard deviation*	*Average [%]*	*Standard deviation*
Pd-NHC (45) – 1[a]	15	98.8	93.2	4.3	57.5	38.1	8.8	100.0	90.9	5.2	-	-	-	-	-	-
	35	100.0	100.6	5.0	70.0	58.2	11.4	100.0	92.2	4.9	-	-	-	-	-	-
	60	100.0	92.3	4.8	87.3	66.0	10.7	100.0	95.4	5.1	-	-	-	-	-	-
	90	100.0	98.0	5.0	97.9	89.6	11.7	100.0	101.5	5.4	-	-	-	-	-	-
	120	100.0	98.9	5.0	100.0	75.4	8.9	100.0	103.2	5.4	-	-	-	-	-	-
Pd-NHC (45) – 2[a]	15	91.2	80.9	6.1	84.4	66.2	7.1	85.6	72.1	3.4	86.3	14.1	73.6	18.5	5.8	1.8
	35	100.0	93.4	7.2	100.0	80.7	7.5	100.0	95.3	4.4	95.0	11.2	86.7	14.1	6.7	2.4
	60	100.0	84.3	6.5	100.0	81.3	7.7	100.0	100.5	4.7	97.9	4.7	86.6	11.3	6.6	2.1
	90	100.0	89.1	6.8	100.0	83.6	7.6	100.0	97.0	4.6	99.7	0.8	93.2	6.2	6.9	2.4
	120	100.0	90.1	6.5	100.0	84.9	7.7	100.0	94.9	4.5	100.0	0.0	91.2	9.2	6.3	1.6
$Pd(OAc)_2$ / NHC-ligand (42)[b]	15	84.7	63.9	9.3	50.5	43.4	5.9	74.8	53.1	6.9	70.0	14.4	53.5	8.4	7.4	1.4
	35	88.0	66.3	7.2	65.9	59.4	6.4	99.9	87.1	7.8	84.6	14.1	71.0	11.8	7.1	0.6
	60	89.7	62.9	6.7	75.9	58.6	5.1	99.8	94.5	9.3	88.5	9.8	72.0	16.0	7.0	1.7
	90	88.7	71.8	8.1	79.5	59.6	4.9	100.0	89.3	8.7	89.4	8.4	73.6	12.2	7.2	1.7
	120	92.8	67.4	7.7	80.9	71.1	5.9	100.0	90.5	9.1	91.2	7.9	76.3	10.1	7.6	1.3
$PdCl2(PPh_3)_2$	15	96.7	29.6	12.1	74.8	19.3	12.7	81.1	21.1	17.3	84.2	9.2	23.3	4.5	14.0	2.3
	35	99.9	66.2	17.3	88.0	44.8	22.2	95.4	52.3	23.2	94.4	4.9	54.4	8.9	20.9	2.6
	60	100.0	71.8	17.2	100.0	55.5	18.2	99.9	59.4	22.4	100.0	0.0	62.2	7.0	19.3	2.3
	90	99.9	74.9	21.1	100.0	65.9	24.7	100.0	62.9	24.1	100.0	0.0	67.9	5.1	23.3	1.6
	120	100.0	73.3	19.2	100.0	53.7	14.8	100.0	62.7	23.1	100.0	0.0	63.3	8.0	19.0	3.4
$Pd(OAc)_2$ / PPh_3[c]	15	75.3	20.5	13.9	83.5	13.0	14.2	62.6	16.4	15.1	73.8	8.6	16.6	3.1	14.4	0.5
	35	95.3	53.4	20.6	95.9	33.6	16.2	88.1	36.2	15.0	93.1	3.5	41.1	8.8	17.3	2.4
	60	100.0	64.9	21.9	100.0	51.8	20.2	99.7	58.7	18.0	99.9	0.1	58.5	5.4	20.0	1.6
	90	100.0	64.1	22.9	100.0	46.1	17.0	99.9	62.8	20.7	100.0	0.0	57.7	8.2	20.2	2.4
	120	100.0	61.8	18.0	100.0	52.9	18.7	100.0	59.8	17.9	100.0	0.0	58.1	3.8	18.2	0.4

[a] Average values for all six experiments. [b] 12% ligand. [c] 22% ligand.

Table F.09: Results for experiments applying different catalysts. Reaction conditions: 10% catalyst (entry), 2 eq. K_2CO_3, DMA (3000 ppm H_2O), 130 °C.

Entry	Time [min]	Experiment 1			Experiment 2			Experiment 3			Conversion BrPyrCz		Yield NICz		Yield PyrCz	
		Conversion BrPyrCz [%]	Yield NICz [%]	Yield PyrCz [%]	Conversion BrPyrCz [%]	Yield NICz [%]	Yield PyrCz [%]	Conversion BrPyrCz [%]	Yield NICz [%]	Yield PyrCz [%]	Average [%]	Standard deviation	Average [%]	Standard deviation	Average [%]	Standard deviation
$Pd(OAc)_2$ / dppf[a]	15	88.2	26.8	21.7	85.8	17.2	17.7	80.6	21.3	15.7	84.9	3.2	21.8	4.0	18.3	2.5
	35	100.0	59.5	31.7	99.8	41.2	24.1	99.9	48.9	20.2	99.9	0.1	49.9	7.5	25.3	4.7
	60	100.0	42.3	27.1	100.0	43.7	22.3	100.0	53.9	23.5	100.0	0.0	46.7	5.2	24.3	2.0
	90	100.0	39.0	28.7	100.0	39.2	18.3	100.0	54.3	22.0	100.0	0.0	44.2	7.2	23.0	4.3
	120	100.0	47.7	27.3	100.0	38.2	18.8	100.0	54.5	20.7	100.0	0.0	46.8	6.7	22.3	3.6
$Pd(OAc)_2$ / PCy_3*BF_4[b]	15	76.3	14.6	21.7	75.0	48.6	22.5	56.7	16.5	28.8	69.3	9.0	26.6	15.6	24.3	3.2
	35	46.6	30.0	27.2	52.0	35.5	35.8	68.4	42.1	38.3	55.7	9.3	35.8	4.9	33.8	4.7
	60	61.4	44.1	25.5	59.0	39.0	42.1	66.9	38.1	32.0	62.4	3.3	40.4	2.7	33.2	6.8
	90	70.2	53.4	26.8	53.7	33.6	37.9	67.9	42.8	39.7	63.9	7.3	43.3	8.1	34.8	5.7
	120	67.0	52.9	26.9	61.7	49.8	46.5	64.9	38.7	32.9	64.5	2.2	47.1	6.1	35.5	8.2
$Pd(OAc)_2$ / JohnPhos[b]	15	73.0	25.0	23.1	65.0	20.1	28.4	71.4	20.2	22.6	69.8	3.5	21.7	2.3	24.7	2.6
	35	90.5	44.9	28.0	78.1	29.4	30.3	87.4	30.6	21.6	85.3	5.3	34.9	7.0	26.6	3.7
	60	97.1	52.9	31.1	87.4	31.7	26.8	91.4	37.5	23.5	91.9	4.0	40.7	8.9	27.1	3.1
	90	99.8	57.3	31.8	88.6	37.8	32.0	94.7	43.2	25.9	94.4	4.6	46.1	8.2	29.9	2.8
	120	100.0	54.8	29.8	91.6	42.5	34.7	97.8	44.1	25.0	96.5	3.6	47.1	5.4	29.8	4.0
$Pd(OAc)_2$	15	39.2	7.7	10.9	4.8	4.6	7.3	53.9	1.7	2.0	32.6	20.6	4.7	2.4	6.7	3.7
	35	58.3	19.3	12.0	58.7	6.0	4.4	47.4	4.0	2.3	54.8	5.3	9.8	6.8	6.2	4.2
	60	84.6	35.0	9.4	29.9	11.1	6.2	42.9	6.1	2.5	52.5	23.4	17.4	12.6	6.0	2.8
	90	96.9	57.1	9.7	76.9	12.4	3.3	44.9	10.5	2.7	72.9	21.4	26.6	21.5	5.2	3.2
	120	99.6	71.3	13.7	65.6	22.3	4.9	46.5	15.0	2.7	70.5	22.0	36.2	25.0	7.1	4.7
	150	-	-	-	36.5	31.6	7.3	-	-	-	-	-	-	-	-	-

[a] 12% ligand [b] 22% ligand

Table F.10: Results from screening investigating the impact of additives and different solvents.

Entry	Time [min]	Experiment 1			Experiment 2			Experiment 3			Conversion BrPyrCz		Yield NICz		Yield PyrCz	
		Conversion BrPyrCz [%]	Yield NICz [%]	Yield PyrCz [%]	Conversion BrPyrCz [%]	Yield NICz [%]	Yield PyrCz [%]	Conversion BrPyrCz [%]	Yield NICz [%]	Yield PyrCz [%]	Average [%]	Standard deviation	Average [%]	Standard deviation	Average [%]	Standard deviation
$Pd(OAc)_2$ / PPh_3 + $BnEt_3NCl$[a]	15	70.2	27.9	22.4	46.4	19.6	15.5	66.9	21.1	20.1	61.2	10.5	22.8	3.6	19.3	2.8
	35	87.4	51.1	31.5	79.5	27.3	14.7	90.1	38.0	24.3	85.7	4.5	38.8	9.8	23.5	6.9
	60	98.9	67.8	31.2	89.4	47.6	17.1	99.7	54.2	25.3	96.0	4.7	56.5	8.4	24.5	5.8
	90	100.0	66.1	28.6	99.4	56.5	15.3	100.0	59.5	29.7	99.8	0.3	60.7	4.0	24.5	6.6
	120	100.0	63.0	27.7	100.0	68.2	18.7	100.0	56.8	25.5	100.0	0.0	62.7	4.7	23.9	3.8
$Pd(OAc)_2$ / PPh_3 + PivOH[b]	15	52.2	11.5	9.6	59.3	10.1	13.3	58.4	9.3	13.5	56.6	3.2	10.3	0.9	12.2	1.8
	35	56.5	28.8	15.0	80.3	17.7	12.5	78.2	15.8	10.8	71.7	10.8	20.8	5.8	12.8	1.7
	60	87.8	48.2	11.6	88.1	33.7	13.1	85.3	26.8	10.4	87.1	1.3	36.2	8.9	11.7	1.1
	90	100.0	69.8	12.3	95.4	67.3	21.3	86.9	54.9	16.2	94.1	5.4	64.0	6.5	16.6	3.7
	120	100.0	62.5	10.5	100.0	67.0	17.3	100.0	73.1	17.3	100.0	0.0	67.5	4.4	15.0	3.2
dioxane[c]	15	24.2	1.5	2.3	0.3	1.2	0.7	-2.1	1.0	0.9	7.4	11.9	1.2	0.2	1.3	0.7
	35	16.8	1.3	1.9	-0.4	1.2	1.2	-3.5	1.1	0.7	4.3	8.9	1.2	0.1	1.3	0.5
	60	15.6	1.2	1.2	-1.3	1.3	0.8	-1.1	1.3	0.9	4.4	7.9	1.3	0.0	1.0	0.2
	90	10.9	1.4	1.4	-2.4	1.3	0.8	-4.5	1.4	0.6	1.3	6.8	1.4	0.1	0.9	0.3
	120	13.0	1.3	0.9	-1.2	1.2	1.0	-4.0	1.5	0.5	2.6	7.5	1.3	0.1	0.8	0.2
	150	14.1	1.3	1.1	1.2	1.2	0.8	-2.1	1.6	1.0	4.4	7.0	1.4	0.2	0.9	0.1
	1440	-	-	-	-0.3	21.2	1.7	-	-	-	-0.3	0.0	21.2	0.0	1.7	0.0
toluene[d]	15	16.5	1.3	1.3	8.1	1.1	0.4	-4.3	0.9	1.0	6.8	8.6	1.1	0.1	0.9	0.4
	35	15.2	1.3	1.1	8.5	1.3	0.4	-6.6	1.1	0.4	5.7	9.1	1.2	0.1	0.6	0.3
	60	12.7	1.6	0.7	9.7	1.6	0.7	-3.9	1.6	0.3	6.2	7.2	1.6	0.0	0.6	0.2
	90	11.5	1.9	0.8	8.7	2.3	0.2	-3.8	2.2	0.3	5.5	6.7	2.1	0.1	0.4	0.3
	120	16.2	2.0	0.5	11.5	2.6	0.3	-2.3	2.7	0.3	8.5	7.8	2.4	0.3	0.4	0.1
	150	6.1	2.8	0.4	13.0	3.3	0.3	-2.6	3.4	0.3	5.5	6.4	3.2	0.3	0.3	0.0
	1440	-	-	-	9.4	16.7	0.9	-	-	-	9.4	0.0	16.7	0.0	0.9	0.0

[a] 10% $Pd(OAc)_2$, 22% PPh_3, 1 eq. $BnEt_3NCl$, 2 eq. K_2CO_3, DMA (3000 ppm), 130°C. [b] 10% $Pd(OAc)_2$, 22% PPh_3, 30% PivOH, 2 eq. K_2CO_3, DMA (3000 ppm), 130°C

[c] 10% Pd-NHC, 2 eq. K_2CO_3, dioxane, 110 °C. [d] 10% Pd-NHC, 2 eq. K_2CO_3, toluene, 110 °C.

Table F.11: Results for experiments investigating different bases. Reaction conditions: 10% Pd-NHC (**45**), 2 eq. base (entry), DMA (3000 ppm H_2O), 130 °C.

Entry	*Time [min]*	*Experiment 1*			*Experiment 2*			*Experiment 3*			*Conversion BrPyrCz*		*Yield NICz*		*Yield PyrCz*	
		Conversion BrPyrCz [%]	*Yield NICz [%]*	*Yield PyrCz [%]*	*Conversion BrPyrCz [%]*	*Yield NICz [%]*	*Yield PyrCz [%]*	*Conversion BrPyrCz [%]*	*Yield NICz [%]*	*Yield PyrCz [%]*	*Average [%]*	*Standard deviation*	*Average [%]*	*Standard deviation*	*Average [%]*	*Standard deviation*
Na_2CO_3	15	18.6	19.8	0.7	22.0	18.7	0.8	10.7	12.1	0.9	17.1	4.7	16.9	3.4	0.8	0.1
	35	32.7	37.6	0.9	40.2	32.0	1.0	33.5	23.9	0.9	35.4	3.4	31.1	5.6	0.9	0.1
	60	50.9	53.3	1.1	61.4	45.3	1.1	40.0	37.3	1.0	50.8	8.7	45.3	6.5	1.0	0.1
	90	71.3	66.0	1.4	77.9	66.5	1.5	55.6	50.7	1.1	68.3	9.4	61.1	7.3	1.3	0.2
	120	86.6	80.7	1.7	94.3	80.7	1.6	76.1	60.5	0.9	85.7	7.5	74.0	9.5	1.4	0.4
	150	96.7	92.4	1.9	99.6	88.0	1.9	84.8	73.1	1.0	93.7	6.4	84.5	8.3	1.6	0.4
	180	100.0	98.8	2.1	100.0	93.8	1.9	92.8	89.5	1.1	97.6	3.4	94.0	3.8	1.7	0.4
	240	100.0	94.9	2.0	100.0	86.2	1.7	99.9	83.0	0.9	100.0	0.1	88.1	5.0	1.5	0.5
K_3PO_4	15	76.2	70.3	6.6	88.5	75.5	4.1	94.1	71.8	4.0	86.3	7.5	72.5	2.2	4.9	1.2
	35	89.4	76.3	7.3	100.0	92.0	5.2	100.0	83.0	4.9	96.5	5.0	83.8	6.4	5.8	1.1
	60	97.1	83.5	7.3	100.0	79.2	4.3	100.0	76.3	4.2	99.0	1.4	79.7	2.9	5.3	1.4
	90	99.8	84.1	7.0	100.0	87.4	4.5	100.0	72.7	4.0	99.9	0.1	81.4	6.3	5.1	1.3
	120	99.5	83.7	6.6	99.0	72.7	3.8	100.0	72.8	3.8	99.5	0.4	76.4	5.2	4.7	1.3
	150	100.0	75.1	5.8	100.0	78.7	3.8	100.0	87.0	5.3	100.0	0.0	80.3	5.0	5.0	0.8
	180	100.0	88.0	6.5	100.0	66.0	3.2	100.0	77.0	4.1	100.0	0.0	77.0	9.0	4.6	1.4
Et_3N	15	11.4	0.4	0.9	33.4	1.0	0.4	21.0	0.8	0.5	21.9	9.0	0.7	0.2	0.6	0.2
	35	7.2	0.5	1.1	24.9	1.3	0.3	42.3	0.8	0.3	24.8	14.4	0.9	0.4	0.6	0.4
	60	32.4	0.3	1.2	45.0	1.3	0.2	55.2	1.0	0.2	44.2	9.3	0.9	0.5	0.5	0.5
	90	-0.6	0.5	1.6	24.0	1.7	0.2	61.0	1.0	0.1	28.1	25.3	1.1	0.5	0.6	0.6
	120	5.3	0.6	1.8	63.2	1.6	0.1	32.3	1.8	0.2	33.6	23.7	1.3	0.5	0.7	0.8
	150	49.1	0.5	2.4	63.1	2.1	0.1	58.5	1.7	0.2	56.9	5.8	1.4	0.7	0.9	1.1
	180	92.3	0.5	3.3	28.7	3.0	0.3	34.8	2.4	0.3	51.9	28.6	2.0	1.1	1.3	1.4
	240	100.0	0.7	5.5	100.0	5.0	19.1	56.4	2.4	0.3	85.5	20.5	2.7	1.8	8.3	7.9
	1200	87.4	4.3	15.9	63.2	19.1	1.6	76.9	5.6	0.4	75.8	9.9	9.7	6.7	6.0	7.0

Table F.12: Results for experiments with reduced catalyst amount. Reaction conditions: 5% Pd-NHC (**45**), 2 eq. K_2CO_3, DMA (3000 ppm H_2O), 130 °C. Average values for all six experiments.

Entry	*Time [min]*	*Experiment 1*			*Experiment 2*			*Experiment 3*			*Conversion BrPyrCz*		*Yield NICz*		*Yield PyrCz*	
		Conversion BrPyrCz [%]	*Yield NICz [%]*	*Yield PyrCz [%]*	*Conversion BrPyrCz [%]*	*Yield NICz [%]*	*Yield PyrCz [%]*	*Conversion BrPyrCz [%]*	*Yield NICz [%]*	*Yield PyrCz [%]*	*Average [%]*	*Standard deviation*	*Average [%]*	*Standard deviation*	*Average [%]*	*Standard deviation*
Pd-NHC 5% - 1	15	50.3	26.1	7.1	47.3	24.4	6.1	44.2	25.6	6.8	-	-	-	-	-	-
	35	61.9	43.2	11.1	52.8	38.0	10.0	61.1	35.4	9.0	-	-	-	-	-	-
	60	71.3	52.7	12.4	67.8	44.7	10.4	63.9	40.6	10.0	-	-	-	-	-	-
	90	81.0	58.4	12.4	79.4	51.0	10.3	78.3	43.2	8.8	-	-	-	-	-	-
	120	88.1	62.7	11.9	86.0	57.2	10.3	84.0	52.4	9.0	-	-	-	-	-	-
	150	92.9	61.2	11.0	91.0	62.3	10.6	89.2	51.6	8.2	-	-	-	-	-	-
	180	95.7	69.8	11.3	95.2	62.0	9.1	93.4	57.6	8.0	-	-	-	-	-	-
	240	98.5	83.6	13.8	97.3	75.2	11.2	96.2	70.3	9.1	-	-	-	-	-	-
	360	100.0	80.2	13.2	100.0	76.8	10.1	99.6	68.9	8.2	-	-	-	-	-	-
	1200	100.0	71.2	9.1	100.0	63.4	7.8	100.0	54.4	5.4	-	-	-	-	-	-
Pd-NHC 5% - 2	15	53.8	21.3	11.9	30.2	22.4	7.2	33.5	23.1	8.6	43.2	8.6	23.8	1.7	7.9	1.9
	35	49.6	30.3	10.8	38.5	29.4	8.6	40.1	29.3	9.3	50.7	9.1	34.3	5.2	9.8	0.9
	60	54.1	34.1	10.5	47.4	36.7	9.0	44.2	36.0	9.9	58.1	10.2	40.8	6.3	10.4	1.0
	90	59.1	40.2	10.7	58.1	44.4	9.1	59.1	42.0	9.6	69.2	10.5	46.6	6.3	10.1	1.2
	120	63.7	46.7	11.1	66.6	53.2	9.4	75.4	46.2	8.3	77.3	9.5	53.1	5.8	10.0	1.3
	180	76.8	45.8	9.9	87.0	57.9	8.0	83.5	57.9	9.0	88.6	6.9	58.5	7.1	9.2	1.1
	240	80.9	52.7	10.0	93.8	67.9	8.1	93.2	58.6	7.6	93.3	5.9	68.0	10.2	10.0	2.1
	360	88.4	57.4	9.1	98.9	79.7	8.8	98.0	74.7	9.2	97.5	4.1	73.0	7.9	9.8	1.6
	1200	97.2	69.0	8.9	100.0	72.9	6.9	100.0	73.8	8.2	99.5	1.0	67.4	6.7	7.7	1.3

Table F.13: Results for experiments with reduced catalyst amount. Reaction conditions: 2% Pd-NHC (**45**), 2 eq. K_2CO_3, DMA (3000 ppm H_2O), 130 °C. Average values for all six experiments.

Entry	*Time [min]*	*Experiment 1*			*Experiment 2*			*Experiment 3*			*Conversion BrPyrCz*		*Yield NICz*		*Yield PyrCz*	
		Conversion BrPyrCz [%]	*Yield NICz [%]*	*Yield PyrCz [%]*	*Conversion BrPyrCz [%]*	*Yield NICz [%]*	*Yield PyrCz [%]*	*Conversion BrPyrCz [%]*	*Yield NICz [%]*	*Yield PyrCz [%]*	*Average [%]*	*Standard deviation*	*Average [%]*	*Standard deviation*	*Average [%]*	*Standard deviation*
Pd-NHC 2% - 1	15	59.1	10.7	9.5	59.3	12.4	7.5	50.8	10.4	8.0	-	-	-	-	-	-
	35	60.9	16.9	11.9	55.1	20.2	12.5	46.2	16.0	11.4	-	-	-	-	-	-
	60	60.7	18.9	12.1	50.8	21.6	14.2	52.5	17.0	10.6	-	-	-	-	-	-
	90	66.0	21.1	11.5	67.0	22.7	12.3	59.8	18.1	9.9	-	-	-	-	-	-
	120	69.5	23.8	11.6	70.4	23.2	11.5	72.8	18.3	8.5	-	-	-	-	-	-
	150	73.5	24.6	10.7	70.8	24.2	11.7	77.3	19.3	7.7	-	-	-	-	-	-
	180	77.4	25.4	10.1	74.4	24.6	10.8	76.2	20.9	8.0	-	-	-	-	-	-
	240	69.6	33.3	13.2	67.7	28.9	13.3	70.5	24.6	9.5	-	-	-	-	-	-
	360	83.2	31.3	9.8	80.3	30.8	11.0	69.2	29.6	10.5	-	-	-	-	-	-
	1200	95.1	37.7	7.6	90.6	47.2	11.0	86.9	45.5	9.1	-	-	-	-	-	-
Pd-NHC 2% - 2	15	31.7	6.4	8.2	25.0	9.6	9.9	31.7	13.0	11.9	42.9	13.9	10.4	2.1	9.2	1.5
	35	33.8	9.5	8.2	43.4	11.4	9.2	42.7	15.2	11.6	47.0	8.8	14.9	3.5	10.8	1.5
	60	40.3	11.7	8.0	51.1	13.0	8.8	50.4	16.6	10.9	51.0	5.9	16.5	3.4	10.8	2.1
	90	42.7	14.2	8.1	52.8	16.1	9.3	60.0	18.2	10.0	58.1	8.3	18.4	2.9	10.2	1.4
	120	53.4	17.0	7.6	55.2	18.3	9.5	59.7	21.7	10.9	63.5	7.7	20.4	2.6	9.9	1.5
	180	61.6	19.0	7.3	51.6	21.9	11.1	60.9	23.7	11.1	67.0	9.6	22.6	2.2	9.7	1.5
	240	61.6	24.0	8.1	61.7	26.0	10.5	47.3	28.6	14.4	63.1	7.9	27.6	3.2	11.5	2.3
	360	59.0	30.5	9.8	72.3	28.1	9.7	66.2	32.7	12.5	71.7	8.2	30.5	1.4	10.6	1.0
	1200	92.0	57.2	9.4	97.5	62.3	14.7	95.0	59.1	14.2	92.9	3.5	51.5	8.7	11.0	2.6

Table F.14: Results for experiments investigating different water contents and influence of protective atmosphere. Reaction conditions: 10% Pd-NHC (**45**), 2 eq. K_2CO_3, DMA, 130 °C.

Entry	*Time [min]*	*Experiment 1*			*Experiment 2*			*Experiment 3*			*Conversion BrPyrCz*		*Yield NICz*		*Yield PyrCz*	
		Conversion BrPyrCz [%]	*Yield NICz [%]*	*Yield PyrCz [%]*	*Conversion BrPyrCz [%]*	*Yield NICz [%]*	*Yield PyrCz [%]*	*Conversion BrPyrCz [%]*	*Yield NICz [%]*	*Yield PyrCz [%]*	*Average [%]*	*Standard deviation*	*Average [%]*	*Standard deviation*	*Average [%]*	*Standard deviation*
	15	86.4	75.0	4.2	80.4	70.0	4.9	-	-	-	83.4	3.0	72.5	2.5	4.5	0.4
	35	96.5	75.5	4.6	94.2	69.5	5.1	-	-	-	95.4	1.1	72.5	3.0	4.9	0.3
	60	99.4	86.0	5.5	97.6	91.1	7.1	-	-	-	98.5	0.9	88.5	2.6	6.3	0.8
37 ppm[a]	90	100.0	80.0	4.7	100.0	92.9	6.9	-	-	-	100.0	0.0	86.4	6.4	5.8	1.1
	120	100.0	91.0	5.7	100.0	90.6	6.8	-	-	-	100.0	0.0	90.8	0.2	6.2	0.5
	1560	100.0	82.6	4.8	-	-	-	-	-	-	100.0	0.0	82.6	0.0	4.8	0.0
	3000	-	-	-	100.0	74.1	4.6	-	-	-	100.0	0.0	74.1	0.0	4.6	0.0
	15	53.8	38.2	4.6	100.0	91.8	3.5	-	-	-	76.9	23.1	65.0	26.8	4.0	0.5
	35	70.1	47.7	5.4	100.0	86.6	3.2	-	-	-	85.1	14.9	67.1	19.4	4.3	1.1
	60	78.6	61.8	6.2	100.0	95.9	3.6	-	-	-	89.3	10.7	78.9	17.1	4.9	1.3
56 ppm[a]	90	93.7	82.5	6.7	100.0	85.1	3.0	-	-	-	96.8	3.2	83.8	1.3	4.9	1.8
	120	99.7	85.3	6.1	100.0	95.1	3.4	-	-	-	99.9	0.1	90.2	4.9	4.7	1.3
	1560	100.0	82.3	5.4	-	-	-	-	-	-	100.0	0.0	82.3	0.0	5.4	0.0
	3000	-	-	-	100.0	71.1	2.2	-	-	-	100.0	0.0	71.1	0.0	2.2	0.0
	15	38.0	4.2	0.9	36.0	4.6	0.6	37.4	4.1	0.6	37.1	0.8	4.3	0.2	0.7	0.2
	35	38.8	8.7	1.2	41.9	8.1	0.8	31.5	8.0	1.2	37.4	4.4	8.3	0.3	1.1	0.2
	60	52.9	17.4	1.3	50.6	15.3	1.1	32.2	16.7	1.8	45.2	9.3	16.4	0.9	1.4	0.3
Air[b]	90	64.6	36.3	2.0	60.2	32.0	1.5	58.4	29.8	2.1	61.1	2.6	32.7	2.7	1.9	0.3
	120	86.0	54.3	2.1	79.4	47.8	1.7	80.8	43.9	2.0	82.0	2.8	48.7	4.3	1.9	0.2
	180	99.7	69.9	2.0	98.1	68.8	1.6	98.0	59.9	1.8	98.6	0.8	66.2	4.5	1.8	0.2
	15	59.6	17.6	9.1	57.6	17.5	9.6	56.1	16.9	9.0	57.7	1.4	17.3	0.3	9.3	0.2
	35	88.5	49.1	10.8	89.6	51.9	11.3	87.2	49.4	11.4	88.4	1.0	50.1	1.3	11.2	0.3
Air – Add.[c]	60	100.0	66.5	10.8	100.0	70.3	11.7	100.0	66.5	11.0	100.0	0.0	67.8	1.8	11.1	0.4
	90	100.0	65.4	10.8	100.0	65.6	10.7	100.0	66.3	10.1	100.0	0.0	65.8	0.4	10.6	0.3
	120	100.0	64.6	10.1	100.0	63.3	10.7	100.0	62.4	10.8	100.0	0.0	63.5	0.9	10.5	0.3

[a] Water content of DMA. Average of two experiments. [b] Absence of protective atmosphere. [c] Addition of 1 ml air during sampling.

Table F.15: Results of screening applying chlorine precursor **XXXIIb**. Reaction conditions: 10% catalyst (entry), 2 eq. K_2CO_3, DMA (3000 ppm H_2O), 130 °C.

Entry	*Time [min]*	*Experiment 1*			*Experiment 2*			*Experiment 3*			*Conversion ClPyrCz*		*Yield NICz*		*Yield PyrCz*	
		Conversion ClPyrCz [%]	*Yield NICz [%]*	*Yield PyrCz [%]*	*Conversion ClPyrCz [%]*	*Yield NICz [%]*	*Yield PyrCz [%]*	*Conversion ClPyrCz [%]*	*Yield NICz [%]*	*Yield PyrCz [%]*	*Average [%]*	*Standard deviation*	*Average [%]*	*Standard deviation*	*Average [%]*	*Standard deviation*
Pd-NHC (45)	15	18.6	17.2	1.1	36.8	28.1	1.0	66.4	65.6	1.5	40.6	19.7	37.0	20.7	1.2	0.2
	35	38.5	23.3	1.1	50.2	31.1	1.1	100.0	101.5	1.8	62.9	26.7	52.0	35.1	1.4	0.3
	60	43.4	28.3	1.2	50.7	34.3	1.3	100.0	99.9	1.7	64.7	25.1	54.1	32.4	1.4	0.2
	90	42.0	35.6	1.4	52.6	41.1	1.4	100.0	103.6	1.9	64.9	25.2	60.1	30.9	1.6	0.2
	120	49.0	39.3	1.4	54.3	44.6	1.5	100.0	103.7	1.8	67.8	22.9	62.5	29.2	1.6	0.2
	150	55.1	44.1	1.3	57.0	50.1	1.6	100.0	100.7	1.7	70.7	20.7	64.9	25.4	1.6	0.2
	180	55.9	44.6	1.4	60.9	53.6	1.6	100.0	105.2	1.8	72.3	19.7	67.8	26.7	1.6	0.2
$PdCl_2(PPh_3)_2$	15	34.4	2.9	5.6	22.5	4.4	6.4	15.5	4.8	7.1	24.1	7.8	4.0	0.8	6.4	0.6
	35	38.7	5.0	8.2	31.1	6.1	9.2	29.5	6.5	10.4	33.1	4.0	5.9	0.6	9.3	0.9
	60	54.9	5.7	6.7	38.3	7.0	8.6	39.2	8.2	10.6	44.1	7.6	7.0	1.0	8.6	1.6
	90	32.1	7.7	8.7	35.9	7.6	8.8	31.2	9.3	11.7	33.1	2.0	8.2	0.8	9.7	1.4
	120	44.6	7.7	7.3	26.8	8.7	9.6	44.4	9.1	9.8	38.6	8.4	8.5	0.6	8.9	1.1
	150	54.3	8.5	6.5	47.1	8.4	7.4	43.1	9.2	9.6	48.2	4.6	8.7	0.4	7.8	1.3
	180	42.0	9.9	7.7	48.0	9.2	7.3	50.7	10.1	8.8	46.9	3.6	9.7	0.4	7.9	0.7